REPUBLIQUE DU CAMEROUN
Paix-Travail-Patrie

UNIVERSITE DE YAOUNDE I

FACULTE DES SCIENCES
CENTRE DE RECHERCHE ET DE FORMATION DOCTORALE EN SCIENCES, TECHNOLOGIES ET GEOSCIENCES
UNITE DE RECHERCHE ET DE FORMATION DOCTORALE PHYSIQUE ET APPLICATIONS
B.P 812 Yaoundé
DEPARTEMENT DE PHYSIQUE

REPUBLIC OF CAMEROON
Peace-Work-Fatherland

THE UNIVERSITY OF YAOUNDE I

FACULTY OF SCIENCES
POSTGRADUATES SCHOOL OF SCIENCE, TECHNOLOGY AND GEOSCIENCES
RESEARCH AND POSTGRADUATE TRAINING UNIT FOR PHYSICS AND APPLICATIONS
P.O.BOX 812 Yaoundé
PHYSICS DEPARTMENT

LABORATORY OF NUCLEAR, ATOMIC, MOLECULAR PHYSICS AND BIOPHYSICS

IMPACT OF ELECTROMAGNETIC INDUCTION AND LIGHT ILLUMINATION OF INFORMATION PATTERN ON COUPLED NEURONS

Thesis

Submitted and defended in Fulfillment of the Requirements for the award of the Degree of **Doctorate/Ph.D** in **Physics**

Speciality: **Nuclear, Atomic, Molecular Physics and Biophysics**

Option: **Biophysics**

By:

Peter NYIFEH

Registration number**: 04T407**

Master of science in Physics

Under the supervision of

EKOBENA FOUDA Henri Paul

Professor

University of Yaoundé I

YEAR : 2025

UNIVERSITE DE YAOUNDE I
UNIVERSITY OF YAOUNDE I

FACULTE DES SCIENCES
FACULTY OF SCIENCE

DEPARTEMENT DE PHYSIQUE
PHYSICS DEPARTMENT

ATTESTATION DE CORRECTION DE LA THESE DE DOCTORAT/Ph.D

Nous, Professeur **HONA Jacques**, Examinateur, et Professeur **BEN-BOLIE Germain**, Président du Jury de la Thèse de Doctorat/Ph.D de Monsieur **Peter NYIFEH**, Matricule **O4T407**, préparée sous la direction du Professeur **EKOBENA FOUDA Henri Paul,** intitulée : « **Impact of electromagnetic induction and light illumination of information pattern on coupled neurons.** », soutenue le **Mardi, 1er Avril 2025**, en vue de l'obtention du grade de Docteur/Ph.D en Physique, Spécialité **Physique Nucléaire, Atomique Moléculaire et Biophysique**, **Option Biophysique,** attestons que toutes les corrections demandées par le Jury de soutenance ont été effectuées.

En foi de quoi, la présente attestation lui est délivrée pour servir et valoir ce que de droit.

Fait à Yaoundé le 15 AVR 2025

Examinateur

Pr. HONA Jacques.

Le Président du Jury

Pr. BEN-BOLIE Germain Hubert

Le Chef de Département de Physique

UNIVERSITE DE YAOUNDE I ★ FACULTE DES SCIENCES ★ DEPARTEMENT DE PHYSIQUE
Le Chef de Département

Pr. NDJAKA Jean-Marie Bienvenu

IMPACT OF ELECTROMAGNETIC INDUCTION AND LIGHT ILLUMINATION ON INFORMATION PATTERN OF COUPLED NEURONS

Submitted and defended publicly in fulfilment of the requirements

for the award of the Degree of Doctor/PhD in Physics,

Option: **Biophysics**

by

Peter Nyifeh

M. Sc. in Physics

Registration Number: **04T407**

Under the supervision of

EKOBENA FOUDA Henry Paul

Professor

April 15, 2024

Dedication

To my late father Bernard NYIBEH NCHETIE.

Acknowledgments

Obviously, no human work can be done without the manifestation of the will of God Almighty. Throughout this process, he blessed me with health, peace, stability and most especially inspiring me with new ideas that gave me the desire and determination to do this research. Also, I would like to express my gratitude to all those who contributed, in whatever manner, to the success of this work.

First of all, I want to thank my supervisor, Professor **EKOBENA FOUDA Henri Paul**. His constant support, guidance, and encouragement have been invaluable throughout the entire process. In addition,

I would also like to express my deepest thanks to the members of jury.

I benefited from Pr **TABI Conrad Bertrand** , Pr **MVOGO Alain** and Dr **TAKEMBO Clovis** a very rich and stimulating research experience.

Special thanks to Pr **NDJAKA Jean-Marie Bienvenu**, Head of Department of Physics at the University of Yaoundé I, for having ordered the processing of the defense file.

I also think about my long years of academic training and cordially thank some of the teachers who gave me scientific knowledge. They are: Pr **OWONO OWONO Luc Calvin**, Pr **WOAFO Paul**, Pr **BEN-BOLIE Germain Hubert**, Pr **KENFACK JIOTSA Aurelien**, Pr **PEMHA Elkana**, Pr **TCHAWOUA Clément**, Pr **ZEKENG Serge**, Pr **NJOMO Donatien**, Pr **MANGUELE Dicoum Eliézer**, Pr **OWONO ATEBA**, Pr **NANA NBENDJO**, Pr **ESSIMBI ZOBO**, Pr **EYEBE FOUDA Armand**, Pr **HONA Jacques**, Pr **MBANE BIOULE**, Pr **SIEWE SIEWE Martin**, Pr **FEWO Serges Ibraid**, Pr **NJANDJOCK NOUCK Philippe**, Pr **DJUIDJE KENMOE Germaine**, Pr **BODO Bertrand**.

A special thanks to Dr **ETEME Alain Sylvain**, Dr **ADAMOU DANG KOKO**, Dr **BELOBO Didier**, Dr **GUIMFACK Boris Anicet** Dr **BINENG Guillaume**, Dr **OWONO Olivier**, Dr **ASSEMBE Patrick** and Dr **TIOMELA TANEFO Sedrique**

Arnaud who shared with me their experience on calculation methods, the use of software essential for the research and interpretation of some complex phenomena.

Additionally, I would like to thank my laboratory mates who supported me with various actions throughout my academic career. I am thinking mainly to: Dr **BANSI KAMDEM Delphin Christel**, Dr **OKALY Joseph Brizar**, Mr **EDOUMA Patrick**.

Furthermore, I wish to express my heartfelt thanks to the parents, brothers, sisters and friends who have distinguished themselves by their immeasurable commitments throughout my academic training. First of all, my late father **Benard NYIBEH NCHETIE** and uncle **NTOKU BETAH John** who did their best before the world separated us. Then my valiant mother **mama MBEH CHENUIVE Esther**, my sisters **Rev Sr Veronica YONAH**, **NYISIKI Belinda MBEKUH**. My daughters and sons also deserve to be thanked at the highest level because, their psychological and material supports have largely contributed to the realization of this work.

Finally, I want to acknowledge my sweetheart **Marcelline NJUH NYIFE**, who not only suggested that it was not too late for me to go back to University and fulfill a lifelong dream, but also gave me emotional support and acted as my literary editor.

Contents

List of Figures

List of Tables

List of Abbreviations

Initials	Meaning	**Initials**	Meaning
NNs	Neural networks	**NLS**	Nonlinear Schrödinger
HR	Hindmarsh-Rose	**DNLS**	Discrete nonlinear Schrödinger
HH	Hodgkin-Huxley	**RK4**	Fourth order Runge-Kutta
FHN	FitzHugh-Nagumo	**LRI**	Long-range interaction
IF	Integrate-and-fire	**CCGL**	Coupled complex Ginzburg-Landau
ML	Morris-Lecar	**ODEs**	Ordinary differential equations
LR	Long-range	**EEG**	Electroencephalography
LF	Low frequency	**IBI**	Inter-burst interval
HF	High frequency	**SDA**	Semi-discrete approximation
MI	Modulational instability	**RK4**	Fourth-order Runge-Kutta
NA	Neuronal activity	**NS**	Neuronal synchronization
CNS	Central nervous system	**EPSPs**	Excitatory post synaptic potentials
NMDA	N-methyl-D-aspartic acid	**GABA**	G-Amino-Butyric Acid
DNA	Deoxyribonucleic acid	**WP**	Waves propagation

Résumé

Les ondes électromagnétiques sont omniprésentes dans notre environnement moderne en raison de l'utilisation croissante des technologies sans fils telles que les téléphones portables, antennes relais et réseau wifi. Cependant, la recrudescence des troubles neurologiques telles que la dépression, l'anxiété, la fatigue chronique et des maladies neurodégénératives comme les maladies d'Alzheimer et de Parkinsons d'après certaines études semblent étroitement liées à l'exposition à ces ondes. Dans cette Thèse, nous étudions l'impact de l'induction électromagnétique et des radiations lumineuses sur la dynamique des réseaux de neurones. Les modèles d'étude sont le modèle de FitzHugh-Nagumo(FHN) et l'Integrate and Fire model (IF) qui décrivent les neurones fonctionnels à partir d'un circuit. Nous modifions le circuit en y introduisant un memristor permettant de simuler l'effet des champs magnétiques internes et externes sur la dynamique du réseau de neurones considéré et un phototube pour générer une excitation dont la valeur dépend de l'intensité de la lumière. Grâce à l'instabilité modulationnelle, la formation d'ondes modulées et la transition de modèle sont étudiées dans un réseau de 100 neurones photosensibles. Les régions de formation d'ondes modulées sont déterminées par l'analyse de la stabilité linéaire. Le taux de croissance de l'IM est tracé et les zones distinctes stable/instable sont présentées. Nous confirmons les résultats analytiques par des simulations numériques dans lesquelles les solutions initiales d'ondes planes conduisent à l'émergence de structures localisées présentant des caractéristiques de pointes, d'éclatements et d'états chaotiques. Il est a noté que le photocourant à haute fréquence transforme les structures localisées en structures de type chaotique, tandis que le flux magnétique à haute fréquence favorise la transition des structures de l'état d'éclatement à l'état de pointes à 2 et 4 périodes. Les résultats trouvés peuvent permettre de mieux comprendre la dynamique de l'influx nerveux dans le cerveau et de développer de nouvelles interventions thérapeutiques pour les troubles neurologiques.

Mots clés: Neurones; influx nerveux; modèle de FitzHugh-Nagumo; memristor; équation discrète de Schrödinger non linéaire; induction électromagnétique; radiation lumineuse; instabilité modulationelle; synchronisation neuronale. structure localisée

Abstract

Electromagnetic waves are omnipresent in our modern environment due to the increasing use of wireless technologies such as mobile phones, relay antennas and wifi network. However, the increase in neurological disorders such as depression, anxiety, chronic fatigue and neurodegenerative diseases such as Alzheimer's and Parkinson's disease according to some studies seem closely linked to exposure to these waves. In this thesis, we study the impact of electromagnetic induction and light radiation on the dynamics of neural networks. The models studied are the FitzHugh-Nagumo model (FHN) and the Integrate and Fire model (IF), which describe functional neurons based on a circuit. We modify the circuit by introducing a memristor to simulate the effect of internal and external magnetic fields on the dynamics of the considered neuron model, and a phototube to generate an excitation whose value depends on the intensity of the light. Thanks to modulation instability, the formation of modulated waves and pattern transition are studied in a network of 100 light-sensitive neurons. Regions of modulated wave are determined by linear stability analysis. The growth rate of the MI is plotted and the distinct areas are presented. We confirm the result by numerical simulations in which the initial plane-wave lead to the emergence of localized structures with the characteristics of spikes, bursts and chaotic states. It should be noted that high-frequency photocurrent transforms localized structures into chaotic ones, while high-frequency magnetic flux promotes the transmission of structures from the bursting state to the peak state at 2 and 4 period. The results found may lead to a better understanding of the dynamics of nerve impulses in brain and to develop new therapeutic interventions for neurological disorders.

Keywords: Neurons; neural networks; nerve impulse; FitzHugh Nagumo model; discrete nonlinear Schrödinger equation;light illumination; electromagnetic induction; modulational instability; neuronal synchronization.

General Introduction

After the discovery of the solitary wave by Scott-Russel in 1834, Zabusky and Kruskal in their work in 1965 showed the existence of a wave called soliton with its applications in particular in the transport of energy and information. The study of the nonlinear effects has recently been undertaken in several fields such Physics, Biology and Chemistry thus the application of physical principles and methods to biological problems called Biophysics tries to explain some properties of the living organisms and their physiology. Understanding the function of the brain, the neuron behavior in response to different kinds of stimuli has received a lot of attention during the last decades, and a critical amount of biological and computational data is now available and makes the field of mathematical neuroscience very active and exciting

Advances in artificial intelligence and brain science also drew much attention recently as they have largely contributed new knowledge on the potential mechanism of information processing in the nervous system related to learning, memory, and cognition [7–9]. Also, the dynamic behavior of neurons is particularly important for understanding information encoding and related diseases in the nervous system (NS). To estimate various neural activities within the brain and its environment, many biophysical laws governing the underlined neural activities have been derived base on various neural models and maps. Various characteristics states such as quiescent, bursting, spiking and chaotic have been accurately mimic as observed from biological systems.

Neurons are the fundamental building blocks of the nervous system, responsible for transmitting and processing information in the form of electrical signals. They are specialized cell that receive, integrate and transmit signals through electrochemical processes.

Neural network have gained significant attention due to their ability to learn from data and make predictions or decisions without been explicitly programmed [1]. To understand how neurons interact within a network, simplified mathematical models are used, with aim to apprehend the essence of their underlying dynamics. The Hodgkin Huxley [2]

and Morris Lecar [3] neuron models are useful to describe the effect of ion channels on membrane potential of neurons. Izhikevich [4] ever gave short comments for most of the neuron model. Ibarz et al. [5] suggested that map-type model could also be effective to produce the dynamical properties in neuronal activities. Perc and Marhl [6] confirmed that excitable neurons that reside in a steady state near a bifurcation point to elliptic bursting oscillations, and it was also found that in addition to the resonant frequency of damped oscillations around the stable focus, another frequency exists that resonantly enhances large amplitude bursts and thus amplifies the information transfer in the system. These results could be helpful to understand the amplification of information transfer in excitable systems. In fact, the FHN model which is a generic model of excitability and oscillatory dynamical behavior particularly creates a very interesting trade-off between theory and experiment.

The cerebral complexity is mainly due to the rich spectrum of activities of interconnected neurons. In fact, the cerebral cortex is made of a huge number of neurons [7], distributed in different compartments and cooperatively interacting for functional activities to be performed [8, 9]. Experimental findings show that cortico-cortical networks display a few prominent characteristics related to complex dynamical features for processing and integration of information by the brain [10]. Explicitly, in neural systems, any perturbation arising in one neuron is transmitted to its neighbors via synaptic coupling, where spike trains are mainly believed to support information transfer and processing across the nervous system [11]. Over the years, the importance of nonlinear waves in neural networks have been extensively investigated for a better understanding of some cooperative behaviors including patterns formation, synchronization and coherence, as they are surely related to normal functioning and generation of some neural ailments [12–14]. Therefore, one of the main goals in neuroscience is to unmask the mechanisms leading to the formation of the subsequent spatiotemporal patterns for a suitable description of brain activities. Human seizures are interesting examples among others, where spatiotemporal events are tributary to seizure episode initiation, development and termination [15]. Other substantial examples include the use of appropriate models on basal ganglia neurons to differentiate pathological network dynamics and regular wave patterns of neural firing [16, 17]. Patterns formation has also been addressed in a network of discrete Rulkov cells [18], with a particular interest in the coupling strength among adjacent nodes [19]. Small-world-networks were constructed, leading to chaotic and synchronous states in HR

neurons with randomly long-range (LR) links among nearest-coupled nodes [20].

The human brain is also known to undergo large activities based mainly on neural oscillations at various frequencies [21, 22]. Low frequency (LF) oscillations modulate activities over broad spatial areas and across long temporal windows, while high frequency (HF) oscillations are restrained to small regions and short temporal windows [23, 24]. For example, pathological high frequency oscillations are the main signature of epileptic cortex [25]. Besides, one of the most resurgent questions in electrophysiology is to know the key frequency related to the pathophysiology of schizophrenia, this because abnormal neural oscillations are found in all frequency bands [23]. Given this, understanding the specificity of frequency abnormalities might be a prosperous avenue to draw the link between disease mechanisms and clinical dysfunction of many neural ailments. Experimentally, the different characteristic frequencies of normal neural activities are known [24], but the most obscure part remains their mode of generation and the appropriate model to be used. Using one-dimensional model, it has not been possible, to the best of our knowledge, to differentiate LF and HF modes. A good example of such recent calculations is the HR model, where one frequency was detected, supposedly the one supporting HF membrane potential oscillations [26]. Albeit one can get a general view of nerve impulse dynamics from these one-dimensional models, it remains however that the human brain contains around $10^{10} - 10^{11}$ neurons, each involved in numerous connections with approximately $10^4 - 10^5$ different neurons [27]. Some formulations, like the cellular automata model of the brain, consider a random distribution of neurons individually involved into numerous connections [28]. Indubitably, neuron systems can display complex dynamical properties in electrical activities, depending on the model and, more importantly, on the type of connections among them. In this regard, it is widely accepted that neurons, in order to discern their collective behaviors, should be connected in networks. For example, two-dimensional (2D) models have been shown to exhibit interesting features and phenomena related to spatial coherence resonance [29, 30] and spatial coherence due to shortcut links [31]. In the same context, networks with 2D coupling have been found to display various synchronization behaviors induced either by finite information delays [32] or attractive and repulsive coupling [33], both related to some pathological states like epileptic seizure [34] and uncontrolled firing [35]. In the 2D-HR model for example, more contributions have been devoted to pattern selection and self-organization in the presence of noise, using boundary initial values and direct numerical simulations [36, 37]. Recently, Xu et

al. [37,38] considered a square lattice of HR neurons and showed that stochastic-like resonance and time-delay may be favourable to the emergence of coherent patterns and spatial regularity in the network. Indeed, spatiotemporal pattern and synchronization dynamics are very crucial in understanding normal function and dysfunction of neuronal systems, but they rely on specific frequencies. Experimentally, such frequencies are known and lots of contributions have been devoted to their subsequent wave patterns, especially those related to pathological rhythmic brain activity in Parkinson's disease, essential tremor, and epilepsies.

The modulational instability (MI) is a phenomenon that occurs in nonlinear systems, where small perturbations can grow and lead to the formation of large-amplitude structures. This technique has been observed in various physical systems, including optics [39], fluid dynamics [40] and plasma physics [41–44]. In some recent contributions, wave modulation, through the activation of MI, has been addressed by Maïna *et al.* [45], where two ephaptically coupled HH networks were shown to exhibit synchronization in terms of trains of solitonic waves. Therefore, MI is one of the direct mechanisms that lead to the formation of solitons and train of waves in systems where there are competitive effects between nonlinearity and dispersion [39–41, 43–45].

This thesis is divided into three chapters that are outlined as follows:

✠ The first chapter focuses on the organization and properties of neurons as the fundamental building block of the nervous system, responsible of transmitting and processing information in the form of electrical signal. We also outline some analytical methods and neuron models, which will result on the choice of the IF and FHN models whose properties and applications are well discussed

✠ In Chapter 2, after the explanation of electromagnetic induction and its relevance to neural activity, we will presents the improved mathematical models developed in this thesis as well as the analytical and numerical methods used to investigate the effects of electromagnetic induction and light illumination in neurons. Some immediate applications are made in order to facilitate the understanding of the used methods. Interestingly, a DNLS equations are derived from generic model and allow to find analytical expression of some MI functions such as critical amplitude along with instability criterion.

✠ The third chapter is devoted to results and interpretations. We first discuss the effects of electromagnetic induction and light illumination on information pattern of coupled neurons. Then the high-low frequency magnetic radiation are studied in a discrete

model of two-dimensional FHN network.

The thesis ends with a general conclusion including the summary of the main results and the futures orientations.

Chapter 1

Literature review on Neurons and Neural Networks

Introduction

Over the past hundred years, biological research has accumulated enormous amount of detailed knowledged about the structure and function of the brain. The elementary processing units in the central nervous system are neurons, which are connected to each other in an intricate pattern. Advances in artificial intelligence and brain science also drew much attention recently as they have largely contributed new knowledge on the potential mechanism of information processing in the nervous system related to learning, memory, and cognition [7–9]. Also, the dynamic behavior of neurons is particularly important for understanding information encoding and related diseases in the nervous system (NS). To estimate various neural activities within the brain and its environment, many biophysical laws governing the underlined neural activities have been derived base on various neural models and maps. Various characteristics states such as quiescent, bursting, spiking and chaotic have been accurately mimic as observed from biological systems.

Neurons communicate by means of electrical impulses (action potentials). The evolution in time of these impulses forms a complex code that supports the treatment of the nervous message. Obviously, the emission of an action potential by a neuron is favored by the electrical properties of its plasma membrane which is ionically permeable. The abundance of neurons in the cerebral tissue sometimes confers them complex and different morphologies, but still retains a basic structure consisting of a cell body, an axon and dendrites.

Naturally in the brain, each neuron can have approximatively ten thousand connections with other neurons, totaling a million billion electrochemical interactions in the nervous system. Neurons interacting with each other via synapses form a network that constitutes a very sophisticated and complex communication system. In a neurons family, the knowledge of inherent properties of individual neuron does not necessarily allow the knowledge of the properties of the network, since the electrical activity of each neuron is influenced by those of the others to which it is connected. In particular the chemical substances of a given afferent neuron for interneuronal communication may slow down or accelerate the nerve impulse transmitting process . This once more makes the phenomenon of neuronal activity (NA) very ambiguous.

To remove the equivocation, researchers have built, on the basis of experimental results, mathematical models, more or less simple, to simulate the different behavior of neurons. Thanks to these mathematical models, it is henceforth possible to obtain spike-shaped patterns like those obtained by Hodgkin and Huxley via experiment on the giant squid axon. Additionally, most of the behaviors related to a neural network are accurately reproduced through these models, although most of which not having biologically specificity, have universal physical fundamentals.

This chapter is divided into two main parts. The first parts presents the neuron as the basic unit of the nervous system with a particular emphasis on its structure and functions, and on the properties of the action potential considered as the elementary electrical signal of the nerve impulse. The second part, in turn, highlights the role played by synapses in the transmission of nerve impulses from one neuron to another in a neural network.

1.1 Nervous system

The nervous system is a complex and highly organized network responsible for coordinating actions and transmitting signals between different parts of the body. It's the body's control and communication center, allowing us to perceive, think, feel and act. The nervous system is divided into two main parts.

1.1.1 The central nervous system (CNS).

- The brain is the control center for thought, memory, emotion and movement.

- The cerebellum: located at the back of the brain, responsable for higher cognitive functions like language, learning and decision-making.
- The cerebrum: it is responsible for higher cognitive functions like language, learning and decision making.
- The brainstem connects the brain to the spinal cord and controls essential functions such as breathing, heart rate and blood pressure.
- The spinal cord: it serves as the major communication pathway between the brain and the rest of the body.

1.1.2 The peripheral nervous system (PNS).

- Ganglia: it act as a relay stations for signals passing between the central nervous system and the periphery.
- The nerves which is a network of nerves that extend from the brain and spinal cord to all other parts of the body.

The nervous system is made up of two types of cells: the glia cells and mainly the nerve cells called neurons.

1.2 Neurons

Neurons are the basic building blocks of the nervous system and are responsible for transmitting information throughout the body.

Human brains comprise tens of billions of neurons, each linked to thousands of other neurons. Thus, the brain has trillions of specialized connections known as synapses. Neurons have many sizes, lengths, and shapes, which determine their functions. As for the most of the biological systems, neuron structure and their various functions are closely dependent.

1.2.1 Structure and Functions

There is a wide variety of neurons, with different shapes and sizes. However, they all have a common structure (see Fig.1.2) comprising:

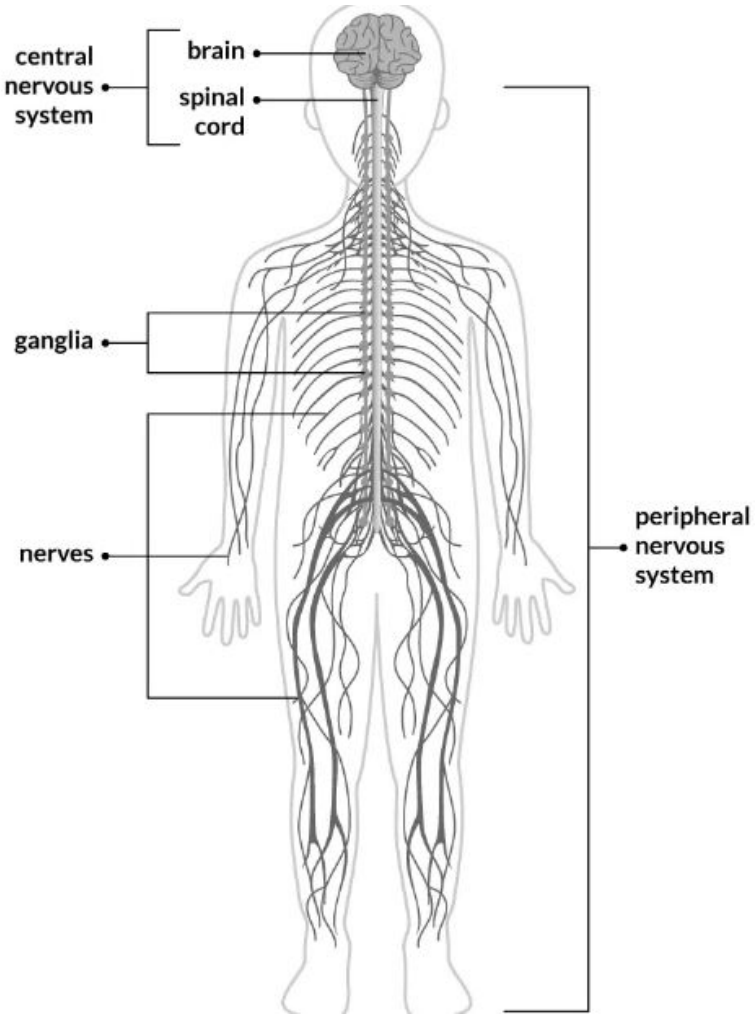

Figure 1.1: Diagram of the nervous system [46]

- the cell body, also called the soma,
- numerous short processes of the soma, called the dendrites;
- the single long nerve fiber, the axon.

The cell body

The cell body, also known as the soma, is the main part of the neuron that contains the nucleus and other organelles necessary for the neuron's metabolic functions. The soma, or cell body, is the processing center of a neuron. When it receives information, it processes it and, if it is sufficient important relative to a certain threshold, sends a signal into the axon. It is responsible for integrating incoming signals from other neurons and generating electrical impulse, known as action potential. Nerve cells contain about $70 - 80\%$ water; the dry material is about 80% protein and 20% lipid. The cell volume varies between

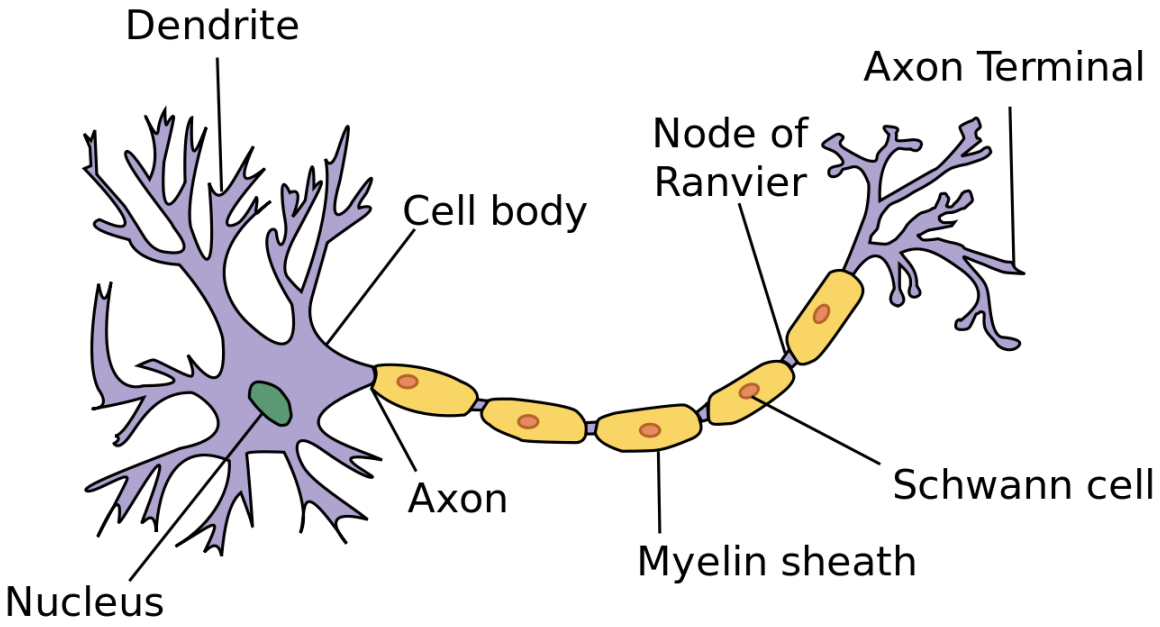

Figure 1.2: Annotated diagram of a neuron [47]

600 and 70.000 μmL. The unique feature of the cell body is that it is the only part of a neuron that contains a cell nucleus in which DNA molecule is confined. Most RNA in a neuron is produced by the cell nucleus. Therefore, most proteins are produced in the cell body and then transported to the entire neuron.

Dendrites

Dentrites are the branch-like structures that extend from the cell body of a neuron. They receive incoming signals from other neurons or sensory receptors and transmit these signals towards the cell body. They function as an "antennae" of the neuron and are covered in specialized structures called synapses, where communication between neurons occurs. When an electrical signal reaches a synapse, it triggers the release of neurotransmitters, which then bind to receptors on the dentritic spines of the receiving neuron. This binding process generates electrical changes in the dentrite, either depolarizing it (excitatory) or hyperpolarizing it (inhibitory), depending on the type of neurotransmitter released. The structure and number of dentrites can vary greatly depending on the type and location of the neuron. Some neurons have only a few short dentrites, while others extensive branching patterns with thousands of dentritic spines. The complexity and connectivity of dentritic arborization play a crucial role in determining how information is processed within neural networks.

Axon is a long, slender projection that carries electrical impulses away from the cell body to other neurons, muscles, or glands. Many neurons do not have axons. For instance, in amacrine neurons, all the neuronal processes are dendrites. Neurons with very short axons are also found. Some axons are covered with a fatty substance called myelin, which acts as an insulating layer and speed up the transmission of electrical signal. The myelin sheath is broken at various points by the nodes of Ranvier, so that in cross section it looks like a string of sausages. The myelin protects the axon, and prevents interference between axons as they pass along in bundles, sometimes thousands at time. The cells that wrap around peripheral nerve fibers (nerve fibers outside of the brain and spinal cord) are called Schwann cells (because they were first described by Theodor Schwann). The cells that wrap around axons within the central nervous system (brain and spinal cord) are called oligodendrocytes. The axon, with its surrounded sheath, is called a nerve fiber. Between each pair of successive Schwann cells is a gap or a node of Ranvier. The axon hillock is where the axon is joined to the cell body. It is from here that the electrical firing, known as an action potential, usually occurs. At the end of the axon, there are small branches called axon terminals that release neurotransmitters into synapses to communicate with other neurons.

1.2.2 Classification of neurons

Neurons can be classified based on various criteria, including their structure, function and location.

Structurally, neurons are classified by the number of processes that originate from the cell body. For this purpose, we have four types of neurons: anaxonic neurons, bipolar neurons, pseudounipolar neurons and multipolar neurons as shown in Fig.1.3.

Anaxonic neurons have dendrites, but no axons. They produce local electrical variations (graded potential), but no action potential.

Bipolar neurons have two extensions that emerge from the cell body: a dendrite and an axon; they are commonly found in sensory organs like retina of the eye.

Pseudounipolar neurons have a single and short extension divided into two branch: one goes towards the central nervous system (CNS), peripheral extension (dendrites to the cell body); and the other, towards the peripheral nervous system, central extension (cell body to the CNS).

Multipolar neurons represent the most common type in the CNS; they have multiple

dendrites and a single axon extending from the cell body.

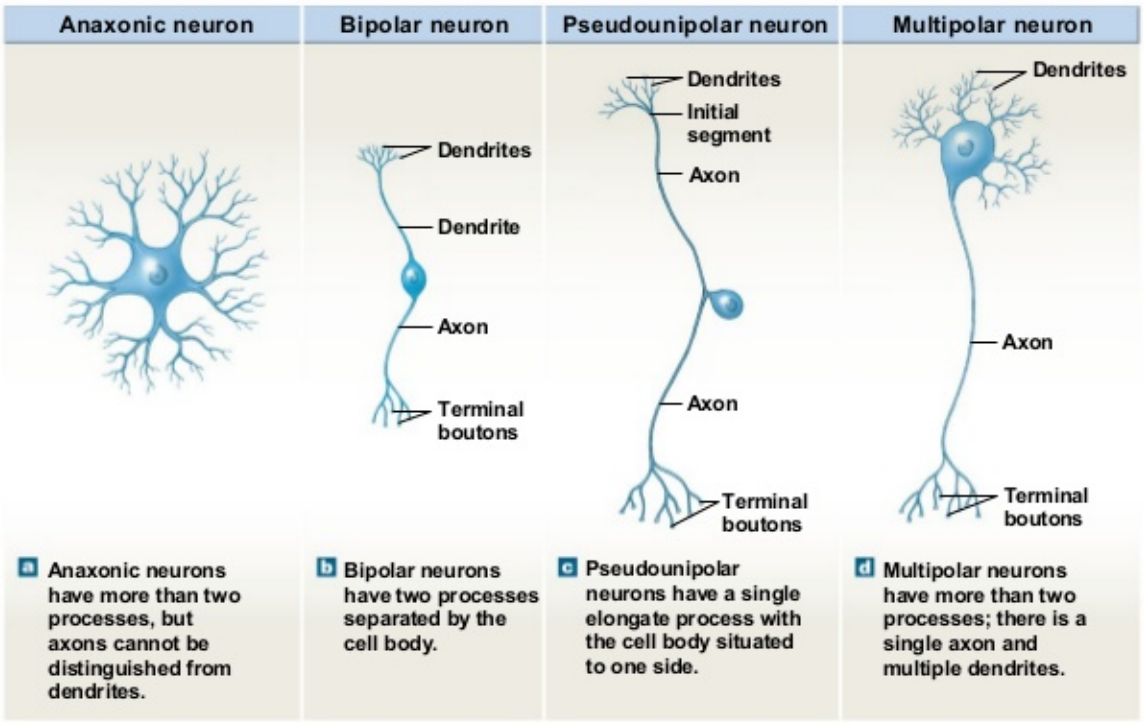

Figure 1.3: Structural categories of neurons [48]

Functionally, neurons can be divided into three functional classes namely sensory (afferent) neurons, interneurons and efferent (somatic motor and autonomic) neurons.

Afferent neurons:

These neurons transmit sensory information (temperature, pressure, light, and other stimuli) from sensory receptor to the CNS. Sensory neurons or afferent neurons are unipolar, bipolar, or multipolar shaped cells that conduct action potentials toward or into the central nervous system. They carry somatic nervous system signals from the skin, joints, skeletal muscles, sensory organs (eyes, ears, mouth, and nose). They also carry autonomic nervous system signals from the visceral organs (heart, lungs, vessels, etc).

In comparison, **motor neurons** (efferent neurons; lower motor neurons) are multipolar shaped cells that transmit signal from the CNS to muscle or glands, enabling movement or secretion. Their cell bodies and dendrites are located in the central nervous system and their axons run inside the nerves to the peripheral organs.

Interneurons (association neurons):

These neurons connect sensory and motor neurons within the CNS, facilitating communication between them. After receiving input from the sensory neurons, the interneurons

perform many complex tasks inside the CNS. First, they integrate, image, and interpret, the sensory information. Next, they form judgments and make needed decisions. Finally, they plan and initiate appropriate response behaviors, which they transfer to the motor neurons.

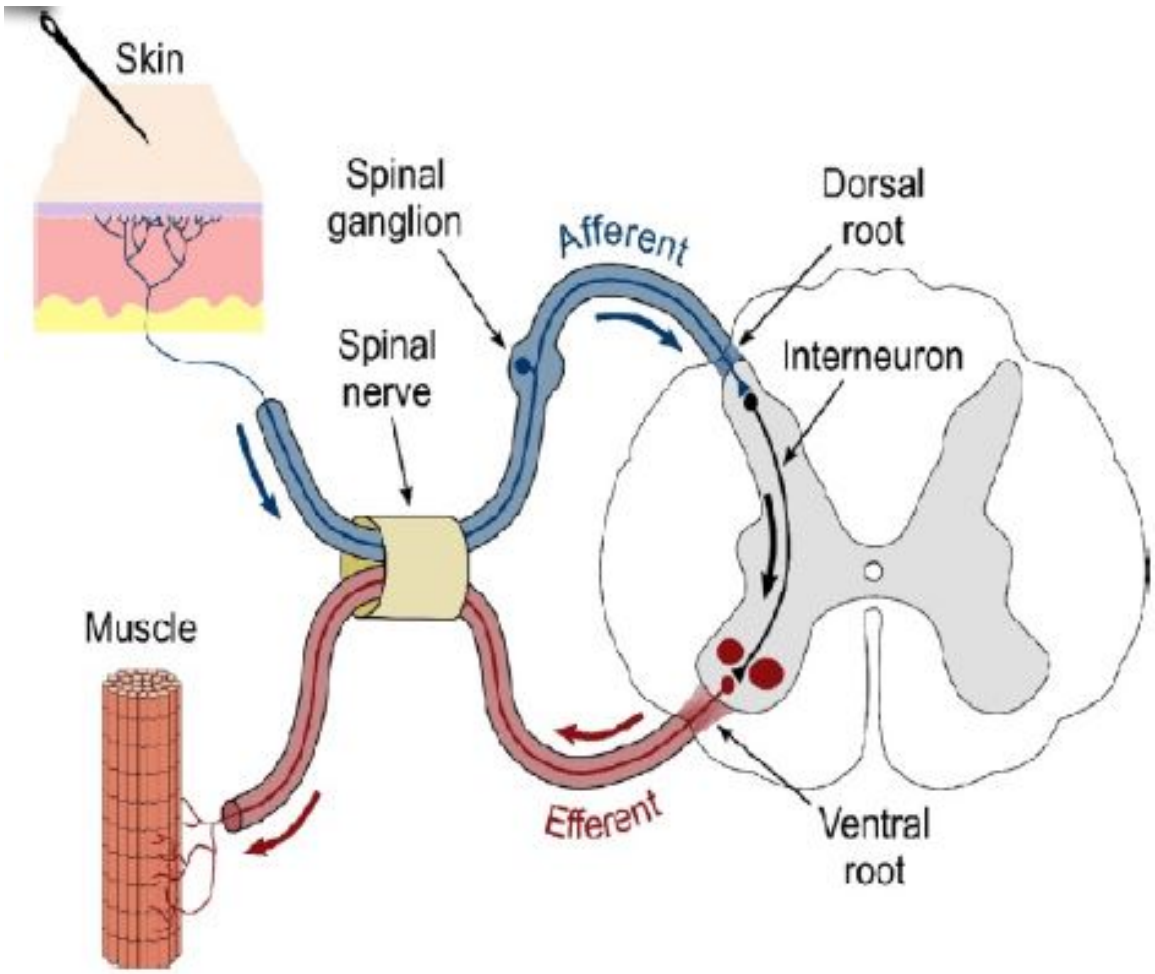

Figure 1.4: Functional neurons [49]

Based on its location criteria, we have:

Central Nervous System (CNS) Neurons:

These neurons are located within the brain and spinal cord.

Peripheral Nervous System (PNS) Neurons:

These neurons are located outside the CNS, such as in sensory ganglia or motor nerves.

1.2.3 Electrical Activity of Neurons

The electrical activity of neurons refers to the generation and transmission of electrical signals within these specialized cells of the nervous system. Neurons are electrically excitable cells that communicate with each other through electrical impulses, known as action potential.

The nervous signal delivered by the neuron is of an electrical nature. This property is an exclusivity of the plasma membrane of the nerve tissue which is very permeable to certain ions. The flow of ions through this membrane is therefore at the origin of a membrane current that reflects the electrical activity of neurons. The ionic unbalance between the intra- and extracellular media of the membrane promotes the electrical activity of the neurons. Therefore, it is important to understand both anatomy and physiology of the cell membrane.

1.2.3.1 Cell membrane

The neuronal membrane, also known as the plasma membrane, is a semi-permeable barrier that surrounds the neurons and separates its internal environment. With its mosaic of proteins, the membrane is responsible for many important functions:

- keeping certain ions and small molecules out of the cell and letting others in,
- accumulating nutrients, and rejecting harmful substances,
- catalyzing enzymatic reactions,
- establishing an electrical potential inside the cell,
- conducting an impulse being sensitive to particular neurotransmitters and modulators .

The membrane is made of lipids proteins-fats and chains of aminoacids. The basic structure of this membrane is a bilayer or sandwich of phospholipids, organized in such a way that the polar (charged) regions face outward and the non polar regions face inward. The external face of the membrane contains the receptors, small specialized molecular regions which provide a kind of "attachment port" for other external molecules, in a scheme analogous to a key and a keyhole. For each external molecule there is a corresponding receptor.

Whenever receptors become attached to a molecule, some alterations of the membrane and in the interior of the cell ensue, such as the modification of permeability to some ions. The main ions found on both sides of the membrane are Na^+ (sodium) ions, K^+ (potassium) ions and Cl^- (chlorite) ions. The schematic view of neuron cell membrane is drawn in Fig.1.5. At rest, the cell membrane is the seat of a resting potential.

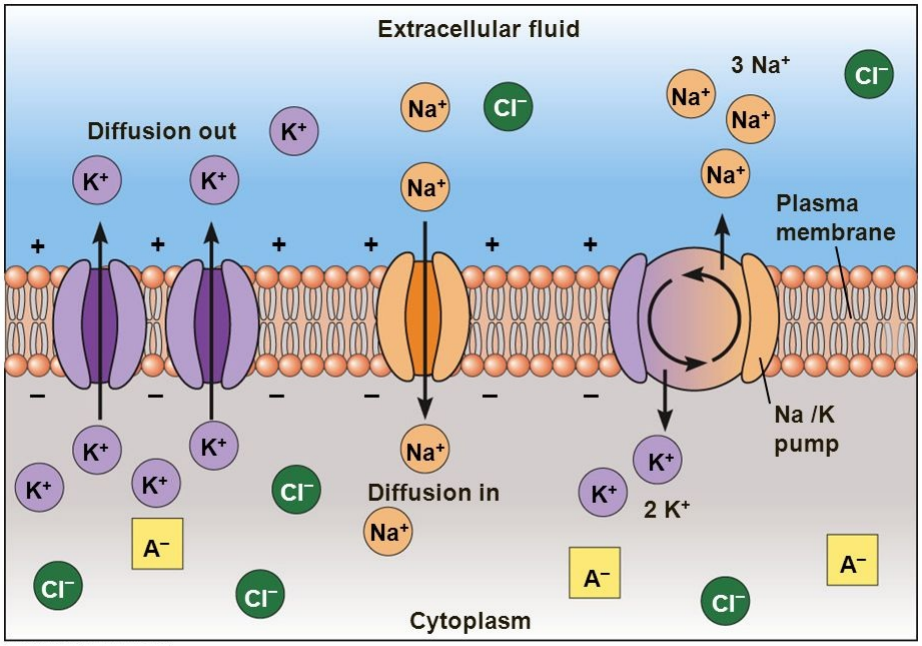

Figure 1.5: Cell membrane flow diagram [50]

1.2.3.2 Resting Potential

Resting potential refers to the electrical charge difference across the cell membrane when a neuron or muscle cell is at rest. In this state, there is a higher concentration of positively charged ions outside the cell compared to inside, creating an electrical potential difference. The relatively static membrane potential of quiescent cells is called the resting membrane potential (or resting voltage). Generally the value of resting potential is about $-70mV$.

Negative value of resting potential is due to:

- presence of large number of positive Na^+ ions towards outside of membrane,
- presence of large number of positive K^+ ions towards inside of membrane,

- zwitterionic protein molecules of cytoplasm behave as negative ions in presence of highly charged K^+,
- $Na^+ - K^+$ ion pump continuously pumps out three sodium ions while only two potassium ions are taken inside the cell.

All these factors mean that the inside of the cell is negatively charged with respect to the outside, hence the existence of a resting potential. However, when cell membrane is excited, the resting potential splits into action potential.

1.2.3.3 Action Potential

The influx and expulsion of ions within cell cause an action. The action potential also referred to as a nerve impulse, it is the electrical potential difference across the plasma membrane. Specifically , potassium and sodium ion are involved. It is a key mechanism by which neurons communicate with each other and transmit information throughout the nervous system. As depicted in Fig.1.6, the action potential displays four transient phases ranging from:

- **Failure phase**.

  The failure phase occurs when the membrane potential fail to reach the threshold level required to generate an action potential. where the action potential is between $-70mV$ and $-55mV$. The limit value $-55mV$ represents the threshold value above which action potential is sustainedly generated. Thus, the action potential obeys to the threshold law. During this phase, the sodium channels open gradually causing the entry of sodium ions inside the cell, but their concentration remains low. At the same time, the potassium channels are inactive and therefore remain closed. The membrane potential remains at a subthreshold level and does not generate action potential, this can result in a failed transmission of signals along the neuron or between neurons leading to a disruption in communication within the nervous system. Malfunctioning ion channels or inhibitory neurotransmitters are factors that can contribute to the failure phase of an action potential

- **Depolarization phase** where the action potential increases from $-55mV$ to $+30mV$, reaches its peak before starting to decrease. It is important to note that this maximum value can not be exceeded whatever the greatest possible value that can reach

the intensity of the stimulus. As a result, the action potential responds to the all-or-nothing law. During this phase, the voltage-gated sodium channels open in response to a stimulus, allowing sodium ions to flow into the cell down their electrochemical gradient. This influx of positive charge causes the membrane potential to become less negative (the inside of the membrane becomes positively charged, while the outside becomes negatively charged) and eventually reach a threshold level triggering an action potential. At the end of this phase, the sodium channels close, becoming inactive, as the potassium channels open.

- **Repolarization phase** occurs when action potential decreases from its maximum value $+30mV$ to their resting state $-70mV$. Throughout this stage, more and more K^+ ions flow towards outside of membrane, thus leading to the initial polarization state where more positive charges are on the outside and more negative charges on the inside.

- **Hyperpolarization phase** occurs when action potential falls below the resting potential value. This is due to the slow closing of the potassium channels and results in a recrudescence of potassium ions outside the cell. As these channels close, the sodium pump will initiate the slow entry of sodium ions into the cell thus allowing the action potential to recover its resting value. At the end of this transition, the sodium channels become active, that is to say close to respond to a new stimulus.

It should also be noted that the time interval separating the onset of depolarization and the end of repolarization constitutes the refractory period during which the cell membrane can not respond to a new stimulus whatever its intensity. Moreover, since action potential is generated locally in the neuron, it becomes like a stimulus and will regenerate along the axon to the synaptic connections. It is said that the action potential undergoes a conduction that is saltatory in the case of myelinated axons and continuous in the case of unmyelinated ones.

In summary, the action potential obeys to four main laws that govern its properties, namely:

- **The threshold law**: the action potential emerges only when the membrane potential reached a certain threshold level which is proportional to the stimulus intensity [52].

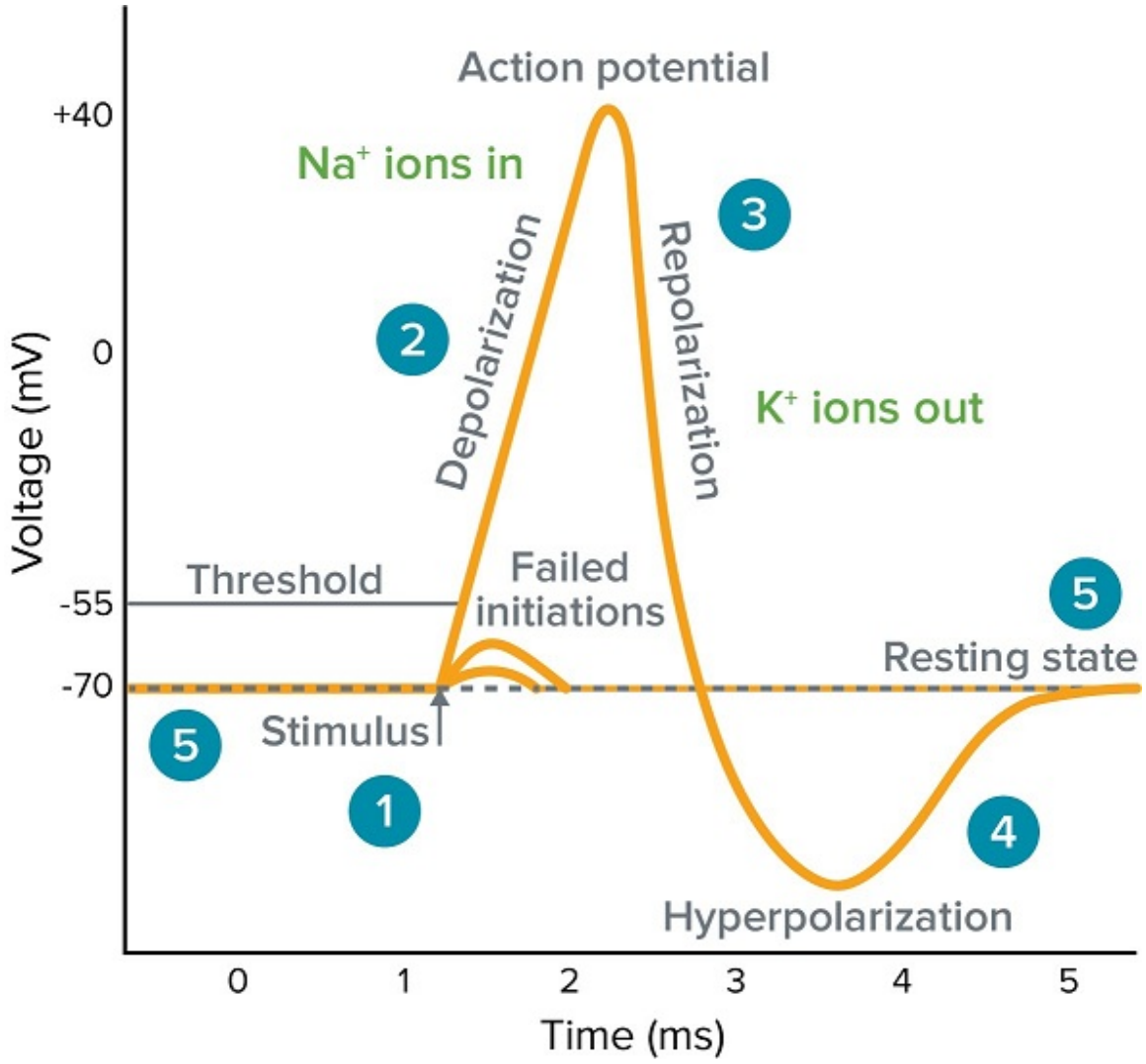

Figure 1.6: Action potential graph [51]

- **The all-or-nothing law**: The amplitude of an action potential is independent of the amount of current that produced it. In other words, larger currents do not create larger action potentials. Therefore, action potentials are said to be all-or-none signals, since either they occur fully or they do not occur at all [53]. The frequency of action potentials is correlated with the intensity of a stimulus. This is in contrast to receptor potentials, whose amplitudes are dependent on the intensity of a stimulus [52].

- **The refractory period law**: each action potential is followed by a refractory period, which can be divided into an absolute refractory period, during which it is impossible to evoke another action potential, and then a relative refractory period,

during which stronger than usual stimulus is required [52]. These two refractory periods are caused by changes in the state of sodium and potassium channel molecules. When closing after an action potential, sodium channels enter an "inactivated" state, in which they cannot be made to open regardless of the membrane potential. This gives rise to the absolute refractory period. Even after a sufficient number of sodium channels have transitioned back to their resting state, it frequently happens that a fraction of potassium channels remains open, making it difficult for the membrane potential to depolarize, and thereby giving rise to the relative refractory period. Because the density and subtypes of potassium channels may differ greatly between different types of neurons, the duration of the relative refractory period is highly variable. The absolute refractory period is largely responsible for the unidirectional propagation of action potentials along axons [52]. At any given moment, the patch of axon behind the actively spiking part is refractory, but the patch in front, not having been activated recently, is capable of being stimulated by the depolarization from the action potential.

- **The law of conduction**: the action potential generated at the axon hillock propagates as a wave along the axon without turning back because of the refractory period law. The currents flowing inwards at a point on the axon during an action potential spread out along the axon, and depolarize the adjacent sections of its membrane. If sufficiently strong, this depolarization provokes a similar action potential at the neighboring membrane patches. This basic mechanism was demonstrated by Alan Lloyd Hodgkin in 1937 [54].

1.2.3.4 Nerve Impulse

It is important to distinguish the concepts of action potential on the one hand, and the nerve impulse on the other hand. In fact, the action potential is an electrochemical signal that results from the depolarization phenomenon of the plasma membrane of neuron, while nerve impulse refers to the transmission of an action potential along the nerve fiber. The nerve pulse propagates through the nerve fiber without decay and with constant velocity. An impulse can be formed and spread because the nerve fiber contains a nonlinear element, which suppresses small deviations from normal state and strengthens big ones. In this case, the nonlinear dependence of the membrane permeability (through which the nerve impulse is spread) from the momentum and the diffusion of ions across the membrane

are balanced. In Ref. [55], it is shown that nonlinearity can actually balance diffusion and, as a result, a running solitary wave with constant speed and shape can occur, i.e, a soliton. A nerve impulse is then an extension of an action potential. Physiological studies have shown that propagation of a nerve impulse through NNs has autowave character. This also allows simulating such processes using soliton theory which describes the form and velocity of propagation of the nervous pulse, stability of its characteristic parameters in time, and process locality with very good precision [56]. The conduction of an action potential along the axon can be continuous or saltatory. In saltatory conduction, an action potential at one node of Ranvier causes inwards currents that depolarize the membrane at the next node, provoking a new action potential there; the action potential appears to "hop" from node to node. This propagation mode enable fast and efficient transduction of electrical signals in the nervous system for certain neuronal axons that are covered with myelin sheaths. However, in the absence of the myelin sheath, the conduction of the nerve impulse proceeds continuously, thus reducing its propagation speed. As a general rule, myelination increases the conduction velocity of action potentials and makes them more energy-efficient. Whether saltatory or continue, the mean conduction velocity of an action potential ranges from 1 meter per second ($m.s^{-1}$) to over $100m.s^{-1}$, and, in general, increases with axonal diameter [54]. In practice, the nerve impulse emitted by a neuron does not remain confined in the latter, it is transmitted to the neighboring neuron via synaptic connections. The recipient neuron in turn transmits it to its nearest neighbor by the same process, and so on until its final destination, which is either the brain or a motor organ. Thus, the path taken by the nerve impulse from its source to its destination constitutes the neural network.

1.3 Neural Networks

Neural networks are a type of machine learning model inspired by the structure and function of the human brain. They consist of interconnected nodes, called neurons, organized in layers. Each neuron receives input from multiple neurons in the previous layer, performs a computation, and passes the output to neurons in the next layer. Therefore, the synapse appears as the main characteristic entity of such a network. Fig.1.7 is an illustration of a simple neural network.

Neural networks achieved remarkable success in various fields like image recognition,

natural language processing, speech recognition and game playing.

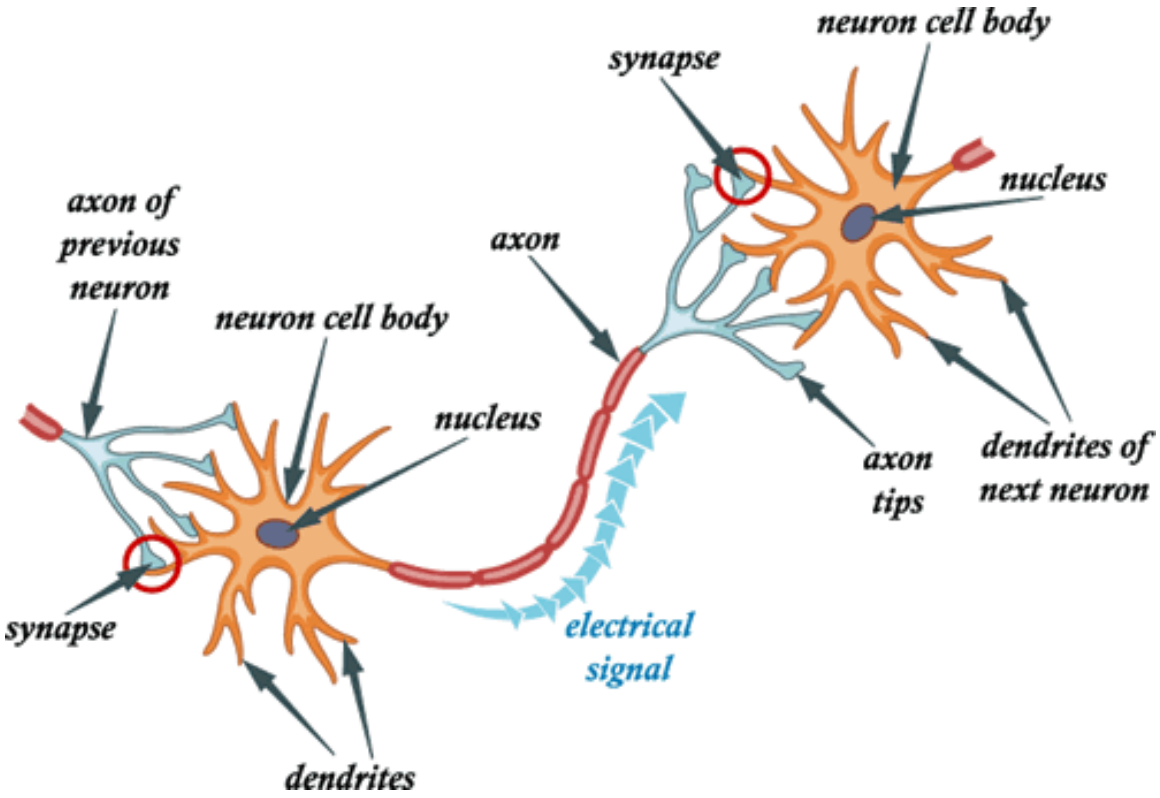

Figure 1.7: A neural network [57]

1.3.1 Synapses

Synapses are key to the brain's function, especially when it comes to memory. They are the junctions where one neuron communicates with other cells. The presynaptic terminal of one cell comes into 'contact' with the postsynaptic membrane of another. It is at these junctions that neurons are excited, inhibited, or modulated. Briefly, the synapse is the system which allows the neurons to communicate between them, it is the place where information passes from a neuron to another. Structurally, we distinguish two types of synapses, electrical and chemical. However, from a functional point of view, there are excitatory, inhibitory and modulatory synapses.

1.3.1.1 Chemical Synapses

In general in chemical synapses (Fig.1.8), action potentials that reach the synaptic knobs cause a neurotransmitter to be released into the synaptic cleft [58]. Neurotransmitters are chemical molecules released at the synapse that, in general, will either excite or

inhibit a reaction in the cell on the other side of the synapse; most axons have the same neurotransmitter at all of their termini. The arrival of the action potential opens voltage-sensitive calcium channels in the presynaptic membrane; the influx of calcium causes vesicles filled with neurotransmitter to migrate to the cell's surface and release their contents into the synaptic cleft [59]. This complex process is inhibited by the neurotoxins tetanospasmin and botulinum toxin, which are responsible for tetanus and botulism, respectively [60]. There are two types of chemical junctions. Type I is an excitatory synapse, generally found on dendrites, type II is an inhibitory synapse, generally found on cell bodies. Different substances are released at these two types of synapse. The direction of flow of information is usually one way at these junctions.

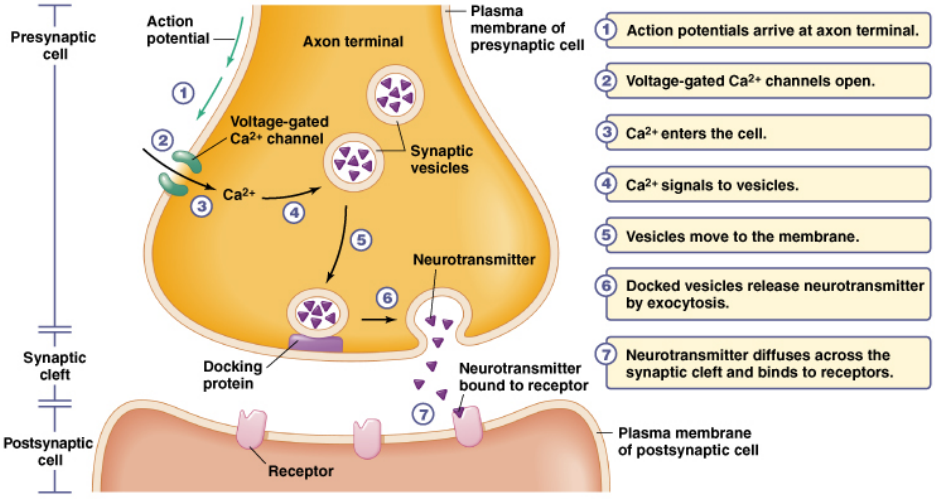

Figure 1.8: Chemical synapse diagram [61].

1.3.1.2 Electrical Synapses

Electrical synapse is a direct electrical coupling between neurons through gap junctions, allowing for rapid transmission of signals. Found in various region of the brain and spinal cord, as well as in cardiac and smooth muscle tisses (Fig.1.9) dispense with the "middleman" of the neurotransmitter, and connect the presynaptic and postsynaptic cells together [62]. When an action potential reaches such a synapse, the ionic currents flowing into the presynaptic cell can cross the barrier of the two cell membranes and enter the postsynaptic cell through pores known as connection [63]. Thus, the ionic currents of the presynaptic action potential can directly stimulate the postsynaptic cell. Electrical

synapses allow for faster transmission because they do not require the slow diffusion of neurotransmitters across the synaptic cleft. Hence, electrical synapses are used whenever fast response and coordination of timing are crucial, as in escape reflexes, the retina of vertebrates, and the heart. Additionally, ions can generally flow both ways at these junctions i.e. they tend to be bi-directional, although there are electrical junctions where the ions can only flow one way, these are know as rectifying junctions. Rectifying junctions are used to synchronize the firing of nerve cells.

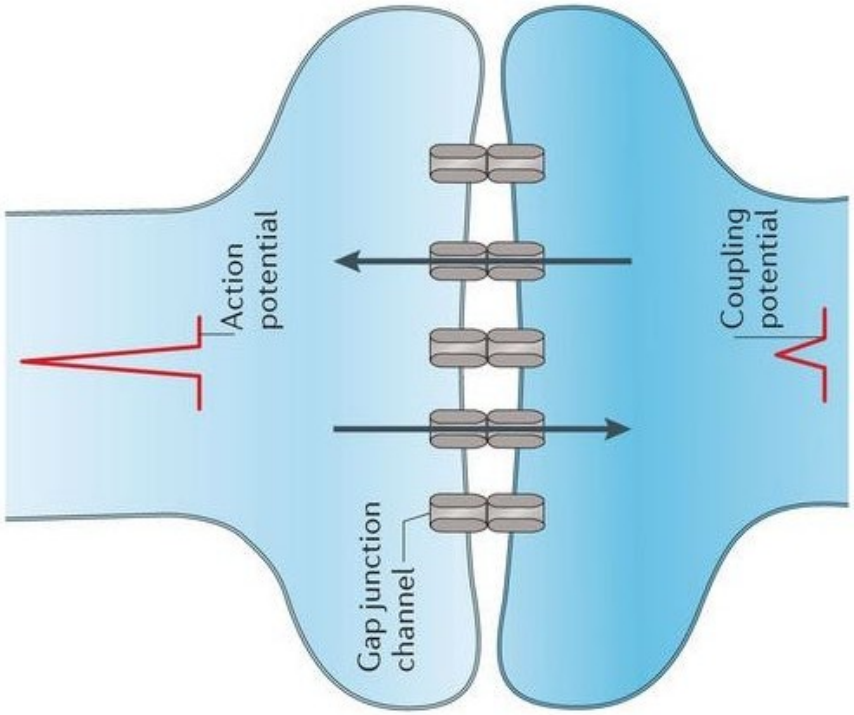

Figure 1.9: Electrical synapse diagram [61]

In short, the comparative table between electrical and chemical synapses is presented below

1.3.1.3 Excitatory Synapses

Excitatory synapses are responsible for transmitting signals that increase the likelihood of an action potential been generated in the postsynaptic neuron. Most excitatory synapses in the brain use glutamate or aspartate as the neurotransmitter. These neurotransmitters bind to non-selective cationic channels that allow for Na^+ and K^+ to pass. As mentioned earlier, it takes many excitatory post synaptic potentials (EPSPs) from these kinds of synapses to depolarize a postsynaptic neuron enough to reach threshold

Electrical synapses	**Chemical synapses**
Cytoplasmic continuity between pre-and post-synaptic cells	No cytoplasmic continuity between pre-and post-synaptic cells
Communicating agent is ionic current	Communicating agent is a chemical transmiter
Essentially no synaptic delay	Significant synaptic delay
Typically bidirectional	Unidirectional
Rare in complex animals	Common in complex animals
Common in simple animals	Rare in simple animals
Direct communication among neurons	Indirect communication among neurons
Post synaptic signal is similar to presynaptic	Post synaptic signal can be different
Only excitatory	Excitatory or inhibitory
synchronized activity	specificity: point to point communication
temperature-insensitive	temperature-sensitive

Table 1.1: Comparative table between electrical and chemical synapses.

and trigger an action potential. A very important subset of synapses in the brain includes a group capable of forming memories by increasing the activity and the strength of the synapse. This process is called long-term potentiation. Long-term potentiation operates at the synapse, using the neurotransmitter glutamate and the receptor known as the N-methyl-D-aspartic acid (NMDA) receptor. The NMDA receptor is unique in that it is both ligand and voltage regulated. When activated by ligands, it becomes permeable to Na^+, but if the charge difference is sufficient, the channel becomes permeable to Ca^{2+} as well. Ca^{2+} can initiate a second messenger cascade that results in an increase in the number of glutamate receptors, thereby increasing the strength of the synapse. The change in strength can last for weeks, months, or even years depending on whether or not the synapse is continually used.

1.3.1.4 Inhibitory Synapses

It may seem somewhat of a paradox to have inhibitory synapses, but the excitability of neurons is essentially governed by a balance between excitation and inhibition. Inhibitory

synapses transmit signals that decrease the likelihood of an action potential been generated in the postsynaptic neuron. The main inhibitory neurotransmitters are G-Amino-Butyric Acid (GABA) and glycine. Both neurotransmitters bind to receptors that result in an increase conductance of Cl^- . Because of the negative charge of Cl^- and the fact that it usually moves into the cell, the effect is to oppose depolarization and cause the membrane to move away from threshold.

The balance between excitatory and inhibitory synaptic input is crucial for proper functioning of the nervous system. an imbalance can lead to various neurological disorders such as epilepsy or schizophrenia. The precise regulation of excitatory and inhibitory synaptic transmission is achieved through complex mechanism involving neurotransmitter release, receptor activation, and modulation by other factors like neuromodulators.

1.3.1.5 Modulatory synapses

Modulatory synapses are those that can be "primed" by neuromodulators so that they are able to respond more powerfully to other inputs. An example of a priming neuromodulator is norepinephrine. By itself, norepinephrine has little effect on synaptic transmission, but when a cell is exposed to norepinephrine first, it will react more powerfully to glutamate.

1.3.2 Functional and behavioral properties of neural networks

The human brain is a cluster of roughly 10^{15} neural networks whose flexibility and adaptability make them powerful tools for solving complex problems across various domain. If the neuron in its individuality is capable of generating, processing and transmitting information, its role remains limited to the microscopic scale. Its natural membership in a network allows it to modulate its activity while giving it still interesting and more promising properties. In general, NNs provide five major cognitive functions [64] namely:

- **Image recognition (Perception)**: it is a sensory property that allows each individual to communicate with his external world through the five senses of sight, hearing, smell, touch and taste. Thus, the perception of an object for example is transmitted to the brain by a specialized neural network for this task, then the information received by the brain is analyzed and then decoded before being sent via another neural network to the receiving organ (the eye) in the form of a real image

of the perceived object.

- **Thought**: it is a mental process that is triggered by internal stimuli. It consists of mental operations that the awake brain performs on internal information stored by a network of neurons. This property involves the networks of cortical neurons and allows the brain to imagine, perform mental or complex calculations and even move from one place to another.

- **Language**: it is a communicative property that use neural networks. Language is one of the most elaborate, complex, and rich brain functions. Its pathological alterations are numerous and, at first sight, often bizarre. The cerebral cortex is a mosaic of specialized areas richly interconnected with each other. When an area is damaged, specific symptoms appear which quench the communication. Even more gravely, when two zones are disconnected, they develop disorders just as specific. Thanks to language, the wording of words becomes possible.

- **Consciousness**:, it is a discerning property of neural networks. It is thanks to it that we make good and bad choices. But it also makes it possible to distinguish sick subjects from healthy subjects. A loss of consciousness can lead to a comatic state surmountable but sometimes irreversible.

- **Memory**: it is one of the most fascinating properties of neural networks. Thanks to memory, enormous amounts of information are recorded during the learning process. It also allows you to remember people or images already seen before. There is long-term memory that can store information over a long period of time and short-term memory that temporarily stores information.

Some behavioral properties such as the rhythm in the alpha and gamma frequency range in the mammalian hypothalamus, NS, spiral and spindle waves formation, sleep oscillations and many others result from the dynamics of set of a neural network. Some of these behaviors are involved in the degradation of brain activity.

1.4 Consequences of neural networks dysfunction

Dysfunction in the transmission of information in neural network can lead to a wide range of pathologies, affecting various aspects of cognition, movement, sensation and

autonomic functions. Here are some prominent examples.

1.4.1 Depression

Depression is characterized A mood disorder characterized by persistent sadness, loss of interest and feeling of hopelessness. It is associated with disruptions in serotonin, norepinephrine and dopamine neurotransmission.

1.4.2 Epilepsy

Epilepsy is a neurological disorder characterized by recurrent seizures. Seizures result from abnormal, excessive electrical activity in the brain. This can be caused by imbalances in excitatory and inhibitory neurotransmission, leading to hyperexcitability of neurons.

1.4.3 Schizophrenia

Schizophrenia is a severe mental disorder characterized by hallucinations, delusions, disorganized thinking and impaired social function. It is thought to involve imbalances in dopamine, glutamate and other neurotransmitter systems.

1.4.4 Multiple sclerosis

An autoimmune disease that attacks the myelin sheath surrounding nerve fibers in the brain and spinal cord. This demyelination disrupts the saltatory conduction of nerve impulses, leading to a variety of symptoms, including muscle weakness, vision problems and fatigue.

1.4.5 Parkinson's disease

Primarily affects motor control, causing tremors, rigidity, bradykinesia (slow movement) and postural instability. It is cause by the degeneration of dopamine-producing neurons in substantia nigra, leading to a disruption in dopamine signaling in the basal ganglia.

1.4.6 Alzheimer's disease

It first affects cognitive function, leading to memory lost, confusion and impaired judgment. The accumulation of amyloid plaques and neurofibrillary tangles disrupts synaptic transmission and neuronal function, eventually leading to cell death.

Conclusion

In summary, understanding the anatomy and physiology of biological neurons with the culminating point of interneuronal communication is essential for comprehending how neural networks function. Neuron's ability to transmit and process information through electrical signals forms the basis for complex cognitive processes observed in living organisms. Roughly speaking, neurons communicate with each other through electrical signals known as action potentials. These electrical impulses are generated when the neuron receives sufficient input from its dendrites which plays the role of the "input device" that collects signals from other neurons and transmits them to the soma. The soma is the central processing unit that performs an important nonlinear processing step: if the total input arriving at the soma exceeds a certain threshold, then an output signal is generated. The output signal is taken out by the axon (output device) which delivers the signals to other neurons. The intricate interplay of neurons in neural networks enables complex information processing, learning, and decision-making capabilities that continue to drive innovation in various fiels.

Chapter 2

Improved models and methodologies

Introduction

Maintening the optimal electrical activities of neurons is highly important for humans as any breakdown dues from any external attack can lead to the collapse of brain resulting in serious diseases and even death in case of injury of the nervous system. In an attempt to understand the collective behaviors of neurons and possible mechanism for neuronal disease. Some theoretical models have been established for computational neuroscience, and some biological neuron model could be helpful to understand plasticity, mode transition in electric activities. For example Liu et al. [65] used photocell to activate a simple FHN neuron and an external optical signal is imposed to excite the photocell in order to generate a time-varying current source. Taking into account two different time constants, Panfilov and Hogeweg [66] modified the standard FHN model for excitable tissue and showed that a spiral wave can break up into an irregular spatial pattern. Takembo et al. [67], reported turbulent electrical activities of coupled FHN neurons under electromagnetic induction and high frequency electromagnetic radiations using the theory of modulational instability(MI).

The phenomenon of the MI studied through the linear stability analysis method unfortunately does not make it possible to make long-term predictions on the manifestations of the phenomenon. However, numerical methods such as the fourth-order Runge-Kutta integration method are generally exploited, not only to give a validity to the linear stability analysis, but also to reveal different patterns of the model. In this chapter, the most prominent computational models will be develop to describe the behavior of neurons and neural networks, Two important neuronal models will also be developed in the framework

of this thesis with a particular focus on network morphology and the synaptic transmission known as the drive belt, or the bridge, which relays the nervous impulse from one neuron to another. Also, we will apply the different analytical and numerical methods mentioned above in order not only to simplify them, but also to solve them.

2.1 Mathematical Neuron Models

The functional complexity of the neuron, and more importantly, the great complexity of a neural network, require the use of new tools beyond simple physiological considerations to better understand the ability of neurons to mutually exchange information. One of the best tools in this regard is the development of mathematical models to accurately simulate the dynamics of nerve impulses as well as the various biological phenomena that it may undergo during its propagation. The models in this category describe the relationship between neuronal membrane currents at the input stage, and membrane voltage at the output stage. The most extensive experimental inquiry in this category of models was made by Hodgkin-Huxley in the early 1950's using an experimental setup that punctured the cell membrane and allowed to force a specific membrane voltage/current.

2.1.1 Hodgkin-Huxley Model

Alan Hodgkin and Andrew Huxley formed one of the most productive and influential collaborations in the history of physiology. Their work, both in the Physiological Laboratory of the Marine Biological Association in Plymouth, provided fundamental insights into nerve cell excitability, won them a share of the 1963 Nobel Prize in Physiology or Medicine as well as laying the foundations for others Nobel Prize-winning work including that of Erwin Neher and Bert Sakmann for their discoveries concerning the function of single ion channels in cells.

The HH model [69] is one of the most important models in computational neuroscience built on the basis of logical physiological assumptions. In biophysically based neural modeling, the electrical properties of a neuron are represented in terms of an electrical equivalent circuit. Capacitors are used to model the charge storage capacity of the cell membrane, resistors are used to model the various types of ion channels embedded in membrane, and batteries are used to represent the electrochemical potentials established by differing intra-and extracellular ion concentrations. In Fig.2.1, we have drawn the HH

electrical equivalent circuit. Based on the simple application of Kirchhoff's laws, Hodgkin and Huxley derived a model of four first-order ordinary differential equations described by:

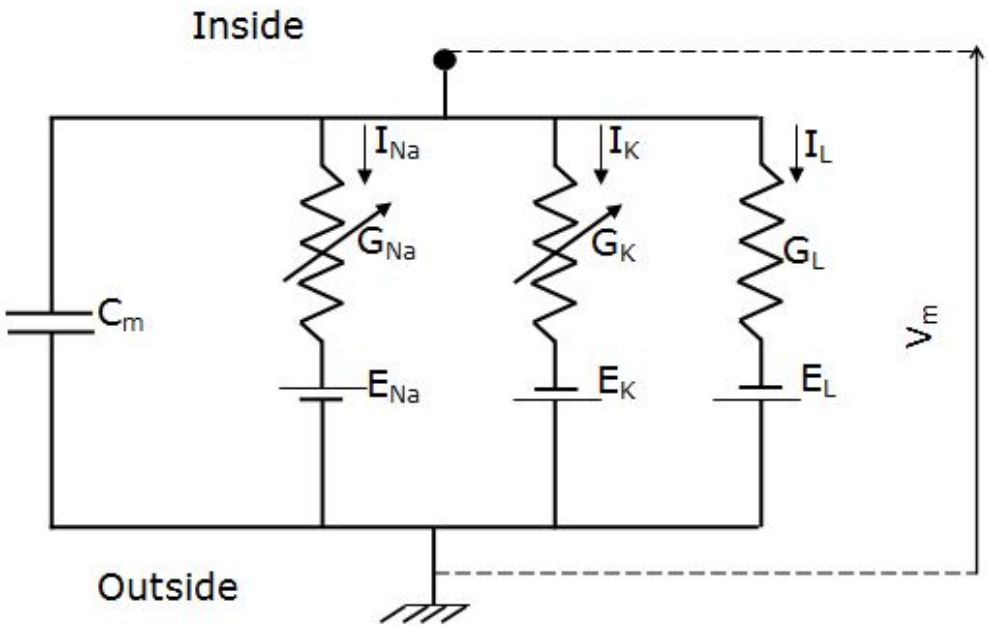

Figure 2.1: Electrical equivalent circuit for a short segment of squid giant axon according to [69]. The capacitor represents the capacitance of the cell membrane; the two variable resistors represent voltage-dependent Na^+ and K^+ conductances, the fixed resistor represents a voltage-independent leakage conductance and the three batteries represent reversal potentials for the corresponding conductances.

$$C_m\dot{V}_m = \bar{G}_K n^4(E_K - V_m) + \bar{G}_{Na} m^3 h(E_{Na} - V_m) + \bar{G}_L(E_L - V_m) + I_{ext}, \tag{2.1a}$$

$$\dot{n} = \alpha_n(V_m)(1-n) - \beta_n(V_m)n, \tag{2.1b}$$

$$\dot{m} = \alpha_m(V_m)(1-n) - \beta_m(V_m)m, \tag{2.1c}$$

$$\dot{h} = \alpha_h(V_m)(1-h) - \beta_h(V_m)h, \tag{2.1d}$$

where (.) denotes the derivative with respect to time. I_{ext} is the current per unit area, and α_i and β_i are rate constants for the $i-th$ ion channel, which depend on voltage but

Parameter	**Unit**	**Value**
C_m	$\mu F.cm^{-2}$	1.0
E_K	mV	$+12$
E_{Na}	mV	-115
E_L	mV	-10.63
$\bar{G}_K$	$mS.cm^{-2}$	36
$\bar{G}_{Na}$	$mS.cm^{-2}$	120
$\bar{G}_L$	$mS.cm^{-2}$	0.3

Table 2.1: HH model parameters [69].

not time. $\bar{G}_n$ is the maximal value of the conductance. n, m, and h are dimensionless quantities between 0 and 1 that are associated with potassium channel activation, sodium channel activation, and sodium channel inactivation, respectively. C_m is the membrane capacitance per unit area, V_m denotes the membrane potential; E_K, E_{Na} and E_L are the potassium, sodium and leak reversal potentials, respectively. The time-dependent functions α_i and β_i are given by:

$$\alpha_n(V_m) = \frac{0.01(10 - V_m)}{\exp\left(\frac{10-V_m}{10}\right) - 1}, \quad \alpha_m(V_m) = \frac{0.1(25 - V_m)}{\exp\left(\frac{25-V_m}{10}\right) - 1}, \quad \alpha_h(V_m) = 0.07 \exp\left(-\frac{V_m}{20}\right),$$

$$\beta_n(V_m) = 0.125 \exp\left(-\frac{V_m}{80}\right), \quad \beta_m(V_m) = 4 \exp\left(-\frac{V_m}{18}\right), \quad \beta_h(V_m) = \frac{1}{\exp\left(\frac{30-V_m}{10}\right) + 1}.$$

The numerical values for the parameters of the HH model are given in the table 2.1. The HH model is known to exhibit only two main features namely tonic and chaotic spiking under the original values of parameters regime. But if the parameters are tuned, the HH model could exhibit other interesting neuro-computational properties including tonic, phasic and chaotic bursting, mixed mode, spike frequency adaptation, spike latency, sub-threshold oscillations, rebound spike or burst just to cite a few [70]. As we have already pointed out above, the HH model is one of the few neural models with a biological meaningful. Such models are important not only because their parameters are biophysically meaningful and measurable, but also because they allow to investigate questions related to synaptic integration, dendritic cable filtering, effects of dendritic morphology, the interplay between ionic currents, and other issues related to single cell dynamics. But one

of its disadvantages is that it has too many time-dependent parameters. Also the number of ordinary differential equations to integrate (in total four) makes its implementation very difficult. That is why Izhikevich [70] said that one can use the HH formalism only to simulate a small number of neurons or when simulation time is not an issue.

2.1.2 Integrate and Fire Model

The integrate and fire model is one of the most widely used models in computational neuroscience that describe the behavior of individual neurons. It assumes that the neuron's membrane potential integrates incoming synaptic currents and fires an action potental when a certain threshold is reached [71]. It is only governed by one ordinary differential equation which describes the dynamics of membrane potential:

$$\dot{v} = a - bv + I, \quad if \quad v \geq v_{th}, \quad v \leftarrow c, \tag{2.2}$$

where v is the membrane potential, I is the input current, and a, b, c and v_{th} are the parameters. It is found that, when the membrane potential reaches the threshold value v_{th}, the neuron is said to fire a spike, and v is reset to c. The IF neuron is Class-1 excitable, i.e., the frequency of tonic spiking of neocortical regular spiking excitatory neurons depends on the strength of the input, and it may span the range from $2Hz$ to $200Hz$, or even greater; it can fire tonic spikes with constant frequency, and it is an integrator (IF neurons prefer high-frequency input; the higher the frequency the more likely they fire). Because of the lack of nonlinear terms in this model, it would be useless to explore it analytically.

2.1.3 FitzHugh-Nagumo Model

The FHN neuron model [72, 73] is a mathematical model that describes the behavior of a neuron. It was developed by Richard Fitzhugh and J. Nagumo in the 1960s as an extension of the HH model. To derive it, FitzHugh and Nagumo have used phase space methods (nonlinear mechanics). Obviously, their approach is, however, not so informative in explaining how trains of impulses occur in the HH equations, where interactions between all four HH variables are essential. This model is described by two ODEs given by:

$$\dot{v} = v(v - a)(1 - v) - w + I, \tag{2.3a}$$

$$\dot{w} = \epsilon(v - \gamma w), \tag{2.3b}$$

where v represents the membrane potential, w is the slow ion current through the membrane and I stands for the input current. Model parameters are such that, $0 < a < 1$, $0 < \epsilon << 1$, $\gamma > 0$ and $1/\gamma - (1 - a + a^2)/3 > 0$, $(1 - a + a^2)/3 - \epsilon\gamma > 0$.

The first equation describes how the membrane potential changes over time while the second described how the recovery variable changes over time

The FHN model is a generalization of the Van Der Pool (VDP) oscillator, whose modified version has been recently proposed with the assumption that the neural environment implies some periodic excitations. The importance giving to the VDP model equation in recent years come from the fact that it describes self-excited or self-sustained oscillations, suitable to described some important processes like those related to brain and cardiac wave [74]. This has been confirmed many years ago by some experimental data published by [75]. The model is often used to study various phenomena in neuroscience, such as action potential generation, neuronal excitability and synchronization of neural activity.

2.1.4 Hindmarsh-Rose Model

One of the most ubiquitous models explored by neuroscientists, the HR model [76] developed by John G. Hindmarch and Rosemary M. Rose in 1984 as an extension of the FitzHugh-Nagumo model. can be described by three ODEs written as:

$$\dot{u} = v - au^3 + bu^2 - w + I, \tag{2.4a}$$

$$\dot{v} = c - du^2 - ev, \tag{2.4b}$$

$$\dot{w} = r[s(u - u_e) - w], \tag{2.4c}$$

where dimensionless variables u, v and w are membrane potential, fast and slow current, respectively. I represents the excitation current, while parameters (a,b,c,d,e,r,s>0). u_e refers to the resting membrane potential which is generally negative and r is the ratio of fast/slow time scales. The original parameters values of this model are $a = 1.0$, $b = 3.0$, $c = 1.0$, $d = 5.0$, $e = 1.0$, $r = 0.006$, $s = 4.0$ and $u_e = -1.60$. In recall, HR model includes fast-variables known as u and v, then the slow variable indicated by w. Since v-variable is known to generate spike activity and w-variable to produce bursting-like activity, HR system exhibits a multi-time-scale spike-burst activity with more suitable values of input current I. The interplay between spiking and bursting regimes within this model allows it to reproduces a rich variety of membrane potential features of thalamic neurons classifying

from regular spiking/bursting, chaotic spiking/bursting or post-inhibitory rebound just to cite a few. Some of such features are graphed in Fig.3.9.

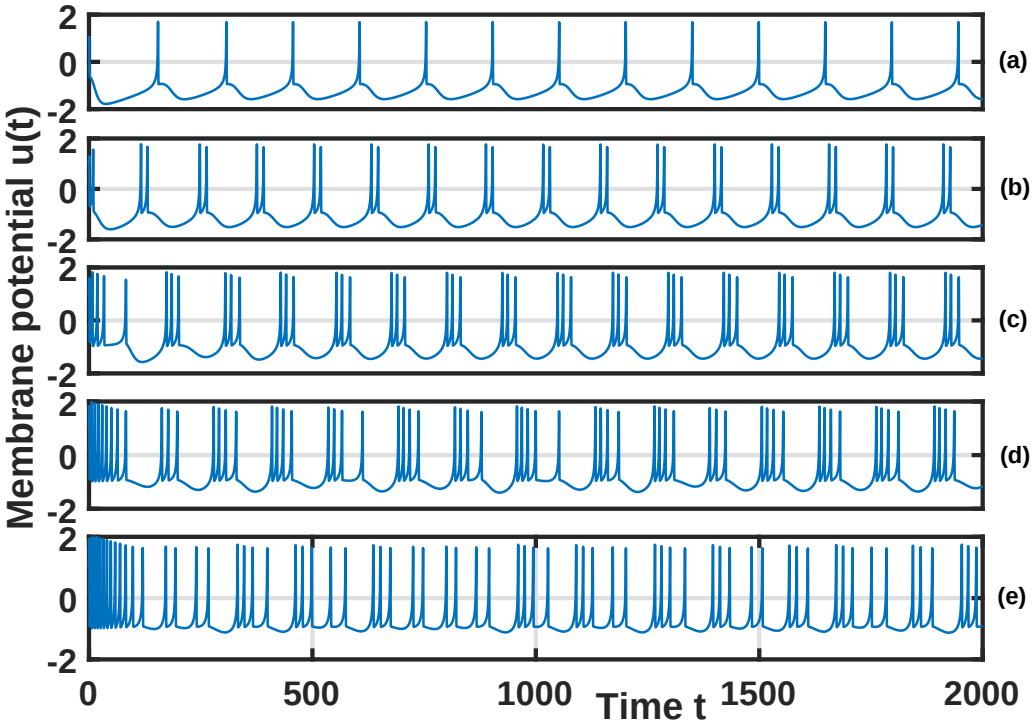

Figure 2.2: Time series of membrane potential $u(t)$ of HR model of thalamic neuron for different values of input current I as (a): $I = 1.5$, (b): $I = 2.0$, (c): $I = 2.5$, (d): $I = 3.0$, (e): $I = 3.3$.

We observe the emergence of spiking activity in panel (a) for $I = 1.5$, regular bursting activity with two spikes per burst in panel (b) for $I = 2.0$, regular bursting activity with three spikes per burst in panel (c) for $I = 2.5$ and irregular bursting activities in panels (c) and (d) for $I = 3.0$ and $I = 3.3$, respectively. The latter are known to fire chaotically. In recall, neuron electrical activity is characterized by a multi-time-scale phenomena accordingly with different values of the external current-like a stimulus: for $1.32 \leq I < 1.57$, spiking activity also known as fasting firing; for $1.57 \leq I < 2.92$, bursting activity also known as slowing firing and chaotic activity when $2.92 \leq I \leq 3.40$; for $I > 3.40$ neuron electrical activity disintegrates into spiking one, but with very high emission frequencies [13].

2.1.5 Izhikevich Model

Izhikevich's formalism [4] is based on a model that reproduces the behavior of biological neurons. This model, described by a set of two first-order ordinary differential equations, is given by:

$$\dot{v} = 0.04v^2 + 5v + 140 - u + I, \tag{2.5a}$$

$$\dot{u} = a(bv - u), \tag{2.5b}$$

with the auxiliary after-spike resetting

$$if \;\; v \geq +30mV, \;\; then \;\; \begin{cases} v \leftarrow c \\ u \leftarrow u + d. \end{cases} \tag{2.6}$$

Here variable v represents the membrane potential of the neuron and u represents a membrane recovery variable, which accounts for the activation of K^+ ionic currents and inactivation of Na^+ ionic currents, and it provides negative feedback to v. The model can exhibit firing patterns of all known types of cortical neurons with the choice of parameters a, b, c and d given in Ref. [4].

2.1.6 Morris-Lecar Model

R. Morris and H. Lecar developed in 1981 a mathematical model [3] which consist of a simple 2-D model that describe oscillations in barnacle giant muscle fiber. It consists of a membrane potential equation with instantaneous activation of Ca current and an additional equation describing slower activation of current. The model reads:

$$C\dot{V} = g_L(V_L - V) + g_K n(V_K - V) + g_{Ca} m_\infty(V)(V_{Ca} - V) + I, \tag{2.7a}$$

$$\dot{n} = \lambda(V)(n_\infty(V) - n), \tag{2.7b}$$

where

$$\begin{aligned} m_\infty(V) &= \frac{1}{2}\left\{1 + \tanh\left[\frac{(V - V_1)}{V_2}\right]\right\}, \\ n_\infty(V) &= \frac{1}{2}\left\{1 + \tanh\left[\frac{(V - V_3)}{V_4}\right]\right\}, \\ \lambda(V) &= \bar{\lambda}\cosh\left[\frac{(V - V_3)}{2V_4}\right], \end{aligned} \tag{2.8}$$

with parameters: $C = 20\mu F.cm^{-2}$, $g_L = 2mS.cm^{-2}$, $V_L = -50mV$, $g_{Ca} = 4mS.cm^{-2}$, $V_{Ca} = 100mV$, $g_K = 8mS.cm^{-2}$, $V_K = -70mV$, $V_1 = 0$, $V_2 = 15mV$, $V_3 = 10mV$, $V_4 = 10mV$, $\bar{\lambda} = 0.1s^{-1}$, and applied current $I(\mu A.cm^{-2})$.

The model can exhibit various types of spiking, but could support tonic bursting only when an additional equation is added, e.g., slow inactivation of Ca current. In this case, the ML model becomes equivalent to the HH model since both have transient inward and persistent outward currents.

The Morris-Lecar model makes it computationally efficient compared to more complex models like Hodgkin-Huxley. However, it also means that certain aspects of neuronal behavior may not be accurately captured by this model. Nonetheless, it remains a valuable tool for understanding basics principles of neuronal excitability.

2.1.7 Similitude and Difference between the Various Models

Without being exhaustive, we have reviewed the most prominent neural models above. They are all mathematical representations of the behavior of neurons. While they share the common goal of simulating neuronal activity, they differ in their level of complexity and the specific aspects of neuronal behavior they focus on.

Some of them have biophysically meaningful and measurable parameters (HH and ML models). The others although not having biophysically meaningful, exhibit the most fundamental properties of thalamocortical spiking neurons, for this purpose we can mention FHN, HR, Izhikevich models. The FHN which is on of the model that caught our attention is often used for bifurcation analysis to study how changes in parameters can lead to different dynamical behaviors such as steady states or oscillations. All other aspects of comparison between these models are contained in the table 2.2. Accordingly, HH, HR and Izhikevich models appear to be the three most powerful neuro-models that accurately reproduce a rich electrical activity of real neurons followed by ML and FHN ones. The IF model, although very simple to handle, do not always exhibit the properties of cortical spiking neurons.

Models	biophysically meaningful	tonic spiking	phasic spiking	tonic bursting	phasic bursting	mixed mode	spike frequency adaptation	class 1 excitable	class 2 excitable	spike latency	subthreshold oscillations	resonator	integrator	rebound spike	rebound burst	threshold variability	bistability	DAP	accommodation	inhibition-induced spiking	inhibition-induced bursting	chaos	# of FLOPS
integrate-and-fire	-	+	-	-	-	-	-	+	-	-	-	-	+	-	-	-	-	-	-	-	-	-	5
integrate-and-fire with adapt.	-	+	-	-	-	-	+	+	-	-	-	-	+	-	-	-	-	+	-	-	-	-	10
integrate-and-fire-or-burst	-	+	+		+	-	+	+	-	-	-	-	+	+	+	-	+	+	-	-	-		13
resonate-and-fire	-	+	+	-	-	-	-	+	+	-	+	+	+	+	-	-	+	+	+	-	-	+	10
quadratic integrate-and-fire	-	+	-	-	-	-	-	+	-	+	-	-	+	-	-	+	+	-	-	-	-	-	7
Izhikevich (2003)	-	+	+	+	+	+	+	+	+	+	+	+	+	+	+	+	+	+	+	+	+	+	13
FitzHugh-Nagumo	-	+	+	-		-	-	+	-	+	+	+	-	+	-	+	+	-	+	+	-	-	72
Hindmarsh-Rose	-	+	+	+			+	+	+	+	+	+	+	+	+	+	+	+	+	+		+	120
Morris-Lecar	+	+	+	-		-	-	+	+	+	+	+	+	+		+	+	-	+	+	-	-	600
Wilson	-	+	+	+			+	+	+	+	+	+	+	+	+	+		+	+				180
Hodgkin-Huxley	+	+	+	+			+	+	+	+	+	+	+	+	+	+	+	+	+	+		+	1200

Table 2.2: Comparison of the neuro-computational properties of spiking and bursting models [77]; of FLOPS is an approximate number of floating point operations (addition, multiplication, etc.) needed to simulate the model during a $1ms$ time span. Each empty square indicates the property that the model should exhibit in principle (in theory) if the parameters are chosen appropriately, but the author failed to find the parameters within a reasonable period of time.

2.2 The improved models under the effect of electromagnetic radiation and light illumination

2.2.1 Concept of electromagnetic induction in neuron

Electromagnetic induction refers to the process by which an electric current is induced in a conductor when it exposed to a changing magnetic field. This phenomenon has been extensively studied in physic and has various applications in technology.

Neurons are fundamentally electrochemical cells. Their electrical activity is driven by the movement of charged ions (sodium Na^+, potassium $-K^+$, chloride $-Cl^+$ and calcium $-Ca^{2+}$ accross their cell membrane. The flow of ions during an action potential not only generates currents but also creates local electric fields around the neuron. These electric fields are essentials for the neuron's own internal dynamics. According to basic physics, any electric current generates a magnetic field around it. The magnetic fields produce by individual neurons are weak, but when many neurons are activated at the same time, it may sum up or interfere with each other, resulting in a collective magnetic field that can be detected outside of the brain or nervous tissue.

According to the Faraday's law of induction, the fluctuation or changes in action potentials in neurons can generate magnet field in the media, thus the electrical activities of neurons will be adjusted under feedback effect. That is to say, the fluctuation of membrane potentials of neurons can change the distribution of electromagnetic field inner and external of neurons; thus, the magnetic flux across membrane and electromagnetic effect should be considered.

The interaction of the electrical and magnetic fields around neurons leads to:

Modulation of neuronal activity: Electromagnetic fields, whether generated internally or apply externally can modulate neuronal activity. These fields can interact with ion channels affecting their gating and, thus, the flow of ions and the generation of action potentials.

Neural oscillations: The rhythmic activity of large populations of neurons results in the generation of brain oscillations, which are synchronized fluctuations in the electrical activity of neurons. These oscillations are reflected in both electrical and magnetic signals, suggesting a strong coupling of electric and magnetic phenomena in brain.

Electromagnetic coupling: The interaction of the electrical and magnetic fields around neurons leads to electromagnetic coupling.

More often, it is claimed that neuronal system can be in good memory to keep normal activities and the memory effect is often described by using time delay term in the model. Indeed, magnetic field or magnet flux storage could be associated with the memory effect. In fact, the neuronal system can be used as a reliable signal processor because slight stimuli on the neuron can be give sensitive response by analyzing the sampled time series.

When it comes to neural networks, electromagnetic induction can have both positive and negative effects. The electromagnetic waves when used properly, contribute to our

well-being through different solutions they provide. Scanners and X-rays in medecine, microwaves and freezers for cooking food and conservation, Wi-Fi, mobile phones,radio for telecommunication. However, improper use of these waves are reported to be responsible of neurological disorders. Research by scientists shows that prolonged presence of these waves can cause some diseases such as depression, chronic fatigue, cell destruction, tumors, cancer, infertility and certain neurodegenerative diseases.

Nowaday electromagnetic induction and radiation are considered in model setting for neurons. However, the presented neuron models seldom consider the effect of electromagnetic induction on membrane potential of neurons. In this case, it is important to set more reliable neuron model so that the effect of electromagnetic induction in neurons could be considered. Lv and Ma [78] recently proposed to describe the memory effect of neuron using magnetic flux. They applied it to the FitzHugh-Nagumo and many other models, where different oscillations modes of electrical activities were reproduced, as well as their response to magnetic flux effects [78]. In the same vein, it was also proposed that the effect of the electromagnetic induction may be studied by introducing a memristor in the neural circuit [79]. Usually, a memristor is introduced in order to achieve the coupling between the membrane potential and the magnetic flux induction, and model the intrinsic origin of electromagnetic induction as the result of the fluctuation of ion concentration [79, 80]. There is a growing interest in understanding the way electromagnetic field interact with the human body, especially their effect on some fundamental brain functions.

2.2.2 The improved Integrate and Fire (IF) neuronal model under the high-low frequency magnetic radiation

The integrate-and-fire neuron model is one of the most widely used models for analyzing the behavior of neural systems. It describes the membrane potential of a neuron in terms of the synaptic inputs and the injected current that it receives. An action potential (spike) is generated when the membrane potential reaches a threshold, but the actual changes associated with the membrane voltage and conductances driving the action potential do not form part of the model.

The integrate-and-fire neuron model has become established as a canonical model for the description of spiking neurons because it is capable of being analyzed mathematically while at the same time being sufficiently complex to capture many of the essential features of neural processing. A number of variations of the model are discussed, together

with the relationship with the Hodgkin-Huxley neuron model and the comparison with electrophysiological data. In the traditional IF model, a neuron's membrane potential is modeled as an electrical circuit with capacitance representing the neuron's membrane, and a resistance representing ions channels. When the membrane potential reaches a certain threshold, the neuron fires an action potential.

Electromagnetic induction resulting from fluctuation in intracellular ion concentration during action potential initiation and propagation in excitable media has been recently included in various neurons and neuronal network [78, 81, 82]. Lv et al. [78], investigated mode transition in the HR neuronal model under magnetic flow. Wang et al. [81], reported energy dependence on action potential of FHN neuron model under electromagnetic induction. Mi et al. [82], investigated dynamical behaviors such as synchronization and wave propagation of coupled neurons under field coupling. Takembo et al. [67], reported turbulent electrical activities of coupled FHN neurons under electromagnetic induction and high frequency electromagnetic radiations using the theory of modulational instability.

In our improved model, electromagnetic induction is considered as an additional factor influencing the neuron's membrane potential. Electromagnetic induction occurs when there is a change in magnetic field strength or direction near a conductor, which can induce an electric current in the conductor.

To incorporate the magnetic field effects into the traditional integrate and fire model, the equation that describes the membrane potential dynamics is modify by introducing a memristor in the circuit.

Memristors are passive electric circuit components, such as inductors, capacitors and resistors, their existence was theorized in 1971 by Leon Chua [68]. From a practical point of view, the memristor can be understood as a variable resistor whose resistance depends, in a nonlinear way, on the amount of current that has previously flowed through it. Additionally, it is a non-volatile device, meaning it retains its state even when disconnected from the current. These properties explain the name that Chua gave them: memristor, combining memory and resistor.

This memory of its history is contained in its physical configuration, so it needs to be both:

1. Physically reconfigurable when subjected to a certain voltage level. This reconfiguration must be reversible, going in both directions, from higher to lower resistivity when

the voltage is positive and vice versa when it is negative.

2. Stable, not changing its state once the current flow through it stops.

In neural network, they can be used as artificial synapses, mimicking the learning and adaptation capabilities of biological neurons. In a simple circuit with a memristor connected in series with a resistor and a voltage source, as current flows through, it's resistance changes, affecting the overall current in the circuit.

We assume that the memristor is flux-controlled and characterized by a smooth continuous cubic monotone-increasing nonlinearity as

$q(\phi) = \alpha\phi + \beta\phi^3$

Where α , $\beta > 0$, the memductance $\varphi(\phi)$ is obtained as $\varphi(\phi) = \frac{dq(\phi)}{d\phi} = \alpha + 3\beta\phi^2$.

According to the Faraday law of electromagnetic induction and description about memristor, the term $k_1\varphi(\phi)x$ could be regarded as additive induction current on the membrane as follow.

$$i' = \frac{dq(\phi)}{dt} = \frac{dq(\phi)}{d\phi}\frac{d\phi}{dt} = \varphi(\phi)V = k_1\varphi(\phi)x \tag{2.9}$$

The improved IF neuronal model driven by a simulation current I is given by

$$\begin{aligned} \frac{dx}{dt} &= a - bx - k_1\varphi(\phi)x + I, \\ \frac{d\phi}{dt} &= kx - k_2\phi, \end{aligned} \tag{2.10}$$

Where x and ϕ describe the membrane potential and magnetic flux variable, respectively. The term $k_1\varphi(\phi)x$ describes the suppression modulation on membrane potential, and it is dependent on the variation in magnetic flux by generating additive faradic current. k_1 is the memristor coupling that bridges the membrane potential and the magnetic flux and hence the effect of electromagnetic induction is realized. $\varphi(\phi) = \alpha + 3\beta\phi^2$ represents memory conductance of flux-controlled memristor, in which, α represents constant conductance, β indicates the feedback rate of magnetic flux, and both depend on the memristor. k_2 and k are induction coefficients dependent on the media.

When synaptic connections are considered, neuronal network are designed, suitable for investigating the collective behaviors of neurons via pattern formation and synchronization. Based on the new IF model with electromagnetic induction, synaptic gap junction coupling with nearest neighbors interaction is proposed to enhance information exchange in the network. The dynamical equations for chain diffusive neuronal network under high-low frequency electromagnetic radiation ϕ_{ext} is given by

$$\begin{aligned}\frac{dx_n}{dt} &= a - bx_n - k_1(\alpha + 3\beta\phi_n^2)x_n + I + D(x_{n+1} - 2x_n + x_{n-1}) \\ \frac{d\phi_n}{dt} &= kx_n - k_2\phi_n + \phi_{ext}.\end{aligned} \tag{2.11}$$

Where $\phi_{ext} = A\cos(2\pi ft) + B\cos(2\pi Nft)$, f and Nf are the frequencies of the magnetic radiation. A, B are amplitudes and N as the frequency factor describing the disparity in the two frequencies. The term $D(x_{n+1} - 2x_n + x_{n-1})$ represents the synaptic gap junction coupling term in the chain neural network, n=1,....,J. J is the number of neurons and D is the strength of the gap junction. The system of equation above will be used later to determine the conditions under which modulated plane wave solutions in the array becomes unstable.

2.2.3 The improved FHN neuron model under the effect of the internal and external magnetic field and light illumination

Phototube and memristor incorporated into the branches of a nonlinear circuit could yield an output voltage controlled by light illumination and electromagnetic induction, respectively. In this way, the biological neuron is thought of as an intelligent and smart processor such that functional nonlinear circuit could be built to perform similar functions. The memristive neuron has been presented in Ref. [83, 84] while the photosensitive neuron presented in Ref. [85]. The memristive photosensitive neuron was also presented by Njitacke et al. in 2023 [85] the FHN circuit obtained from the modification of the previous model investigated in Ref. [96] by adding a memristive device as a fifth branch of the neuronal circuit to mimic the effect of the magnetic field on the dynamics of the proposed neuron circuit. The circuit represented in Fig 2:1 is, an improved FHN neuron circuit under the effect of the internal/external magnetic field and light is built. The first branch of the circuit is made up of a phototube and a resistor used to generate an excitation current whose value varies according to the intensity of light and the material property of the cathode. The second branch is made up of a capacitor which enables to generate the output voltage of the membrane potential. The third branch was realized using an inductor, a resistor, and a DC source to generate a time-varying current. The fourth branch is built using a nonlinear resistor to perform the nonlinear relation between the voltage and current. The current from that nonlinear resistor can be given as

$iN = -\frac{1}{\rho}(v - \frac{v^3}{3v_0^2})$ [96]. Finally, the fifth branch is realized by a memristor, used to simulate the effect of the internal and the additional external magnetic fields on the dynamics of the considered neuron model. For the considered model, the value of the induction current from the memristive device is given in Eq. (2:3)

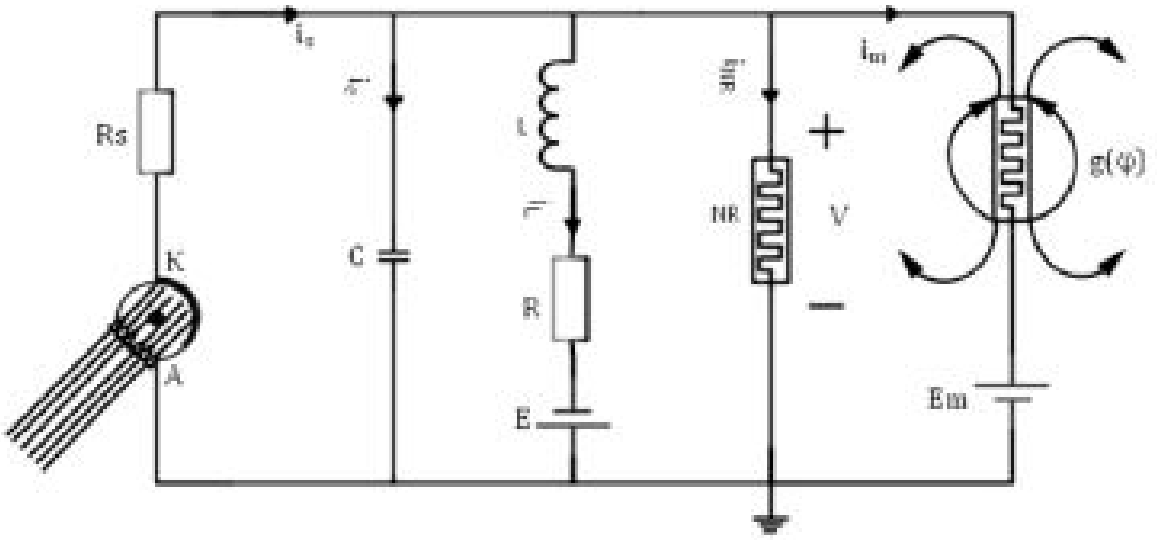

Figure 2.3: circuit of the improved FHN neuron under the internal and external magnetic field effects and light exposure [85]

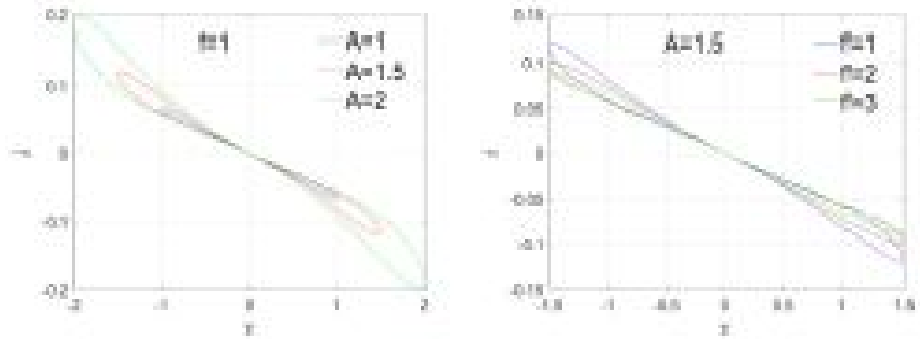

Figure 2.4: Fingerprint of the memristive current when varying both the amplitude and the frequency of model [85]

Inspired by the photoelectric effect, a phototube is incorporated into a simple neural circuit, and then the output voltage and dynamics become sensitive to external illumination within a specific frequency band. The firing modes are also dependent on the amplitude and frequency band in the illumination. In this paper, the signal outputs from

a chaotic circuit are used as external optical signals, which are filtered and encoded by a phototube. Then, the functional neural circuit is excited to present a variety of firing modes and patterns. An exponential function of the filtering wave is proposed to discover the biophysical mechanism for frequency selection in the retina as most of wave bands of the external illumination are absorbed in the cathode material of the phototube while a specific band is effective in inducing a photocurrent for stimulating the visual neurons. Based on our light-sensitive neural circuit and model, external illumination is filtered and firing modes in the neuron are reproduced; furthermore, the mode transition induced by parameter shift is also investigated in detail. This result discovers the signal processing mechanism in the visual neurons and provides helpful guidance for designing artificial sensors for encoding optical signals and for repairing abnormalities in the retina of the visual system.

$$\begin{cases} i_m = g(\phi)(v - E_m) = k_0'(-\alpha' - 3\beta'\phi^2)(v - E_m) \\ \dfrac{d\phi}{dt} = k_1' v - k_2'\phi \end{cases} \tag{2.12}$$

Where E_m stands for a reversal potential [87]. $g(\phi) = k_0'(-\alpha' - 3\beta'\phi^2)$ is the memductance of the flux control memristor. k_0' represent the gain of the induction current, while k_1' and k_2' are respectively the coefficients of the contribution of the magnetic flux in the intercellular media and extracellular media. Using the discrete values α'=0.01, β'=0.3, k_0'=5.7, k_1'=0.1, k_2'=1.8 while varying A and f for $v = A\sin(ft)$ with E_m=0.

When applying the well-known $Kirchhoff's$ electrical circuit law to Fig. 1, Eq. (2) describing the dynamics of the considered neuron circuit is obtained.

$$\begin{cases} C\dfrac{dv}{dt} = \dfrac{v_s - v}{R_s} - i_L - i_N - i_m \\ L\dfrac{di_L}{dt} = v + E - Ri_L \end{cases} \tag{2.13}$$

Replacing i_N and i_m by their previous values,

$$\begin{cases} C\dfrac{dv}{dt} = \dfrac{v_s - v}{R_s} - i_L + \dfrac{1}{\rho}(v - \dfrac{v^3}{3v_0^2}) - k_0'(-\alpha' - 3\beta'\phi^2)(v - E_m) \\ L\dfrac{di_L}{dt} = v + E - Ri_L \\ \dfrac{d\phi}{dt} = k_1' v - k_2'\phi + e_e xt \end{cases} \tag{2.14}$$

Performing the following change of variables and parameters, we obtain:

$x = \frac{v}{v_0}$, $y = \frac{\rho i_L}{v_0}$, $t = \frac{1}{\rho C}$, $\rho = \frac{\phi}{v_0 \rho C}$. $\varepsilon = \frac{\rho}{R_s}$, $\alpha = \rho\alpha'$, $\beta = v_0^2\rho^3C^2\beta'$, $e_m = \frac{E_m}{v_0}$, $c = \frac{\rho^2 C}{L}$, $a = \frac{E}{v_0}$, $b = \frac{R}{\rho}$, $k = k_0'$, $k_2 = k_2'\rho C$, $\frac{\rho v_s}{v_0 R_s} = \frac{\rho v_{SN}}{v_0 R_s}\sin(w_1\rho C t + I_\alpha)$, $e_{ext} = \frac{E_{ext}}{v_0} sin(W_2\rho C t)$, $a_1 = \frac{\rho v_{SM}}{v_0 R_s}$ $w_1 = W_1\rho C$ $a_2 = \frac{E_{ex}}{v_0}$, $w_2 = W_2\rho C$

$$\begin{cases} \dot{x} = x(1-\epsilon) - \frac{1}{3}x^3 - y + a_1\sin(w_1 t + l_\alpha) - k_0(-\alpha - 3\beta\varphi^2)(x - e_f) \\ \dot{y} = c(x + a - by) \\ \dot{\varphi} = k_1 x - k_2\varphi + e_{ext} \end{cases} \tag{2.15}$$

Based on the variable change, the following dimensionless values are provided for parameters of our considered neuron model a=0.7, b=0.8, c=0.1, $\epsilon = 0.25$, $a_1 = 0.6$, $a_2 = 4$, $l_\alpha = 0.1$ $\alpha = 0.01$ $\beta = 0.3$, $k_1 = 0.01$, $k_2 = 1.8$, $w_1 = 0.5$, $w_2 = 10$, $k_1 = 5.7$, $e_m = 0.99$

The term $a_1\sin(w_1 t + l_\alpha)$ is a varying external forcing that maps the photocurrent from the phototube due to light illumination.

-$k_0(-\alpha - 3\beta\varphi^2)(x - e_f)$ is the negative feedback memristive current originating from electromagnetic induction due to the internal effect to bioelectricity from ions exchange across the cell membrane as well as exposure to external magnetic flux. k_0 is the memristive coupling strength that couples the membrane potential (x) and the magnetic flux variable(φ)

The term $e_{ext} = a_2\sin(\omega t)$ is the external magnetic flux forcing originating from electromagnetic radiation exposure [88]. $k_2\varphi$ measures the magnetic flux leakage.

The photosensitive memristive neurons are considered to be couple locally in a chain with nearest neighbor interaction. The network can be written as.

$$\begin{cases} \dot{x}_i = x_i(1-\epsilon) - \frac{1}{3}x_i^3 - y_i + a_1\sin(w_1 t + l_\alpha) - k_0(-\alpha - 3\beta\varphi^2)(x_i - e_f) \\ +D(x_{n+1} - 2x_n + x_{n-1}) \\ \dot{y}_i = c(x_i + a - by_i) \\ \dot{\varphi}_i = k_1 x_i - k_2\varphi + e_{ext} \end{cases} \tag{2.16}$$

where $i = 1.....N$, N and D are the positions of node in the lattice and synaptic coupling, respectively. ϵ =0.25, D = 0.05, a = 0.6.

2.3 Analytical and Numerical methods

2.3.1 Multiple scale expansion in the discrete approximation

The multiple scale in a discrete asymptotic expansion has been successfully applied to various physics problem such as fluid dynamics, plasma physics and nonlinear optics. It provides powerful tool for understanding complex systems and predicting their behavior under different conditions. Develop by J. Leon and M. Manna [89], the multiple-scale allow to deduce simplified equations from a basic model without loosing its characteristic features. The method consist of analyzing a system or phenomenon at different levels or scales. More specifically, the method generates a hierarchy of (small) scales for the space and time variations of the envelopes of a fundamental (linear) plane wave and all the overtones. Moreover, the scale is directly related to the (small) amplitude of the wave itself. The scaling of variables is performed via a Taylor expansion of the frequency $\omega(k)$ in power of a small deviation of the wave number k. This deviation from the linear dispersion relation is, of course, generate by a nonlinearity. The multiple scale method is quite appropriate for the study of boundary value problems and leads to a DNLS equation (with reversed space-time), the goal being the study of a nonlinear dispersive chain with dispersion relation $\Omega(Q)$ where Ω represents the wave frequency and Q the wavenumber of the carried wave. The physical problem we are concerned with is the following: the stimulation of the first neuron in the chain network (say $n = 0$) initiates an action potential (wave packet) having oscillation angular frequency ω and wave number k. Due to nonlinear effects within the network, Ω and k deviate by υ from the natural frequency Ω' and k'. This is summar (or is submitted to an external force) at frequency Ω. Would the chain be linear that this oscillation would propagate without distorsion as the plane wave $\exp[i(\Omega t + Qnd)]$, with d being the lattice spacing. But the nonlinearity induces some deviations from the value Ω, namely, the wave propagates with actual frequency ω and wave number q that are define as:

$$\omega = \Omega + \epsilon\lambda, \quad \text{and} \quad q = Q + \epsilon\frac{\lambda}{v_g} + \epsilon^2 c_g\lambda^2 + ... \tag{2.17}$$

where $v_g = \frac{\partial\Omega}{\partial Q}$ is the group velocity and $2c_g = \frac{\partial^2 Q}{\partial\Omega^2}$ represents the group velocity dispersion. λ is a small deviation from the natural frequency Ω.

The principle of this method can be summarized as follow: given a discrete differential

equation in the form

$$F(\ddot{u}_n, \dot{u}_n(t), u_n(t), u_{n+j}(t), u_{n-j}(t), u_n^2(t), u_n^3(t), ..., u_n^r(t)) = 0. \tag{2.18}$$

One first seeks a solution of Eq.(2.21) in the form of a Fourier expansion in harmonics of the fundamental $A(n,t) = \exp[i(\Omega t + Qnd)]$, where the Fourier components are developed in a Taylor series in power of the small parameter ϵ measuring the amplitude of the initial wave, that is to say

$$u_n(t) = \sum_{p=1}^{\infty} \epsilon^p \sum_{l=-p}^{p} \psi_p^{(l)}(m,\tau) A^{(l)}(n,t). \tag{2.19}$$

Note that the above serie includes all overtones $A(n,t) = \exp[i(\Omega t + Qnd)]$ up to order p. These are generated by the nonlinear terms which explain that the corresponding coefficients are of maximum order ϵ^p. Here we have the real valued condition

$$\psi_p^{(-l)}(m,\tau) = \left(\psi_p^{(l)}(m,\tau)\right)^*, \tag{2.20}$$

with the asterisk denoting complex conjugations. The slow variables $\xi_n = m$ and $\tau_n = \tau$ are introduced via

$$\tau = \epsilon(t + \frac{nd}{v_g}), \;\; m = \epsilon^2 n. \tag{2.21}$$

We then insert solution (2.22) into Eq.(2.21) to obtain a linear homogeneous system for $\psi_p^{(l)}(m,\tau)$ polynomial in $A^{(l)}(n,t)$. Finally we can proceed to collect and solve different orders of ϵ^p and harmonics l, order (p,l) in the obtained equation or system of equations. Note that it is enough to consider $l > 0$ as negative values follow from the reality condition (2.23). The culminating stage comes from order $(3,1)$ where the cubic DNLS equation is derived. In addition, the general formulas of this method are given as follows:

$$\begin{aligned} u_{n+j} - u_{n-j} = & \left[A^{(l)}(n+j,t) - A^{(l)}(n-j,t)\right]\psi_p^{(l)}(m,\tau) \\ & + \epsilon\left[A^{(l)}(n+j,t) + A^{(l)}(n-j,t)\right]\left(\frac{jd}{v_g}\right)\frac{\partial}{\partial\tau}\psi_p^{(l)}(m,\tau) \\ & + \frac{\epsilon^2}{2}\left[A^{(l)}(n+j,t) + A^{(l)}(n-j,t)\right]\left[\psi_p^{(l)}(m+j,\tau) - \psi_p^{(l)}(m-j,\tau)\right] \\ & + \frac{\epsilon^2}{2}\left[A^{(l)}(n+j,t) - A^{(l)}(n-j,t)\right]\left(\frac{jd}{v_g}\right)^2\frac{\partial^2}{\partial\tau^2}\psi_p^{(l)}(m,\tau) \end{aligned} \tag{2.22}$$

and

$$\begin{aligned} u_{n+j} - 2u_n + u_{n-j} = &\left[A^{(l)}(n+j,t) - 2A^{(l)}(n,t) + A^{(l)}(n-j,t)\right]\psi_p^{(l)}(m,\tau) \\ &+ \epsilon\left[A^{(l)}(n+j,t) - A^{(l)}(n-j,t)\right]\left(\frac{jd}{v_g}\right)\frac{\partial}{\partial\tau}\psi_p^{(l)}(m,\tau) \\ &+ \frac{\epsilon^2}{2}\left[A^{(l)}(n+j,t) + A^{(l)}(n-j,t)\right]\left(\frac{jd}{v_g}\right)^2\frac{\partial^2}{\partial\tau^2}\psi_p^{(l)}(m,\tau) \\ &+ \frac{\epsilon^2}{2}\left[A^{(l)}(n+j,t) - A^{(l)}(n-j,t)\right]\left[\psi_p^{(l)}(m+j,\tau) - \psi_p^{(l)}(m-j,\tau)\right] \end{aligned} \tag{2.23}$$

2.3.2 Runge-Kutta numerical integration method

The Runge-Kutta numerical integration methods are a family of implicit and explicit iterative techniques used to approximate the solution of ordinary differential equations (ODEs) [90] . These methods were developed around 1900 by the German mathematicians Carl Runge and Martin Kutta.

The basic idea behind Runge-Kutta methods is to break down the ODE into a series of smaller steps and approximate the solution at each step. The specific coefficients and derivative terms depends on the order of the Runge-Kutta method being used. The most commonly used order is 4, known as the fourth-order Runge Kutta methods(RK4). This methods uses four intermediate steps to estimate the solution at each time steps. The main steps can be express as follows:

$$\dot{y} = f(t,y), \quad y(t_0) = y(0), \tag{2.24}$$

where y is an unknown function (scalar or vector) of time t, which we would like to approximate; we are told that $\dot{y}$, the rate at which y changes, is a function of t and of y itself. At the initial time t_0 the corresponding y-value is y_0. The function f and the data t_0, y_0 are given. Therefore the formulas of RK4 method are given by:

$$\begin{aligned} y(n+1) &= y(n) + \frac{1}{6}(k_1 + 2k_2 + 2k_3 + k_4) \\ t(n+1) &= t(n) + h \end{aligned} \tag{2.25}$$

for $n = 0, 1, 2, 3, ...$, using

$$\begin{aligned} k_1 &= hf\bigg(t(n), y(n)\bigg) \\ k_2 &= hf\bigg(t(n) + \frac{h}{2}, y(n) + \frac{k_1}{2}\bigg) \\ k_3 &= hf\bigg(t(n) + \frac{h}{2}, y(n) + \frac{k_2}{2}\bigg) \\ k_4 &= hf\bigg(t(n) + h, y(n) + k_3\bigg) \end{aligned} \tag{2.26}$$

where $h > 0$ represents the step-size and n stands for the iteration number. $y(n+1)$ is the RK4 approximation of $y(t_{n+1})$, and the next value $(y(n+1))$ is determined by the present value $(y(n))$ plus the weighted average of four increments, where each increment is the product of the size of the interval, h, and an estimated slope specified by function f on the right-hand side of the differential equation. The RK4 method is a fourth-order method, meaning that the local truncation error is on the order of $O(h^5)$, while the total accumulated error is on the order of $O(h^4)$. Note that the above results are necessary and sufficient to find the numerical solutions of Eq.(2.24) as long as it remains continuous. However, considering a discrete model, one needs moreover to these results, additional conditions called boundary conditions whose choice depends on the studied problem. Throughout our experiments, we have adopted periodic boundary conditions since the different models explored are assumed to be cyclic. For example, a network of N neurons with nearest neighbors interactions obeys the following boundary conditions

$$x(0) = x(N) \;\text{ and }\; x(N+1) = x(1) \tag{2.27}$$

Overall, Runge-Kutta numerical intergration methods are powerful tools for solving ODEs numerically. They offer a good balance between accuracy and computational efficiency and have become a standard technique in many scientific disciplines.

Conclusion

This chapter has been organized around two main themes. Firsly, the most prominent computational models have been develop to describe the behaviour of neurons and neural networks. It appears that the HH and ML models hold biologically acceptable properties, since the parameters of these two models have been deduced experimentally, unlike other

models whose basic principle was to simulate the biological behaviour of neurons observed experimentally. We focused our attention on the FHN and the IF models that are often used for bifurcation analysis to study how changes in parameters can lead to different dynamical behaviors such as steady states or oscillations. the two models have been improved to provide more accurate representations of the complex interactions between electromagnetic induction or light illumination and neural activity. By incorporating memristors and photocells into a simple FitzHugh-Nagumo circuit to detect and process external magnetic flux and light radiation.

The above models have been handled by means of some analytical and numerical methods. The RK4 method with periodic boundary conditions has also been presented for the numerical simulations.

Chapter 3

Results and Discussion

Introduction

Many processes in living systems are oscillatory. Biological rhythms occur at all levels of biological organization, from unicellular to multi-cellular organisms, with periods ranging from fractions of a second to years. Besides quite obvious examples of biological oscillations such as beating of heart, lung respiration, the sleep-wake cycle..... These rhythms find their roots in the many regulatory mechanisms that control the dynamics of living cells. For example, neural and cardiac rhythms at the single cell level are associated with the regulation of voltage-dependent ion channels metabolic oscillations originating from the regulation of enzyme activity, pulsatile intercellular signals and intracellular calcium oscillation associated with receptor activity, while regulation of gene expression in hypothalamic neurons underlies circadian rhythms.

MI has been shown to be efficient pathway to energy localization in biological molecules as well as discrete systems, in general [91, 92]. It result from the interplay between non linearity and dispersion. Indeed nonlinear waves and solitons initiated from MI have been showed to be suitable for complex computations, learning and describing nerve pulse in the neuronal network for real applications in one and two dimensional coupling [93, 94]. Dispersion , on the other hand, is less relevant to neural networks but can arise in certain types of neural dynamics. In this chapter, after applying the multiple scale expansion method to solve our generic system of equations, we performed the linear stability analysis on the results obtained. Using parameters from our analytical predictions, numerical simulations will be performed and spatiotemporal evolutions of plane waves are investigated to evaluate the long-time of the modulated waves evolving in the network under

memristive and photosensitive parameter.

3.1 Modulated wave patterns in a IF neural networks

Here the effect of high-low frequency electromagnetic radiation on our network dynamics through the memristor coupling k_1 and the disparity in frequency N are investigated both analytically and numerically.

3.1.1 Derivation of a Nonlinear Schrodinger Equation (NLSE) with coefficients depending on the electromagnetic induction feedbacks and synaptic coupling strength between neurons

Based on the IF model with electromagnetic induction, synaptic gap junction coupling with nearest neighbor interaction is proposed to enhance information exchange in the network. The dynamical equations for chain diffusive neuronal network under high-low frequency electromagnetic radiation ϕ_{ext} is given by

$$\begin{aligned} \frac{dx_n}{dt} &= a - bx_n - k_1\left(\alpha + 3\beta\phi_n^2\right)x_n + I + D(x_{n+1} - 2x_n + x_{n-1}). \\ \frac{d\phi_n}{dt} &= kx_n - k_2\phi_n + \phi_{ext} \end{aligned} \tag{3.1}$$

Where ϕ_{ext}= Acos$(2\pi ft)$+ Bcos$(2\pi Nft)$. f and Nf are the frequencies of the magnetic radiation, with respective amplitudes A and B. N is a frequency factor describing the disparity in the two frequencies. The term $D(x_{n+1} - 2x_n + x_{n-1})$ represents the synaptic gap junction coupling term in the chain neural network with nearest neighbors interaction. The subscript n represents the node position in the network, n=1,...,J. J and D represents the number of neurons and strength of the gap junction, respectively. The parameters are selected as a=1.05, b=1.80, l=1.04, k=0.9, α=0.40, $\beta = 0.02$, $k_2 = 1.50$, D=0.50 and J=500. We used to determine the condition under which modulated plane wave solutions in the array becomes unstable, resulting in the formation of localized wave patterns with solitonic traits. The effect of electromagnetic induction via the memristor coupling are investigated under magnetic radiation.

The system of coupled nonlinear discrete differential equations represented by Eqs.(3:1) is very difficult to be resolved analytically. In this light we proceeded by applying the

powerful multiple scale expansion presented previously, so as to derive a more suitable amplitude equation on which linear stability and instability have been successfully applied. In the process, the first lattice site in the network annotated n=1 is stimulated at the original frequency Ω. It is worth noting that frequency simplifies to the natural frequency in case $\epsilon = 0$. We designed a state vector solution for Eqs.(3:1) as $P_n(t) = x_n(t), \phi_n(t)$ having the generalized unperturbed forms given by

$$\begin{aligned} x_n(t) &= \int d\omega \chi(\omega) e^{i(wt+q_0 n)}. \\ \phi_n(t) &= \int d\omega \phi(\omega) e^{i(wt+q_0 n)} \end{aligned} \tag{3.2}$$

Where $\hat{P}(\omega) = \{\hat{\chi}(\omega), \hat{\phi}(\omega)\}$. We use the change of variables $\tau_n = \epsilon(t+n/u_g)$ and $\zeta_n = \epsilon^2 n$, with $c_g = 1$. The trial generalized solutions are then represented in the form

$$\begin{aligned} x_n(t) &= A(n,t)\chi(\zeta_n,). \\ \phi_n(t) &= A(n,t)\phi(\zeta_n,) \end{aligned} \tag{3.3}$$

with $A(n,t) = e^{i(\Omega t+qn)}$. This approach introduces a new network number m which supports a large grid . For a given n, the available the set of network points that can be considered are $..., n-N, n, (n+N)...$,.written as a function of the slow variable m as $\{..., (n+N) \to (m-1),\ n \to m,\ (n+N) \to (m+1)..., \}$. We set ϵ^2 =1/N due to the pronounced discretness effects.

By making use of the Fourier series in power of the parameter ϵ

$$\begin{aligned} x_n(t) &= \sum_{p=1}^{\infty} \epsilon^p \sum_{l=-p}^{p} \chi_p^{(l)}(\chi_n, \tau) A^{(l)}(n,t), \\ \phi_n(t) &= \sum_{p=1}^{\infty} \epsilon^p \sum_{l=-p}^{p} \phi_p^{(l)}(\zeta_n, \tau) A^{(l)}(n,t), \end{aligned} \tag{3.4}$$

With $\chi_p^{-l}(m,\tau) = (\chi_p^l(m,\tau)^{)}*$ and $\phi_p^{-l}(m,\tau) = (\phi_p^l(m,\tau)^{)}*$. By substituting Eqs.(3.4) into Eqs.(3.1), we obtain

$$\sum_{p=1}^{\infty}\epsilon^p\sum_{l=-p}^{p}\big[\epsilon\frac{\partial}{\partial\tau}\chi_p^l(m,\tau)+i\omega l\chi_p^l(m,\tau)\big]A^l(n,t)$$
$$=a-b\big(\sum_{p=1}^{\infty}\epsilon^p\sum_{l=-p}^{p}\chi_p^l(m,\tau)A^l(n,t)\big)+I-k_1\big[\alpha+3\beta\big(\sum_{p=1}^{\infty}\epsilon^p\sum_{l=-p}^{p}\phi_p^l(m,\tau)A^l(n,t)\big)^2\big]$$
$$+D\big[\sum_{p=1}^{\infty}\epsilon^p\sum_{l=-p}^{p}2(\cos(ql)-1)\chi_p^{(l)}(m,\tau)+\epsilon(\frac{2i}{v_g})\sin(ql)\frac{\partial}{\partial\tau}\chi_p^l(m,\tau) \tag{3.5}$$
$$+\epsilon^2(\frac{1}{v_g})^2\cos(ql)\frac{\partial^2}{\partial\tau^2}\chi_p^l(m,\tau)+i\epsilon^2\sin(ql)(\chi_p^{(l)}(m+1,\tau)-\chi_p^{(l)}(m-1,\tau))\big]A^l(i,t). \tag{3.6}$$

$$\sum_{p=1}^{\infty}\epsilon^p\sum_{l=-p}^{p}\left[\epsilon\frac{\partial}{\partial\tau}\phi_p^l(m,\tau)+i\omega l\phi_p^l(m,\tau)\right]A^l(i,t)$$
$$=k\left[\sum_{p=1}^{\infty}\epsilon^p\sum_{l=-p}^{p}\phi_p^{(l)}(m,\tau)A^s(i,t)-k_2\left(\sum_{p=1}^{\infty}\epsilon^p\sum_{s=-p}^{p}\phi_p^l(m,\tau)A^l(n,t)\right)\right]$$

The above coupled system is solve at different order of ϵ, with the corresponding harmonics l.

At the order (1,l), with l=0, we obtain

$$\chi_1^0(m,\tau)=\phi_1^0(m,\tau)=0. \tag{3.7}$$

For l=1, we obtain the dispersion relation

$$[i\Omega-2D(\cos(q)-1)-b-\alpha k_1]\,[i\Omega+k_2]=0 \tag{3.8}$$

for which our system admit non trivial solutions:

$$\begin{aligned}\chi_1^1(m,\tau)&=\chi(m,\tau)\\ \phi_1^1(m,\tau)&=\frac{k}{k_2+i\Omega}\times\chi(m,\tau)\end{aligned} \tag{3.9}$$

At the order (2, l), for l=0, we obtain the solution

$$\chi_2^0(m,\tau)=\phi_2^0(m,\tau)=0. \tag{3.10}$$

At l=1, a system of equations with a zero determinant is obtained, satisfying the Fredholm condition given by

$$V_g=2iD\sin(q). \tag{3.11}$$

We search for solutions in the form

$$\begin{aligned}\psi_2^1(m,\tau) &= \pi(m,\tau)\\ \phi_2^1(m,\tau) &= \frac{k_1}{k_2+i\Omega}\times\pi(m,\tau) - \frac{k_1}{(k_2+i\Omega)^2}\frac{\partial\pi(m,\tau)}{\partial\tau}\end{aligned} \tag{3.12}$$

with $\chi(m,\tau)$ is been arbitrary function. For l=2, we obtain the solution in the form

$$\chi_2^2(m,\tau) = \phi_2^2(m,\tau) = 0 \tag{3.13}$$

Finally, by resolving the system for $\chi_3^1(m,\tau) and \phi_3^1(m,\tau)$, at p=3 and l=1, it yields the nonlinear amplitude equation:

$$-i\gamma(\chi_{m+1}-\chi_{m-1}) + \alpha_2\frac{\partial^2\chi_m}{\partial\tau^2} + \beta_2|\chi_m|^2\chi_m = 0 \tag{3.14}$$

where

$$\begin{aligned}\gamma &= D\sin(q).\\ \beta_2 &= \frac{\cos(q)}{D\sin^2(q)}\\ \alpha_2 &= 3\beta k_1 k^2\left[\frac{1}{(k_2+i\Omega)^2} + \frac{2}{(k_2)^2-(i\Omega)^2}\right]\end{aligned} \tag{3.15}$$

Eqs.(3.14) is a nonlinear amplitude differential equation with coefficients $\gamma, \beta_2, \alpha_2$ dependent on the electromagnetic induction feedbacks and synaptic coupling strength between neurons. This spatiotemporal confirms information processing in the brain is not localized in a given neuron but it is done collectively within network in both space and time. The global forms of Eqs.(3.14) are well documented equations, already obtained in other domains of nonlinear physics including charge transport in DNA [95] and myocardial action potential propagation [92]

3.1.2 Linear stability analysis and modulated wave patterns

We consider the plane wave $\chi_m = Ae^{i(\nu m-\Delta\tau)}$ as the solution for the amplitude Eqs.(3.14). The complex amplitude and frequency are related to the perturbation wave number ν via the nonlinear dispersion relation

$$\Delta^2 = \frac{-\beta_2}{\alpha_2}\times\left[|A|^2 + \frac{2D\sin(q)}{\beta_2}\sin(\nu)\right] \tag{3.16}$$

The wave solution above will be unstable for $\Delta^2 < 0$. This condition depends simultaneously on the signs of the terms $\frac{-\beta_2}{\alpha_2}$ and $|A|^2 + \frac{2D\sin(q)}{\beta_2}\sin(\nu)$. Considering $\sin(\nu) =$

1, unstable wave will be generated for

$$|A|^2 > \frac{2D\sin(q)}{\beta_2} = A_{cr}^2, with \frac{-\beta_2}{\alpha_2} < 0. \tag{3.17}$$

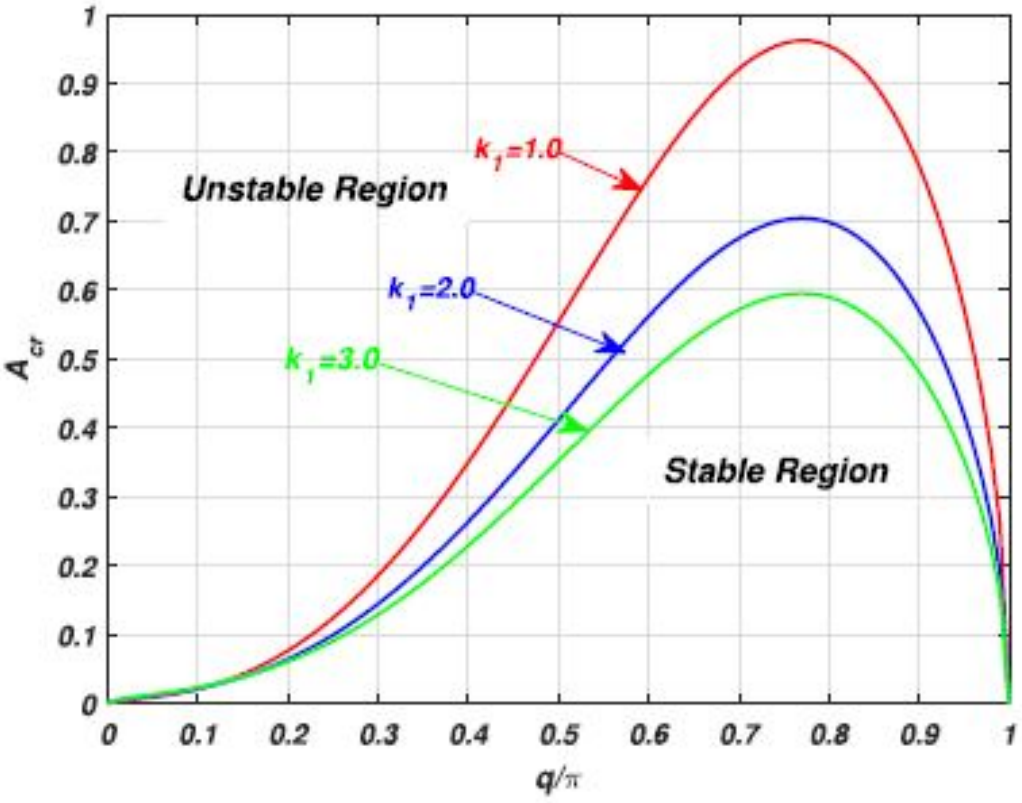

Figure 3.1: Critical amplitude vs wave number for D=0.50, k=0,9 $\alpha = 0.40$, $\beta = 0.02$ and $k_2 = 1.50$. The stable (SR) and unstable regions (UR) of modulational instability (MI) are presented. .

It is understood from the instability condition given by Eqs.(3.14) that when the parameters fall inside the unstable zone, unstable wave pattern emerges in the network following the mechanism of modulational instability (MI). We plot the growth rate of instability versus the wave number q and present the results in Fig. 3.1. More so, the stable and unstable regions are clearly displayed. It is found that smaller values of the wave number falls in the unstable region and hence favors the formation of localized wave pattern. When performing our numerical simulations, we select q=0.1 π, Furthermore, by varying the values of the memristor coupling, it is observed that the growth rate of instability decreases with increases in the memristor coupling. That is higher electromagnetic induction feedback reduces the critical amplitude, consequently, the network becomes less

susceptible to disruptions from external stimuli or internal fluctuations, making it more resistant to sudden chaotic bursts of activity. In order to validate this analytical prediction, we intergrate numerically our generic model.

Indeed, the linear stability analysis cannot give impulse information about the long-time evolution of the modulated waves evolving in the network because it is based on the linearization around an unperturbed plane wave. To verify our analytical predictions, Eqs.(3.1) is integrated numerically using the fourth-order Runge-Kutta computational scheme, with step size h = 0.001. The transient period for calculation is set at 10 000 time units. Initial conditions are chosen in accordance to the plane wave solution of Eqs.(3.14). Indeed, initial conditions are perturbed plane waves having amplitude A = 0.20, wave number q = 0.1π and modulation wave number $\nu = 0.5\pi$ picked from the unstable regions of the modulational instability as indicated on Fig.3.1. To discern the effect of electromagnetic induction through the memristor coupling, on the bearing of localized structures by our discrete system, we set $k_1 = 1.20$, where the network is exposed to a high-low frequency electromagnetic radiation $\phi_{ext} = 25\cos(2\pi ft) + 25\cos(2\pi Nft)$, with f = 0.04 and N = 10. We note the intrinsic parameter values selected correspond to a point which belongs to the unstable region of the growth rate presented in Fig.3.1, which according to the figure obtained, the instability is predicted for plane waves with these wave numbers.

In order to study the spatial and temporal dynamics of electrical activity within the network, the 3D pattern of the emerging pattern of nerve impulse for a network of 500 identical cells is presented in Fig.3.2. while the spatiotemporal pattern is presented in Fig. 3.3 [panel (a)] and the corresponding time series at the node position n = 100 [panel b_1], n = 200 [panel b_2] and n = 400 [panel b_3] are presented in Fig.3.3.

It is found that the 3D pattern obtained in Fig.3.2 are nonlinear waves with temporal periodic-like structures This suggest potential interference with neural activity confirms by analycal prediction presented in Fig 3.1. This could impact neuronal communication and potentially leading to disruptions in brain function or signaling pathways.

Fig.3.3 [panel (a)] presents the spatiotemporal pattern of the membrane potential of 500 neurons in the network, where Time runs from top to bottom and Lattice site from left to right. It consist of alternate band of bright and dark regions. Bright regions suggest simultaneous firing of neurons, while dark regions indicates periods of inactivity or quiescence across the network. In this bright regions, different firing patterns are expected.

The spatiotemporal patterns clearly portrait bright bands with different intensities brightness, suggesting mixed or irregular firing patterns. This alternating pattern could signify coordinated bursts of activity followed by periods of rest in the neural network.

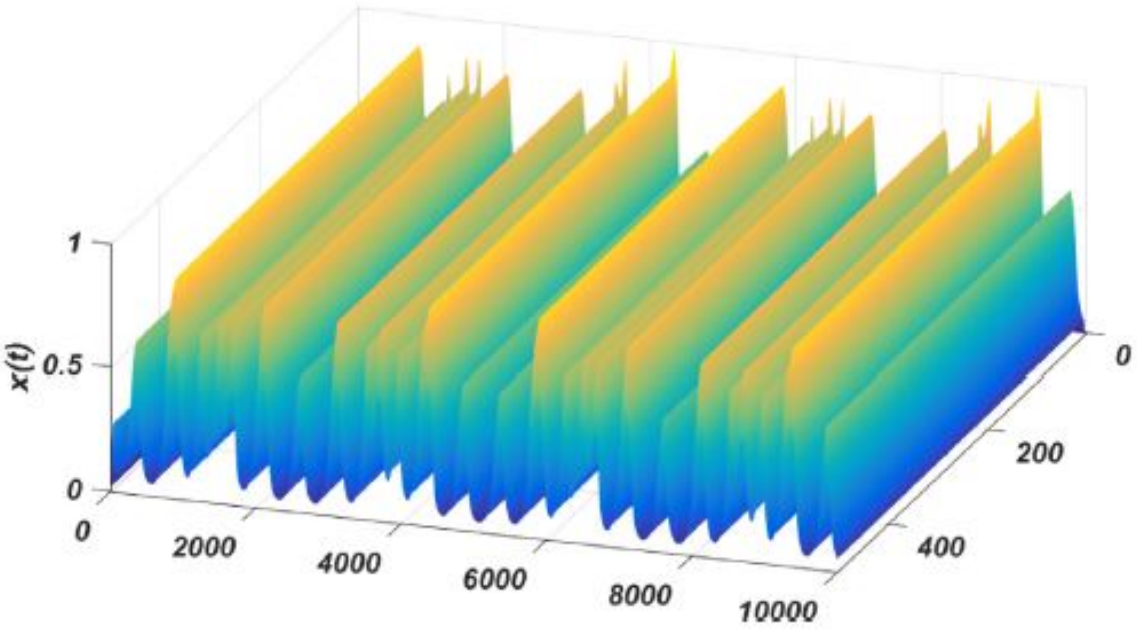

Figure 3.2: 3D Feature of the nerve pulse in a lattice with 500 cells and recorded over a period of t=10000, where $k_1 = 1.20$, D=0.50, A=25.0 B=25.0, f=0.04, N=10.

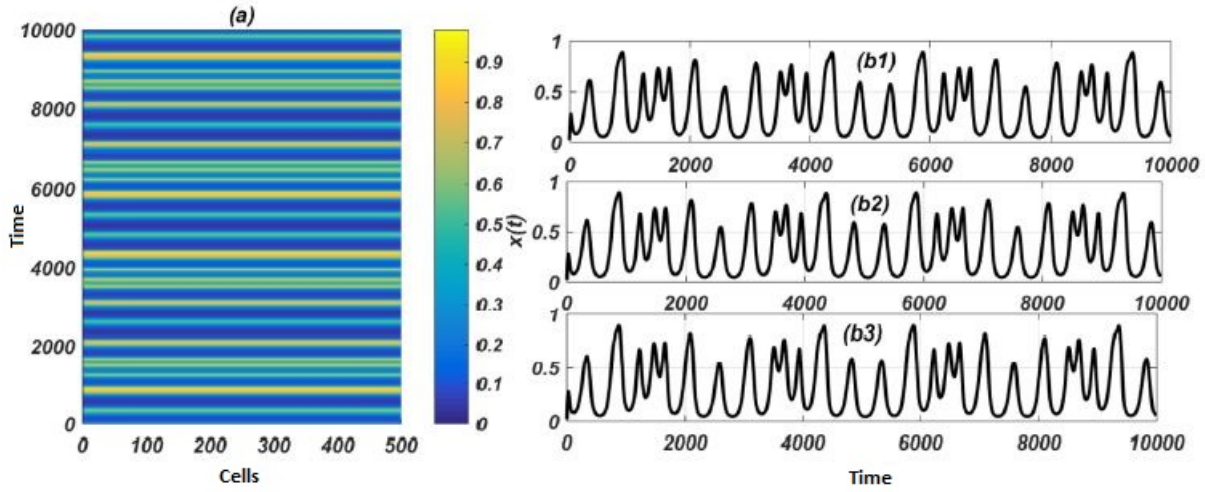

Figure 3.3: Spatiotemporal (a) and temporal features (b) of the nerve impulse presented in Fig. 3.2

The time series in Fig.3.3 presents mixed/irregular firing patterns of the network.

These irregular firing patterns could be clearly due to the exposure of the network to electromagnetic radiation.The network is no longer firing in a simple, repeating, pattern, but is exhibiting more complex rhythms with multiple frequencies. This confirms the work reported in Ref. [96, 97]. Furthermore, the time series taken at different lattice site and presented in Fig. 3.3 [panel (b1) . (b3)] show nonlinear waves pattern with similar dynamics, suggesting synchronization. This could be very powerful from biophysical perspective where intermittent neural synchronization has been linked to Parkinson's disease Ref. [101] which is characterized by tremors, rigidity and impaired movement thought to arise from abnormal activity in the brain basal's ganglia. The improved IF model exposed to high-low frequency electromagnetic radiation could thus be a vital prototype relevant for understanding the potential mechanism of intermittent synchrony in Parkinson disease. It is well known that depending on the value of the memristor coupling k_1 selected, one should expect different behaviors of the system. By increasing the strength of k_1, its effect on pattern formation are presented Fig. 3.4, Fig.3.5 and Fig. 3.6.

It is found in Fig.3.4, Fig.3.5 and Fig.3.6 that the spatiotemporal patterns are greatly modified as the value k_1 are changed. Indeed , higher electromagnetic induction feedback gain suppresses excitability k_1=2.50 in Fig 3:4, k_1=2.90 in Fig 3:5 and k_1=3.10 in Fig 3:6, by reducing the spatiotemporal pattern to a homogeneous and quiescent state. Furthermore, we examine the effect of high-low frequency electromagnetic radiation on our network dynamics. Since we are using a superposition of two fields, we concentrate on the effect of disparity in frequency (N) of the two fields. The results are presented in Figs. 3.7, 3.8 and 3.9. It is observed in Figs. 3.7, 3.8 and 3.9, that as the value of N increased, the localized patterns are modified. At a small value of N (N = 1) in Fig. 3:7, the system presents regular spatiotemporal pattern, whereby the bright bands correspond to the regions where the neurons are firing. Indeed, the thin structures found in Fig. 3:7 correspond to individual spikes inside a burst. This is confirmed by its corresponding time series , where spikes are observed. It is found that as N increases as in Figs. 3:8 and 3:9, mode transition in firing state occurs Figs. 3:8 and 3:9. This factor (N) thus proofs efficient in ensuring rich dynamic states in the network.

Overall, these approaches have advanced our understanding of how external stimuli can influence neural activity, information processing and have potential implications for fields such as neuroscience, especially as the rise in the use of wireless technologies such as mobile phones, relay antennas, wifi network and other portable instruments have increased

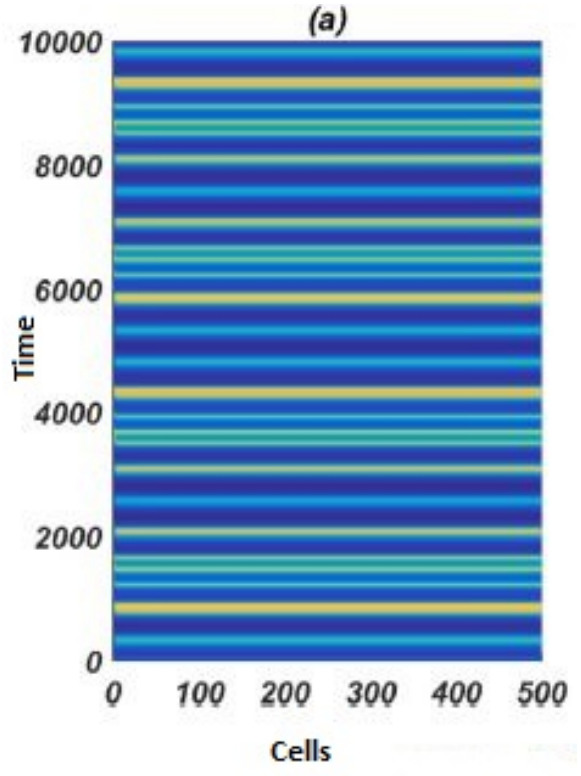

Figure 3.4: spatiotemporal pattern where time runs from top to bottom and lattice site from left to right. for (a) $k_1 = 2.50$.

electromagnetic interactions with human biological cells, notably neurons. It is found that the collective behaviors of neurons as well as the electrical activities are dependent on the distribution of magnetic flux. It reveal that electromagnetic induction can modulate the formation of wave patterns and mode in electrical activities. Under high-low frequency electromagnetic radiation, the electromagnetic induction gain via the memristor could effectively suppress excitability to a homogeneous spatiotemporal pattern, with quiescent state.

3.2 Modulated wave patterns in a FHN neural networks

Neurons in the cerebral cortex are interconnected and form networks for activity coordination and cooperative behaviors, including pattern formation, impulses, synchronization and coherent structures [98–100]. Particularly, exploring spatiotemporal patterns dynamics behaviors in neuronal system are crucial for brain function, encoding informa-

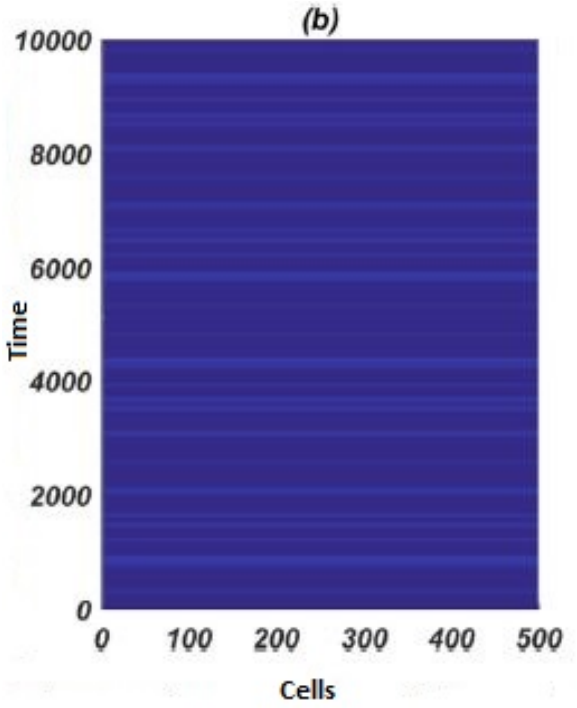

Figure 3.5: spatiotemporal pattern where time runs from top to bottom and lattice site from left to right for (b) $k_1 = 2.90$.

tion, driving behavior. A general view, from experimental and theoretical studies, is that brain oscillations are excellent candidates in conveying information from the brain to organs and may adopt a broad range of features related to either normal or pathological behaviors.

Electromagnetic fields and light illumination have been shown to modulate the activity and connectivity of neurons, leading to changes in their information processing capabilities. These external pattern formation in FHN model under magnetic flow and light illumination will be investigate through the MI technique. In that respect, effects of some parameters on nonlinear patterns such as the memristor coupling, light illumination, external stimulus current and magnetic radiation are investigated both analytically and numerically.

3.2.1 Derivation of Cubic Nonlinear Schrodinger Equation (CNSE)

As a reminder, Eqs.(2.16) has three equations with three unknowns, describing the effects of light illumination and magnetic flow in the FHN model. Based on the discrete

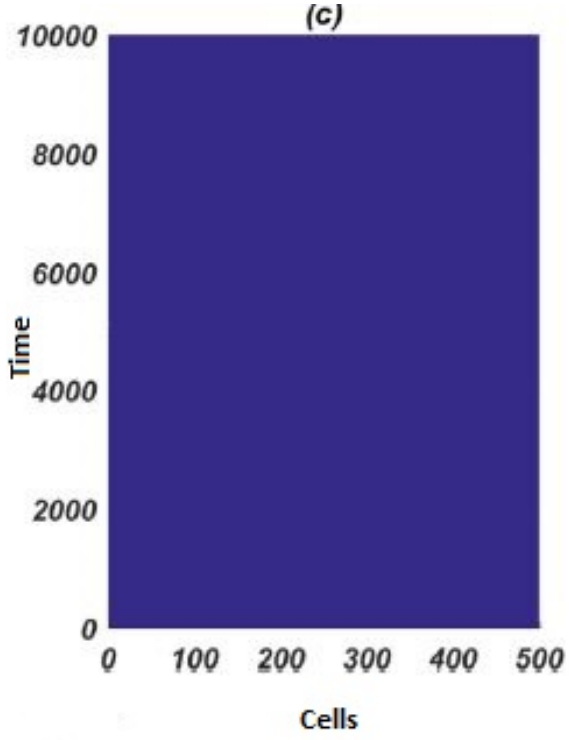

Figure 3.6: spatiotemporal pattern where time runs from top to bottom and lattice site from left to right for (c) $k_1 = 3.10$.

asymptotic expansion method, the solutions to the system of equations are considered wave packets, whereby the amplitudes and carrier waves are kept discrete. This approach permits us to obtain a more manipulable equation from Eqs.(2.16) for which linear stability analysis will be discussed.

The stimulation of the first neuron in chain network initiates an action potential (wave packets) having oscillation angular frequency ω and wave packet k. Due to nonlinear effects within the network, ω and k deviate by ϑ from the natural frequency ω' and k'. This is summaarized by the relation $\omega = \omega' + \epsilon\vartheta$ and $\vartheta k = k' + \epsilon\frac{\vartheta}{u_g} + \epsilon^2 c_g \vartheta^2 + ...$, with $u_g = \frac{\partial\omega}{\partial k}$ and $\frac{1}{2c_g} = \frac{\partial^2\omega}{\partial k^2}$. Furthermore, by introducing a new network number m that supports a large grid in such that for any i, possible sets of network points..., i-1, i, i + N,..., are taken as a function of a the slow variable m as $..., (i-N) \to (m-1), i \to m, (i+N) \to (m+1)...,$. Consequently, the solution of Eqs.(2.16) can be expressed as Fourier expansions, whose components are calculated in a Taylor series in powers of ϵ given as follow:

$$U_i(t) = \sum_{p=1}^{\infty} \epsilon^p \sum_{s=-p}^{p} \hat{U}_p^{(s)}(\zeta_i, \tau_i) e^{j(ki+\omega t)}, \tag{3.18}$$

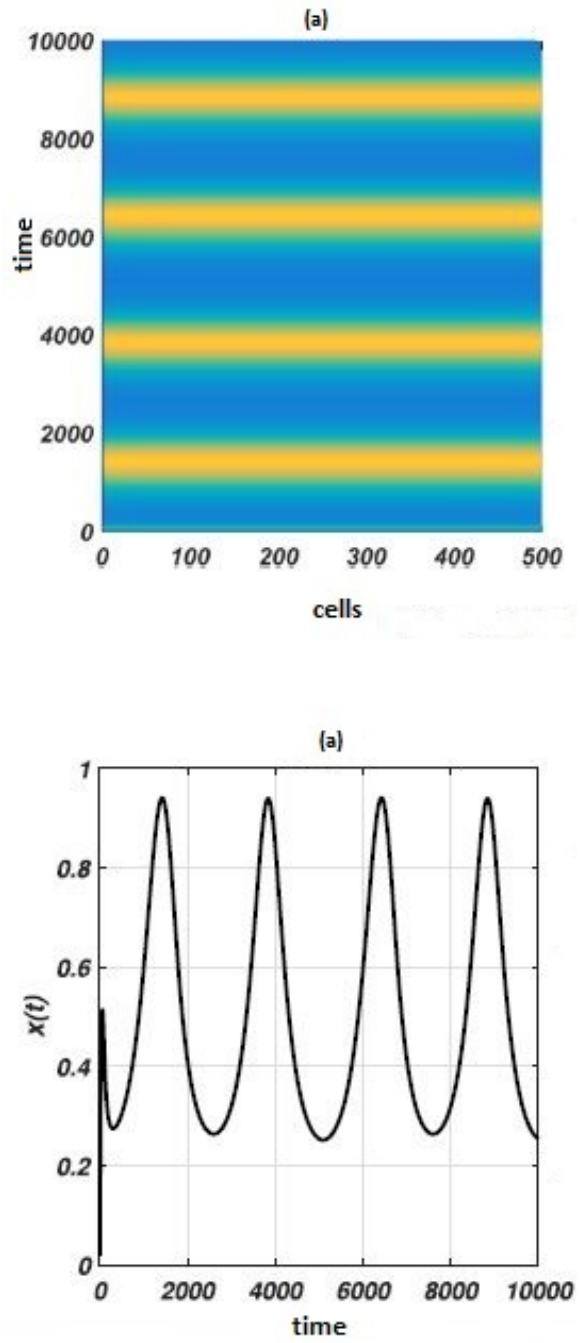

Figure 3.7: spatiotemporal pattern where time runs from top to bottom and lattice site from left to right and membrane potential time series patterns for n=200 (a)N=1.

with $U_i(t) = \{x_i(t), y_i(t), z_i(t)\}$ and $\hat{U}_p^{(s)}(\zeta_i, \tau_i) = \{\hat{x}_p^s(\zeta_i, \tau_i), \hat{y}_p^s(\zeta_i, \tau_i), \hat{\varphi}_p^s\}$ being the slowly modulation amplitude of the plane wave $e^{j(ki+\omega t)}$, where $j^2 = -1$ $\tau_i = \epsilon(t + \frac{i}{u_g})$ and $\zeta_i = \epsilon^2 i$. The slowly modulated amplitude $\hat{U}_p^{(l)}$ respects the reality condition $\hat{U}_p^{(-l)} = \hat{U}_p^{(-l)}*$. By substituting Eqs.(3.18) in Eqs.(2.16), we obtain the system of equations:

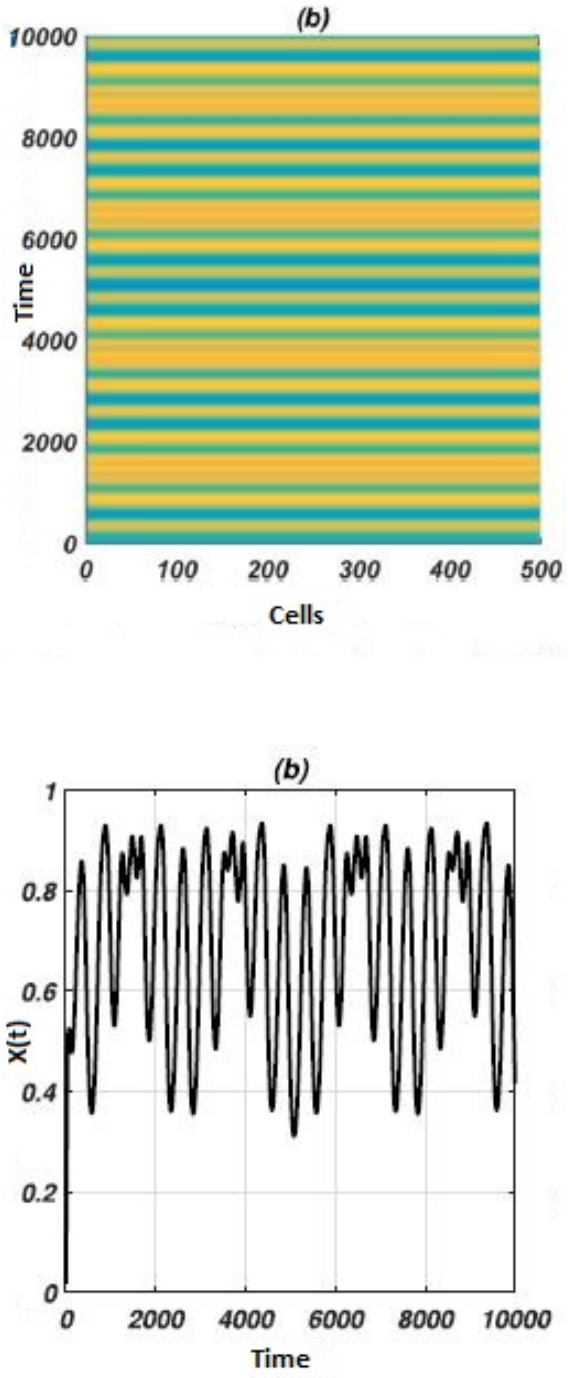

Figure 3.8: spatiotemporal pattern where time runs from top to bottom and lattice site from left to right and membrane potential time series patterns for n=200 (a) N=10.

$$\sum_{p=1}^{\infty}\epsilon^p\sum_{l=-p}^{p}\left[\epsilon\frac{\partial}{\partial\tau}x_p^{(s)}(m,\tau)+j\omega s x_p^{(s)}(m,\tau)\right]A^s(i,t)=(1-\varepsilon)\sum_{p=1}^{\infty}\epsilon^p\sum_{l=-p}^{p}x_p^{(s)}(m,\tau)A^s(i,t)$$
$$-\frac{1}{3}\left(\sum_{p=1}^{\infty}\epsilon^p\sum_{s=-p}^{p}x_p^{(s)}(m,\tau)A^s(i,t)\right)^3-\left(\sum_{p=1}^{\infty}\epsilon^p\sum_{s=-p}^{p}y_p^{(s)}(m,\tau)A^s(i,t)\right)$$
$$-k_0\left[-\alpha-3\beta\left(\sum_{p=1}^{\infty}\epsilon^p\sum_{s=-p}^{p}\varphi_p^{(s)}(m,\tau)A^s(i,t)\right)\right]\left[\sum_{p=1}^{\infty}\epsilon^p\sum_{s=-p}^{p}X_p^{(s)}(m,\tau)A^s(i,t)-e_f\right]$$
$$+D\sum^{\infty}\epsilon^p\sum^{p}\left(2(\cos(ks)-1)x_p^{(s)}(m,\tau)+\epsilon\left(\frac{2j}{}\right)\sin(ks)\frac{\partial}{}x_p^{(s)}(m,\tau)\right.$$

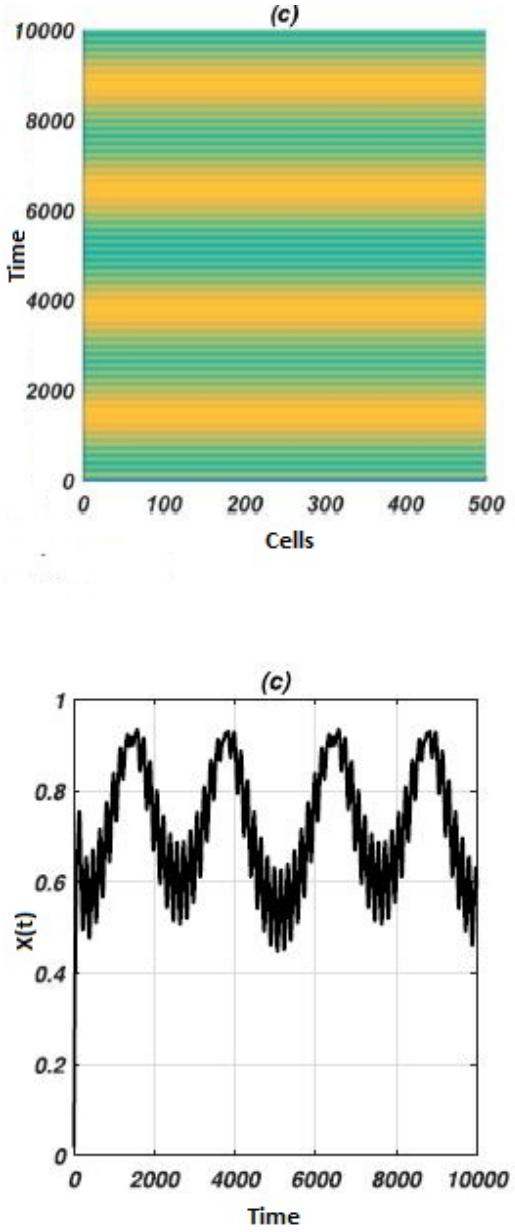

Figure 3.9: spatiotemporal pattern where time runs from top to bottom and lattice site from left to right and membrane potential time series patterns for n=200 (a) N=25.

$$\begin{aligned}&\sum_{p=1}^{\infty}\epsilon^{p}\sum_{l=-p}^{p}\left[\epsilon\frac{\partial}{\partial\tau}y_{p}^{(s)}(m,\tau)+j\omega s y_{p}^{(s)}(m,\tau)\right]A^{s}(i,t)\\&=c\left[\sum_{p=1}^{\infty}\epsilon^{p}\sum_{l=-p}^{p}x_{p}^{(s)}(m,\tau)A^{s}(i,t)+a-b\left(\sum_{p=1}^{\infty}\epsilon^{p}\sum_{s=-p}^{p}y_{p}^{(s)}(m,\tau)A^{s}(i,t)\right)\right]\end{aligned}\tag{3.20}$$

$$\sum_{p=1}^{\infty}\epsilon^p\sum_{l=-p}^{p}\left[\epsilon\frac{\partial}{\partial\tau}\varphi_p^{(s)}(m,\tau)+j\omega s\varphi_p^{(s)}(m,\tau)\right]A^s(i,t)$$
$$=k_1\left(\sum_{p=1}^{\infty}\epsilon^p\sum_{l=-p}^{p}x_p^{(s)}(m,\tau)A^s(i,t)\right)+k_2\left(\sum_{p=1}^{\infty}\epsilon^p\sum_{s=-p}^{p}\varphi_p^{(s)}(m,\tau)A^s(i,t)\right)+a_2\sin(\omega_2 t).$$

(3.21)

For different values of p, Eqs.(3:19), Eqs.(3:20), Eqs.(3:21) are solved at different orders of ϵ. At the first order p=1, the order ϵ^1, gives the system;

$$\begin{aligned}
&\sum_{s=-1}^{s=1}\left[(js\omega-1+\varepsilon+\alpha k_0-2D(\cos ks-1))\,x_1^s+y_1^s\right]A^s(i,t)=0\\
&\sum_{s=-1}^{s=1}\left[-cx_1^s+(js\omega+bc)\,y_1^s\right]A^s(i,t)=0\\
&\sum_{s=-1}^{s=1}\left[-k_1x_1^s+(js\omega+k_2)\,\varphi_1^s\right]A^s(i,t)=0
\end{aligned}\tag{3.22}$$

Solving Eqs.(3:22) for s=0 yields $U_1^0(m,\tau)=0$ $\left(x_1^0(m,\tau)=y_1^0(m,\tau)=\varphi_1^0(m,\tau)=0\right)$. At s=1, we obtain a linear system of equations in terms of $x_1^1, y_1^0 and \varphi_1^0$ summarized by

$$AU_1^1(m,\tau)=0\tag{3.23}$$

with Since $U_1^1(m,\tau)\neq 0$, it implies the determinant of A is null, giving the relation

$$[j\omega-1+\varepsilon-\alpha k_0-2D(\cos(k)-1)]\,x\,(j\omega+bc)+c=0\tag{3.24}$$

The dispersion relation given by Eqs.(3:24) above is dependent on the memristive coupling k_0. The corresponding group volocity is obtained as:

$$\frac{2jD\sin(k)(j\omega+bc)}{2j\omega+bc-1+\varepsilon+\alpha k_0-2D(\cos(k)-1)}\tag{3.25}$$

If we let $x_1^1(m,\tau)=x_m$ then we can solve for $y_1^1(m,\tau)$ and $\varphi_1^1(m,\tau)$ in Eqs.(3:23) such that

$$\begin{aligned}
y_1^1(m,\tau)&=\left(\frac{c}{j\omega+bc}\right)x_m\\
y_1^1(m,\tau)&=\left(\frac{k_1}{j\omega+k_2}\right)x_m
\end{aligned}\tag{3.26}$$

In the same manner, for p=1, 2, the order ϵ^2, s=0 gives a system of equations in terms of x_2^0 , y_2^0, φ_2^0

$$\begin{aligned} x_2^0(m,\tau) &= \frac{6\beta k_0 e_f k_1^2}{(\varepsilon - 1 - \alpha k_0 + 1/b)((j\omega)^2 - k_2^2)}|x_m|^2, \\ y_2^0(m,\tau) &= \frac{6\beta k_0 e_f k_1^2}{b(\varepsilon - 1 - \alpha k_0 + 1/b)((j\omega)^2 - k_2^2)}|x_m|^2, \\ \varphi_2^0(m,\tau) &= \frac{6\beta k_0 e_f k_1^3}{k_2(\varepsilon - 1 - \alpha k_0 + 1/b)((j\omega)^2 - k_2^2)}|x_m|^2, \end{aligned} \tag{3.27}$$

for s=1 we obtain a system of equations in terms of x_2^1 , y_2^1 and φ_2^1 such that with $x_2^1 = \delta(m,\tau)$, we obtain:

$$\begin{aligned} y_2^1(m,\tau) &= \frac{c}{j\omega + bc}\delta(m,\tau) - \frac{c}{(j\omega + bc)^2}.\frac{\partial x_m}{\partial \tau}, \\ \varphi_2^1(m,\tau) &= \frac{k_1}{j\omega + k_2}\delta(m,\tau) - \frac{ck_1}{(j\omega + bc)^2}.\frac{\partial x_m}{\partial \tau}. \end{aligned} \tag{3.28}$$

and for s=2 we obtain a system of equations in terms x_2^2, y_2^2 and φ_2^2.

$$\begin{aligned} x_2^2(m,\tau) = Ax_m^2 &= \frac{-3\beta k_0 e_f k_1^2 (2j\omega + bc)}{[(2j\omega + bc)(2j\omega + \lambda) + c]\,(j\omega + k_2)^2}x_m^2, \\ y_2^2(m,\tau) &= \frac{-3c\beta k_0 e_f k_1^2}{[(2j\omega + bc)((2j\omega + \lambda) + c)](j\omega + k_2)^2}x_m^2, \\ \varphi_2^2(m,\tau) &= \frac{-3\beta k_0 e_f k_1^3 (2j\omega + bc)}{[(2j\omega + bc)(2j\omega + \lambda) + c]\,(j\omega + k_2)^2\,(2j\omega + k_2)}x_m^2, \end{aligned} \tag{3.29}$$

with $\lambda = -1 + \varepsilon - \alpha k_0 - 2D(\cos(2k) - 1)$. Finally, when p=1, 2, 3, the order ϵ^2 s=0 gives a system of equations in x_2^s, y_2^s and φ_2^s. For s=1 we obtain a system equations in terms of x_2^1, y_2^1 and φ_2^1 such that by making use of previous relations, where $x(m,\tau) = x(\tau)$ we obtain

$$jP\,(x_m + 1 - x_m - 1) + Q\frac{\partial^2 x_m}{\partial \tau^2} + R|x_m|^2 x_m = 0 \tag{3.30}$$

where

$$\begin{aligned} P &= D\sin(k), \\ Q &= \frac{-D\cos(k)}{(ju_g)^2} - \frac{c}{(j\omega + bc)^3}, \\ R &= 3\beta k_0 k_1^2\left(\frac{1}{(k_2 + j\omega)^2} + \frac{2}{(k_2)^2 - (j\omega)^2}\right) - 1 - \frac{6\beta k_0 e_f k_1^2 \bigwedge}{(k_2 - j\omega)(k_2 + 2j\omega)}. \end{aligned} \tag{3.31}$$

The obtained equation above is a nonlinear differential difference equation having features of Discrete Nonlinear Schrödinger Equation (CNSE)

3.2.2 Analytical analysis of MI

To remind the critical amplitude is the minimum strength or intensity of a stimulus required to trigger an action potential or a neural response. Understanding the critical amplitude in neurons is crucial for studying neural excitability and information processing in the nervous system, such critical amplitude should be useful to predict the MI phenomenon in our system.

Due to MI in nonlinear and dispersive media, a plane impulse wave could become unstable under modulation. By injecting a perturbation $x_m(\tau) = x_0 e^{j(\mu m - \pi\tau)}$ into Eqs.(3:30), the nonlinear relation obtained is given by

$$\pi^2 = \frac{1}{Q'} \times \left(\frac{-2D\sin(k)\sin(\mu)}{R} + |x_0|^2 \right) \tag{3.32}$$

with $Q' = \frac{Q}{R}$. Modulated wave emerge when $\pi^2 < 0$. By taking into consideration discreteness effect, $\sin(\mu)$ is bounded and thus we set $\mu = \frac{\pi}{2}$. If $Q < 0$ then unstable wave is possible when.

$$\pi^2 = \frac{1}{Q'} \times \left(\frac{-2D\sin(k)\sin(\mu)}{R} + |x_0|^2 \right) < 0 \tag{3.33}$$

$$|x_0|^2 > \frac{2D\sin(k)}{R} = x_{cr}^2 \tag{3.34}$$

The graph of growth rate related to the critical amplitude $x_{cr} = x_{cr}(k)$ is plotted for synaptic strength D=0.04 and presented in fig 3.10.

The critical amplitude-wave number parameter space in Fig 3.10 is divided into two distinct regions namely the Stable Region(SR) and the Unstable Region(UR). It is expected from numerical findings that when parameters are picked from UR. modulated wave will emerge from the network lattice.

3.2.3 Numerical analysis of MI

The linear stability analysis does not give any information about the long time evolution of the modulated waves, since it is mainly based on the linearization around an unperturbed plane wave. We therefore intend to perform full numerical simulations on the generic system given by Eqs.(2.16). Results are obtained via the fourth-order Runge-Kutta computational scheme, with step time h=0.01. The initial conditions are selected

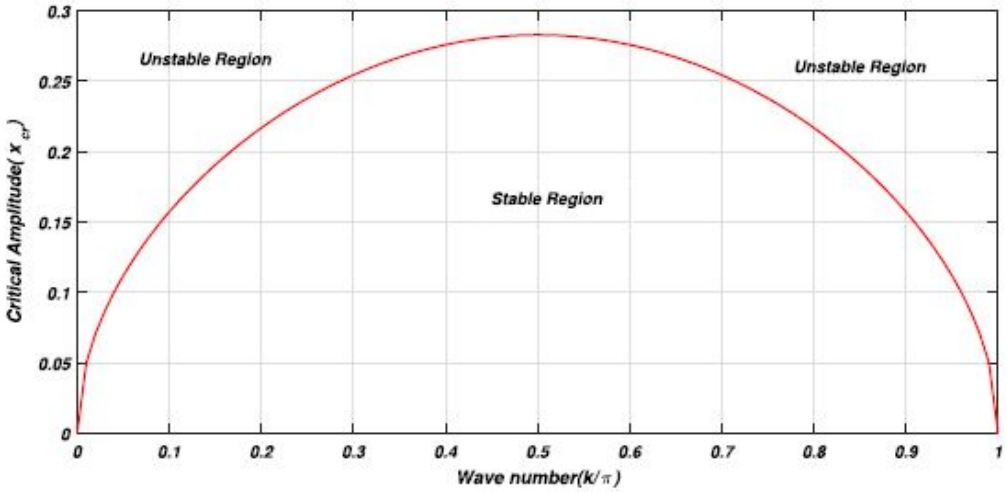

Figure 3.10: Critical amplitude vs wave number for D=0.04, $k_0 = 5.7$ and $b = 0.8$. Stable Region (SR)and Unstable Region (UR) of modulational instability (MI) are presented. .

to correspond to slightly modulated plane waves, having corresponding normal and perturbed wave numbers set at $k = 0.1\pi$ and $\mu = 0.5\pi$. Numerical simulation permits the study of the long-time evolution of the modulated waves evolving in the network under memristive, photosensitive parameter. This evolution in patterns is related to the hidden structure of information coding in the network [103]. Analyzing these patterns will help to gain deeper insights into how the brain works and how we can better understand and treat neurological disorder.

Firsly, we examine the effect of light illumination on the spatiotemporal patterns of membrane potential. We fix the amplitude at $a_1 = 0.4$ and we evaluate the dependence possible information coding on the frequency ω_1. The results are presented in Fig 3.11, Fig 3.12 and Fig 3.13. In Fig 3.11, $\omega_1 = 0.10$, in Fig 3.12 $\omega_1 = 0.18$, while in Fig 3.13, $\omega_1 = 0.18$ $\omega_1 = 0.20$,

The result in Fig 3.11, Fig 3.12 and Fig 3.13 confirm that evolution of collective dynamical behaviors via pattern formation in the network depends on the external stimuli from light illumination on each node. At low frequency exposure in Fig 3.11, the network presents a state characterized by alternate quiescent and firing pattern. This structure corresponds to the spiking state of the network. As the frequency of light exposure is increased to greater value in Fig 3.13, there is destruction of the initially coherent pattern into a partially disorder state which could be linked to chaotic state. This results prove that variety of different collective electrical activities could be induced under different

frequency of light illumination. Photosensitive neurons can thus capture and convert external optical signals thereby realizing the encoding of the signal. Remarkably, the obtained patterns in Fig. 3:13 might also be a route to chimera states which has been widely discussed recently in neuronal system. [38, 79].

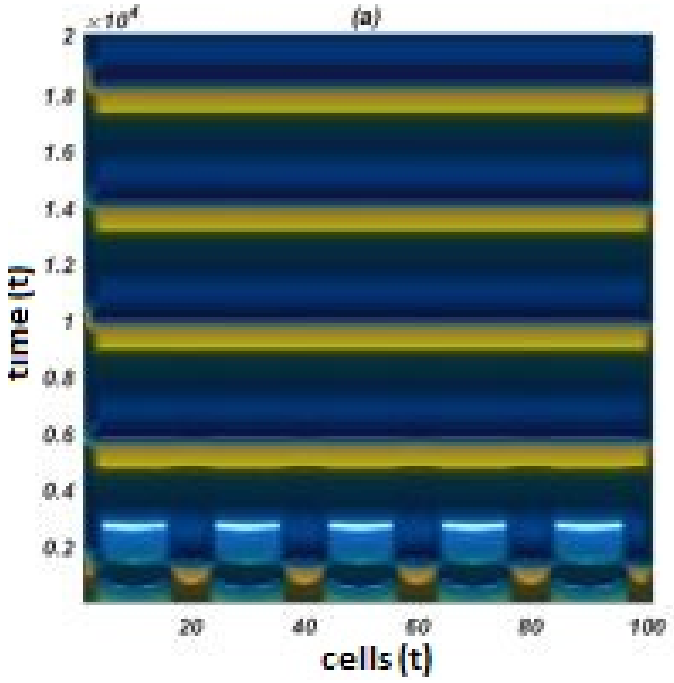

Figure 3.11: Spatiotemporal patterns of membrane potential calculated for each frequency of photocurrent from light illumination; (a) $\omega_1 = 0.10$, with $a_1 = 0.4$.

Furthermore, we evaluate the dependance of patterns on the frequency of external magnetic flux related to the electromagnetic induction. We fix the amplitude at $a_2 = 4.0$ and we vary the angular frequency ω_2. The results presented in Fig. 3.13, Fig. 3.14 and Fig. 3.15 , where (a) $\omega_2 = 0.50$, (b) $\omega_2 = 8.0$, and (c) $\omega_2 = 10$.

The results in Fig 3.14, Fig. 3.15 and Fig 3.16 confirm varieties of firing patterns such as bursting state as well as 2-period and 4-period spiking states can be induced in the network under electromagnetic radiation exposure. At low frequency external magnetic flux in Fig 3.14, the spatiotemporal pattern presents localized patterns corresponding to bursting state. In Fig. 3.15, the 2-period spiking state is observed and at a higher frequency in Fig. 3.16, we observe a 4-period spiking state.

Apart from light illumination, thermal fluctuation can significantly modulate excitability of neurons by influencing gated channel conductance.

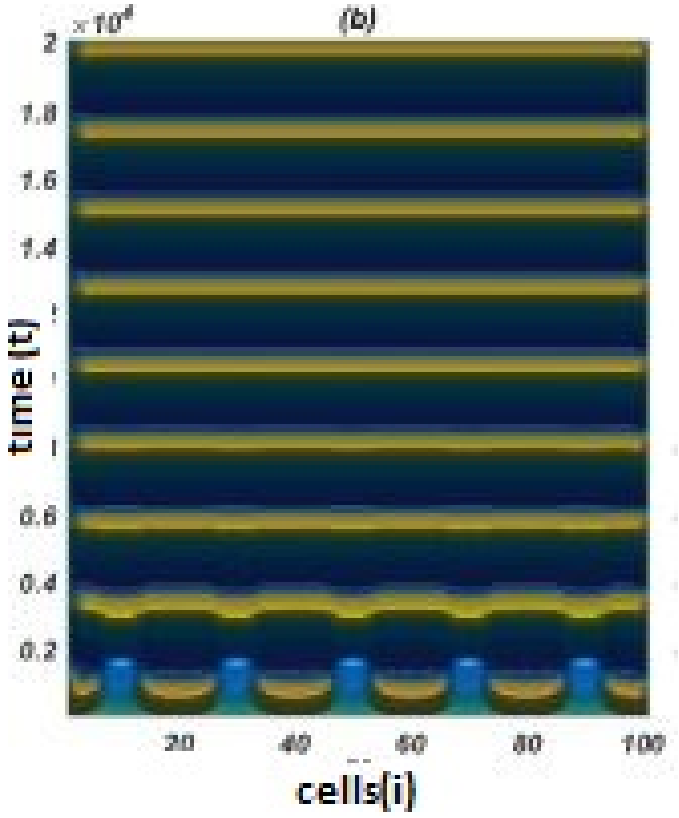

Figure 3.12: Spatiotemporal patterns of membrane potential calculated for each frequency of photocurrent from light illumination;(b) $\omega_1 = 0.18$, with $a_1 = 0.4$.

The above work was devoted to modulated impulse formation and pattern transition in a chain network of memristive photosensitive neurons have been discussed through modulational instability. Using parameters taken from the unstable zone, the longtime evolution of initial plane wave solutions confirm the presence of localized modulated impulses with features of spiking and bursting states as obtained in real biological experiments

Conclusion

In this chapter, we demonstrate that electromagnetic induction and light illumination have a significant impact on the information pattern of coupled neurons. The use of modulational instability and the RK4 algorithm allowed for a detailed analysis of the effects of these external stimuli on the behavior of neuronal network. It is noted that light frequencies and magnetic field can significantly modulate the excitability of neurons by influencing the conductance of different ion channel. By intensifying the electromagnetic

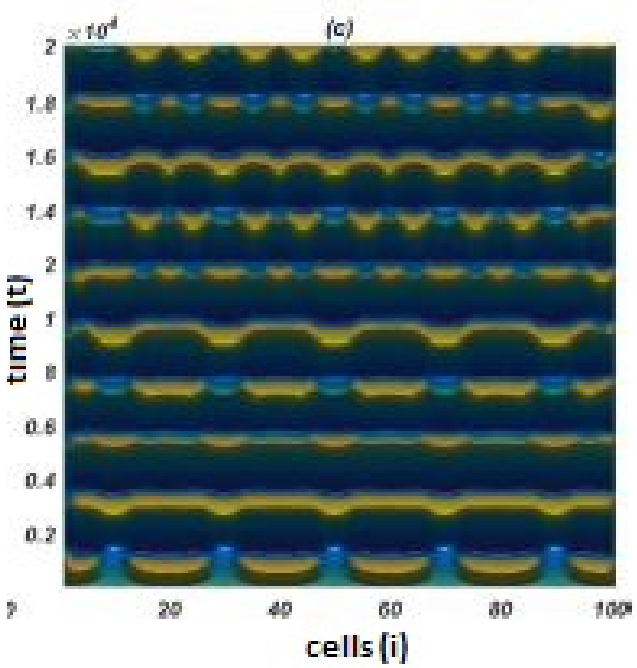

Figure 3.13: Spatiotemporal patterns of membrane potential calculated for each frequency of photocurrent from light illumination;(c) $\omega_1 = 0.20$, with $a_1 = 0.4$.

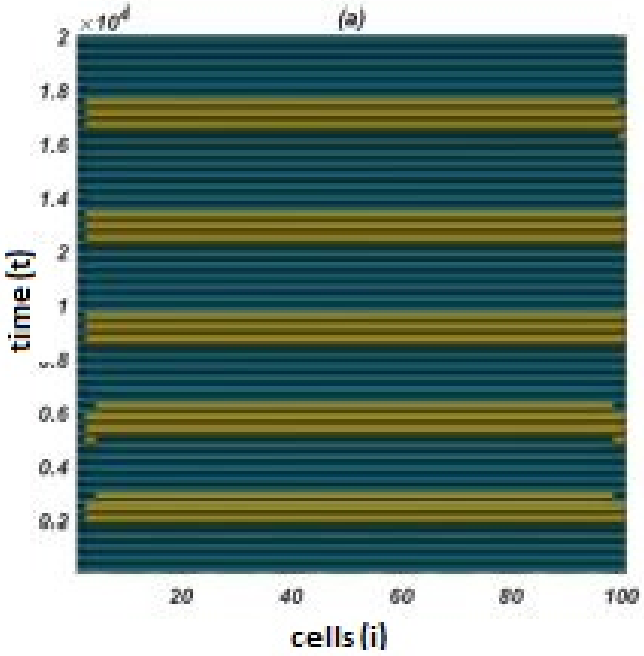

Figure 3.14: Spatiotemporal patterns of membrane potential calculated for each frequency of external magnetic flux; (a) $\omega_2 = 0.5$ with $a_1 = 4.0$.

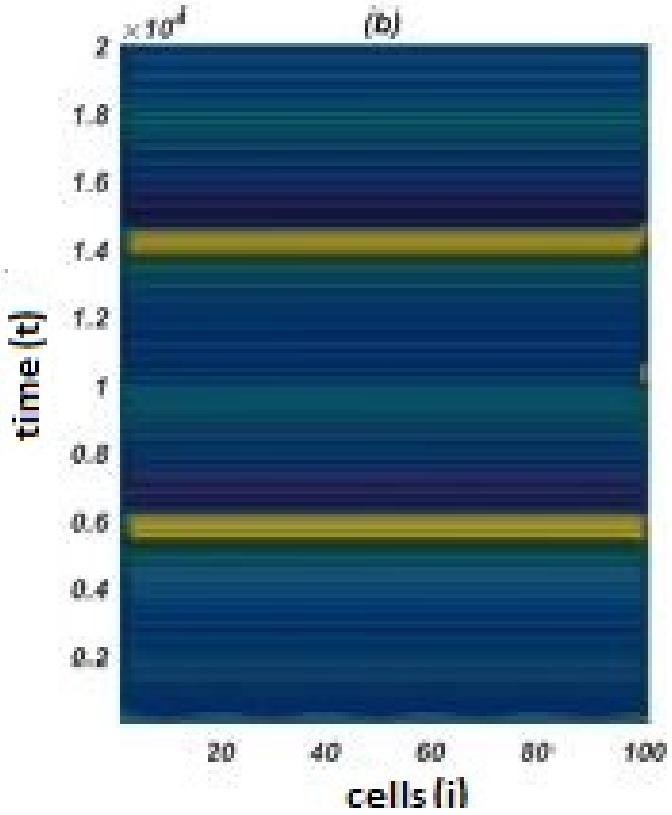

Figure 3.15: Spatiotemporal patterns of membrane potential calculated for each frequency of external magnetic flux; (b) $\omega_2 = 8$, with $a_1 = 4.0$.

radiation, there is a gradual disappearance of the patterns, this could provide indications and a better understanding of sudden heart and nerve failures when cells are exposed to high electromagnetic radiation.

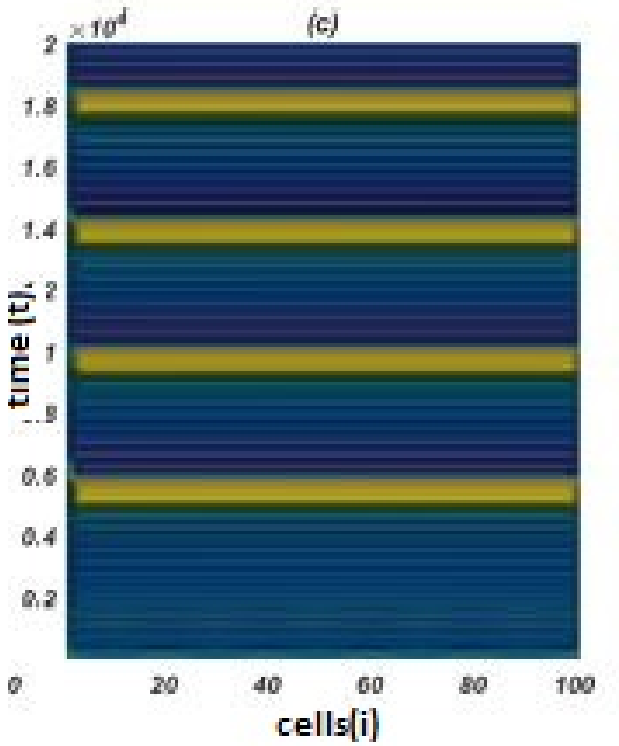

Figure 3.16: Spatiotemporal patterns of membrane potential calculated for each frequency of external magnetic flux; (c) $\omega_2 = 10$, with $a_1 = 4.0$.

General Conclusion

Summary

In this thesis, we study the effects of electromagnetic induction and light illumination on the phenomena of wave propagation and neuronal synchronization that are associated with the transport and transfer of nerve impulses in biological neural networks. To investigate the mechanism by which electromagnetic induction affects the electrical activity of neurons and mastering the mechanisms underlying the dynamics of nerve impulses under the influence of light illumination, we develop two mathematical models: the Integrate-and-Fire model and the FitzHugh-Nagumo model.

To achieve our main goals, the work of this thesis has been subdivided into three chapters: Chapter I presents the literature review. After a brief review of the physiology and anatomy of neurons with emphasis on the functioning of synapses as the bridges that connected two neurons in neuronal network, some basic ideas necessary for understanding neuronal communication are presented. Mathematical models of biological neurons are also presented.

In Chapter II, the two models, objects of the study, are presented. we develop an improved IF neuronal model using the additional magnetic flux variable to describe the time varying electromagnetic field, and its feedback on the membrane potential realized using the memristor. In the second model, memristors and photocells are incorporated into a simple FitzHugh-Nagumo circuit to detect and process external magnetic flux and light radiation. The above models have been handled by means of some analytical and numerical methods. In that context, the DNLS equation describing the spatiotemporal dynamics of envelop soliton has been derived in the discrete approximation. The RK4 method with periodic boundary conditions has been used in the numerical simulations for integrating of original models.

In chapter III, the results of the thesis are presented. It is noted that neuronal network can be deformed and wave propagation destroyed when exposed to continuous diverse electromagnetic radiations light frequencies and magnetic field can also significantly modulate the excitability of neurons by influencing the conductance of different ion channels.

Future orientations

The work of this thesis has contributed to the improvement of mathematical FHN and the leaky IF models to better understand the dynamics of nerve impulses in NNs. Most of the investigations carried out aimed at studying the phenomena of wave propagation and NS as a function of certain parameters, the number of which is not exhaustive. That is why we are prospecting other research directions that include:

- Thermal fluctuation which can significantly modulate excitability of neurons by influencing gated channel conductance. It is expected that in future project, a thermistor can be incorporated into a functional circuit to detect temperature fluctuation. In that way, the effect of thermal fluctuation on the potential mechanism of information coding in brain micro-circuits could be uncovered.

- Synchronization in memristive neurons with no synapse coupling.

- NS in amplitude modulation revealed two distinct regimes, direct and indirect synchronization regimes. It is therefore very important to study the phenomenon of NS in frequency modulation when the detected HF and LF modes are mixed.

- The formation and removal of spiral waves in cardiac cells have also attracted much attention in recent decades. Unfortunately, the detection of such waves which result from the inhomogeneities of the target media has been done only either numerically or experimentally. Therefore analytical finding of these survival waves could open new horizons in neuroscience.

- Experiment findings have revealed perfect correlation between NA and DNA double strand dynamics in the brain. We therefore need to develop mathematical models allowing to prove that theoretically. Some of such models could be useful to study coupling effects between DNA dynamics and neuronal activity in order to investigate for instance, the role of DNA dynamics in NS.

References

[1] S. Haykin. Neural Network and Learning Machines. 3rd edition. Pearson; 2008.

[2] A. L. Hodgkin and A. F. Huxley. A quantitative description of membrane current and its application to conduction and excitation in nerve. J. Physiol. (Lond), **117**, 500-544 (1952) .

[3] C. Morris, H. Lecar. Voltage oscillations in the barnacle giant muscle fiber. Biophys. J. 35, 193-213 (1952)

[4] E. M. Izhikevich. Which model to use for cortical spiking neurons? IEEE Trans. Neural Netw. **15**, 1063-1070 (2004)

[5] B. Ibarz, J. M. Casado, M. A. F. Sanjuan. Map-basedmodels in neuronal dynamics. Phys. Rep. **501**, 1-74 (2011)

[6] M. Perc, M. Marhl. Amplification of information transfer in excitable systems that reside in a steady state near a bifurcation point to complex oscillatory behavior. Phys. Rev. E **71**, 026229 (2005).

[7] G. Gerstner and W. M. Kistler, "Spiking Neuron Models" (Cambridge University Press, pp1-4) (2002).

[8] C. C. Hilgetag and M. Kaiser, Neuroinformatics **2**, 353 (2004).

[9] O. Sporns, D. Chialvo, M. Kaiser and C. C. Hilgetag, Trends Cogn. Sci. **8**, 418 (2004).

[10] G. Zamora-López, C. Zhou and J. Kurths, Front. Neurosci. **5**, 83 (2011).

[11] S. Raghavachari and J. A. Glazier, Phys. Rev. Lett.**82**, 2991 (1999).

[12] A. S. Landsman and I. B. Schwartz, Nonli. Biomed. Phys. **1**, 126 (2007).

[13] Q. Y. Wang, Z. S. Duan, M. Perc and G. R. Chen, EPL **83**, 50008 (2008).

[14] T. Nowotny, R. Huerta and M. I. Rabinovich, Chaos **18**, 037119 (2008).

[15] S. J. Schiff, T. Sauer, R. Kumar and S. L. Weinstein, Neuroimage **28**, 1043 (2005).

[16] C. G. McConnell, R. Q. So, J. D. Hilliard, P. Lopomo and W. M. Grill, J. Neurosci. **32**, 15657 (2012).

[17] M. D. Bevan, P. J. Magill, D. Terman, J. P. Bolam and C. J. Wilson, Trends Neurosci. **25**, 523 (2002).

[18] N. F. Rulkov, Phys. Rev. Lett. **86**, 183 (2001).

[19] Q. Y. Wang, Z. S. Duan, L. Huang, G. R. Chen and Q. S. Lu, New J. Phys. **9**,383 (2007) .

[20] M. S. Wang, Z. H. Hou and H. W. Xin Chem. Phys. Chem. **7**, 579 (2006).

[21] G. Buzsaki and X. J. Wang, Annu. Rev. Neurosci. **35**, 203 (2012).

[22] G. Buzsaki and A. Draguhn, Science **304**, 1926 (2004).

[23] L. V. Moran and L. E. Hong, Schiz. Bull. **37**, 659 (2011)

[24] A. Draguhn, R. D. Traub, D. Schmitz and J. G. R. Jeffreys, Nature **394**, 189 (1998).

[25] G. M. Ibrahim, S. M. Wong, R. A. Anderson, G. Singh-Cadieux, T. Akiyama, A. Ochi, H. Otsubo, T. Okanishi, T. A. Valiante, E. Donner, J. T. Rutka, O. C. Snead III and S. M. Doesburg, Exper. Neurol. **251** 30 (2014).

[26] F. M. Moukam Kakmeni, E. M. Inack, and E. M. Yamakou, Phys. Rev. E **89**, 052919 (2014).

[27] V. Braitenberg and A. Schüz, Statistics and Geometry of Neuronal Connectivity, Springer-Verlag, Berlin, 1998.

[28] L. Acedo, E. Lamprianidou, J.-A. Moraño, J. Villanueva-Oller and R.-J. Villanueva, Physica A **435** 111 (2015).

[29] M. Perc, Phys. Rev. E **72**, 016207 (2005).

[30] M. Perc and M. Marhl, Phys. Rev. E **73**, 066205 (2006).

[31] B. K. Bera, S. Majhi, D. Ghosh and M. Perc, EPL **118**, 10001 (2017).

[32] S. Majhi, M. Perc and D. Ghosh, Sci. Rep. **6**, 39033 (2016).

[33] S. Majhi, M. Perc and D. Ghosh, Chaos **27**, 073109 (2017).

[34] V. Volman, M. Perc and M. Bazhenov, PLoS ONE **6**, e20572 (2011).

[35] D. Guo, M. Chen, M. Perc, S. Wu, C. Xia, Y. Zhang, P. Xu, Y. Xia and D. Yao, EPL **114**, 30001 (2016).

[36] J. Ma, Y. Xu, C. Wang and W. Jim, Physica A **461**, 586 (2016).

[37] Y. Xu, C. Wang, M. Lv and J. Tang, Neurocomput. **207** 398 (2016).

[38] G. Tang, K. Xu and L. Jiang, Phys. Rev. E **84**, 046207 (2011).

[39] A. Mohamadou, B. E. Ayissi and T. C. Kofané, Phys. Rev. E **74**, 046604 (2006) .

[40] T. B. Benjamin and J. E. Feir, J. Fluid Mech. **27**, 417 (1967) .

[41] A. D. Koko, C. B. Tabi, H. P. F. Ekobena, A. Mohamadou and T. C. Kofané, Chaos **22**, 043110 (2012) .

[42] C. B. Tabi, I. Maïna, A. Mohamadou, H. P. F. Ekobena and T. C. Kofané, EPL **106**, 18005 (2014) .

[43] G. R. Y. Mefire, C. B. Tabi, A. Mohamadou, H. P. F. Ekobena and T. C. Kofané, Chaos **23**, 033128 (2013).

[44] C. B. Tabi, A. Mohamadou and T. C. Kofané, Eur. Phys. J. E **32**, 327 (2010) .

[45] I. Maïna, C. B. Tabi, A. Mohamadou, H. P. F. Ekobena and T. C. Kofané, Chaos **25** 043118 (2015).

[46] Clark-Evans . The brain and nervous system in two french renaissance (scientific) poets: Pernette du Guillet and Guillaume du Bartas. Bibliothèque d'humanisme et Renaissance, 289-303, 65(2) (2003).

[47] Fullick, Ann. Edexcell IGCSE Biology Revision Guidel. p. 40. ISBN 9780435046767 (1984).

[48] http://physiologyplus.com/classification-of-neurons-by-structure-and function (consulted on april, 2023)

[49] S. Alessandro, Extracting muscle synergies from human steady and unsteady locomotion: methods and experiments. PhD thesis, 08 (2018).

[50] http://opentextbc.ca/anatomyandphysiology/chapter/12-4-the-action-potential (consulted on may, 2023)

[51] http://www.psych.ualberta.ca/ITL/ap/ap.swf (consolted on may, 2023)

[52] D. Purves , G.J. Augustine, D. Fitzpatrick, W.C. Hall, A.-S. Lamantia, J.O. McNamara and L.E. White, Neuroscience(4th Ed.) 26 (2008)

[53] T. Sasaki, N. Matssuki and Y. Ikegaya, science **331**, 599 (2011)

[54] A. L. Hodgkin, J. Physiol. **90**, 183 (1937)

[55] A. N. Kohmogorov, I. G. Petrowskij, N. C. Piskunov, Annual Eugenics **7**, 255 (1937).

[56] L.L. Rubchinsky, C. Park, R.M. Worth, Nonlinear Dynam. 329-346, 68 (2012).

[57] http://www.researchgate.net/publication/327882341 (Online; accessed 14-Jan-2021)

[58] T.C. Suudhof, Handb. Exp. Pharmacol. **184**, 1 (2006).

[59] D.A. Rusakov, Neuroscientist .**12**, 317. (2006).

[60] Y.Humeau, F Dousseau, N .J. Grant and B. Poulain, Biochimie. **82**, 427 (2000).

[61] http://www.zoology.ubc.ca/ gardner/synapses (consulted on may, 2023)

[62] G. Zoidl and R. Dermietzel, Cell Tissue Res. **310**, 137 (2002)

[63] P. R. Brink, K. Cronin and S. V. Ramanan, J. Bioenerg. Biomembr. **28**, 351 (1996).

[64] E. Godaux, Cent Milliards de Neurones, Collection la science *apprivoisèe* (2006).

[65] Y. Zhang ,Y. Xu , Z. Yao , J. Ma . A feasible neuron for estimating the magnetic field effect. Nonlinear Dynam 102(3):1849Ű67(2020).

[66] A. Panfilov and P Hogeweg, Phys. Lett.A **176**, 295 (1993) .

[67] C.N. Takembo, A. Mvogo, H.P. Ekobena, T.C. Kofane, Nonlinear Dynam. **95** (2) 1067-1078 (2019).

[68] L. Chua. Memristor-the missing circuit element. IEEE Transactions on Circuit Theory, **18** 507-519 (1971).

[69] A.L. Hodgkin and A.F. Huxley, J. Physiol., **177**, 500 (1952).

[70] E. M. Izhikevich, IEEE Trans. Neural Networks, **14** 1569-1572 (2003).

[71] J. Woo, SH. Kim, K. Han, M. Choi. Characterization of dynamics and information processing of integrate-and-fire neuron models. J Phys A **54**, :445601 (2021).

[72] R. FitzHugh, Biophys. J. **1** 445 (1961).

[73] J. Nagomo, S. Arimoto and S. Yoshizawa, Proc. IRE **50** 2061 (1962).

[74] L. D. Silva, F. H. Hocks, A. Smits and L. H. Zitterberg, Kybernettik **15**, 25-37 (1997).

[75] M. E. Brandt, Int. j. Psychophys. **26**, 285-298 (1997).

[76] J. L. Hindmarsh and R. M. Rose, Proc. R. Soc. London Ser-B **221** 87 (1984).

[77] E. M. Izhikevich, IEEE Trans. Neural Networks **15** 1063 (2004) .

[78] M. Lv, C. Wang, R. Guodong, J. Ma, X. Song, Nonlinear Dynam. **85**, 1479-1490 (2016).

[79] Kesheng XU, Wenwen Huang, Baowen Li, Mukesh Dhamala and Zonghua Liu, EPL, **102**, 50002 (2013).

[80] A. Mvogo, C. N. Takembo et al., Phys. Lett. A **381**, 2264-2271 (2017)

[81] G. Wang, Y. Xu, M. Ge, L. Lu, Y. Jia, Int. J. Electron. Commun.(AEU)**120** 153209 (2020).

[82] M. Lv, J. Ma, Y.G. Yao, F. Alzahrani, Sci. China Tech. Sci. **62** 448-457 (2019).

[83] C. N. Takembo et al., Physica A **593**,126891 (2022) .

[84] J. L. Hindmarsh and R. M. Rose, Nature **296**, 162 (1982)

[85] Z. T. Njitacke, J. Ramadoss, C.N. Takembo, K. Rajagopal, J. Awrejcewicz. Chaos Solitons Fractals **167**, 113014 (2023) .

[86] Y. Zhang, F. Wu, C. Wang, J. Ma, Physica A **521** 519-530 (2019).

[87] Wu F, Hu X, Ma J. Estimation of the effect of magnetic field on a memristive neuron. Appl Math Comput **432**, 127366 (2022).

[88] Y. Xu , J. Ma Pattern formation in a thermosensitive neural network. Commun Nonlinear Sci Numer Simul; 111:106426 (2022).

[89] J. Leon, M. Manna, J. Phys. A: Math. Gen., **32**, 2845 (1999).

[90] L.P. Devries and E.J. Hasbun, A first course in computational

[91] A.S. Tankou, C.N. Takembo, G.H. Ben-Bolie, P. Owona Ateba, PLoS ONE **14** (6) e0214989 (2019).

[92] C.N. Takembo, A. Mvogo, H.P. Ekobena, T.C. Kofane, Nonlinear Dyn. **381** 95 (2) 1079-1098 (2019).

[93] C.N. Takembo, A. Mvogo, H.P. Ekobena, T.C. Kofane, Nonlinear Dynam. **96**, 1083-1093 (2019) .

[94] C.N. Takembo, A. Mvogo, H.P. Ekobena, T.C. Kofane, Internat. J. Modern Phys. B **32** 1850165 (2018).

[95] C.B. Tabi, A. Mohamadou, T.C. Kofané, Chaos **19** 043101 (2009)

[96] Y. Zhang, C. Yi, J. Zheng. Neural Comp and Appl. **20**, 1 - 7 (2011).

[97] M. Ge, Y. Yia, Y. Xu, L. Yang, Nonlinear Dynam. 515-523 (2018).

[98] A. S. Landsman and I. B. Schwartz, Nonlin. Biomed. Phys. 1 (2007).

[99] Y. H. Xie, Y. B. Gong, Y. H. Hao and X. G. Ma, Biophys. Chem. 146 126(2010).

[100] U. Ernst, K. Pawelzik and T. Geisel, Phys. Rev. Lett. 74 1570(1995).

[101] L.L. Rubchinsky, C. Park, R.M. Worth, Nonlinear Dynam. **68** 329-346 (2012).

[102] Q. Zhou, D.Q. Wei, Nonlinear Dynam. **105** 753-765 (2021).

[103] E. Kengne, E. Nkouankam, A. Lakhssassi, Nonlinear Dyn. **104**, 1 (2021).

[104] Y. Xu and J. Ma, Commun. Nonlinear Sci. Numer. Simul. **111**,(2022) 106426

List of publications

✠ **P. Nyifeh**, Z.T. Njitacke, C.N. Takembo, A. Mvogo, H. P. Ekobena Fouda, and J. Awrejcewicz, *Unstable wave patterns of information in neural network under light illumination and magnetic field*, International Journal of Modern Physics B (2024) 2450200.

✠ C.Ntahkie Takembo , **P. Nyifeh**, H. P. Ekobena Fouda, T.C. Kofané, *Modulated wave pattern stability in chain neural networks under high-low frequency magnetic radiation*, Communications in Nonlinear Science and Numerical Simulations Physica A **593** (2022) 126891.

Physica A 593 (2022) 126891

Contents lists available at ScienceDirect

Physica A

journal homepage: www.elsevier.com/locate/physa

Modulated wave pattern stability in chain neural networks under high–low frequency magnetic radiation

C. Ntahkie Takembo [a,*], P. Nyifeh [b], H.P. Ekobena Fouda [b], T.C. Kofane [c]

[a] Department of Electrical and Electronic Engineering, College of Technology, University of Buea I, P.O. Box 63, Buea, Cameroon
[b] Laboratory of Biophysics, Department of Physics, Faculty of Science, University of Yaounde I, P.O. Box 812, Yaounde, Cameroon
[c] Laboratory of Mechanics, Department of Physics, Faculty of Science, University of Yaounde I, P.O. Box 812, Yaounde, Cameroon

ARTICLE INFO

Article history:
Received 1 October 2021
Received in revised form 20 December 2021
Available online 11 January 2022

Keywords:
Integrate and Fire neural network
Electromagnetic induction
Modulational instability
High–low frequency electromagnetic radiation
Brain disorder

ABSTRACT

The dynamics of localized modulated action potential induced through modulational instability (MI) in a diffusive array of coupled neurons under high–low frequency magnetic radiation is investigated both analytically and numerically in the frame work of the improved Integrate and Fire model. The improved model includes the magnetic flux variable which takes into account the effect of electromagnetic induction set up from the variation in intracellular distribution of ions concentration during action potential propagation. The coupling between the magnetic flux variable and the membrane potential variable is realized using the memristor. High–low frequency magnetic radiation is imposed as periodic forcing currents on the magnetic flux variable. Through the powerful discrete multiple scale expansion, the nonlinear system of coupled equations are simplified to a lone nonlinear amplitude differential equation, on which linear stability analysis is carried out. It is found that high memristive coupling stabilizes the growth rate of instability. The stable and unstable zones of MI portrait are clearly dependent on the memristive coupling. Numerical experiment is performed and it confirms data picked from the unstable zone lead to the formation of localized modulated wave patterns with some traits of synchronization. Extensive numerical simulations revealed higher memristive coupling suppresses the excitability of the lattice to quiescent state, with homogeneous spatiotemporal patterns. The sample time series of the membrane potential showed high–low frequency magnetic radiation factor (N) promotes mode transition from spiking to bursting-like state. This could provide new insights to develop a new therapy in controlling abnormal brain state using magnetic radiation.

1. Introduction

Understanding the potential mechanism of information encoding and mode transition in the nervous system has been extensively investigated using neurons and neuronal networks [1–6]. Realistic neuron models are basically mathematical quantification of neuron's characteristics. These models are thus vital tools in exploring the biological behaviors of neurons. Neurons can effectively communicate either electrically, chemically, autaptically, or emphatically with neighbors [3,5,7–12]. Electrical communication is possible via the axons and dendrons of neurons as well as through gap junction proteins [7,8]. Chemical communication is through the use of neurotransmitters [9]. Autaptical communication is through the use of autapse; a specific synapse made from auxiliary loop [10–12]. Emphatic communication is by

* Corresponding author.
E-mail address: takembo.ntahkie@ubuea.cm (C.N. Takembo).

https://doi.org/10.1016/j.physa.2022.126891
0378-4371/

a transient electrical field produced by population of spikes [3,5]. Communication amongst neurons creates neuronal networks. Reliable neuronal networks relies can reproduce neuronal collective behaviors in an interacting environment. Indeed, the brain counts billions of interconnected neurons and synaptic links vital for efficient processing and exchange of information. Using neuronal networks, various complex cooperative behaviors such as pattern formation [6,13,14] and synchronization [15,16] have been extensively reported. The first neuron model made from nonlinear equations was presented by Hodgkin and Huxley [17]. It showed how membrane potential of neuron is related to the flow of currents across the cell membrane of the squid giant axon. From this seminal work, various simplified models have been constructed such as FitzHugh–Nagumo (FHN) model [18,19], Hindmarsh–Rose model(HR) [20], Morris–Lecar model [21], Izhikevich neuron model [22] and the Integrate and Fire (IF) model [23,24]. The choice of the different neuronal models are the ability of the model to exhibit the natural expression of a neuron and its computational efficiency. The merits of the Izhikevich neuron model is that it takes into account both biological concepts similar to the Hodgkin–Huxley model, and is computationally cost-effective, like the IF model [25].

Electromagnetic induction resulting from fluctuation in intracellular ion concentration during action potential initiation and propagation in excitable media has been recently included in various neurons and neuronal networks [26–30] . Lv et al. [26], investigated mode transition in the HR neuronal model under magnetic flow. Wang et al. [27], reported energy dependence on action potential of FHN neuron model under electromagnetic induction. Mi et al. [28], investigated dynamical behaviors such as synchronization and wave propagation of coupled neurons under field coupling. Ge et al. [31] discussed wave propagation and synchronization driven by chemical autapses in neuronal network. Takembo et al. [29], reported turbulent electrical activities of coupled FHN neurons under electromagnetic induction and high frequency electromagnetic radiations using the theory of modulational instability(MI). Liu et al. [32] reported mode transition in electrical activity of a hybrid neural model driven by electromagnetic induction. Hou et al. [33] reported different firing responses in an HR neural model driven by the depolarization field effect. Indeed, polarization and magnetization can occur when the network is exposed to continuous electromagnetic field and thus the distribution of charges and electric field in the cells are rearranged and regulated to change the response in action potential.

MI has been shown to be an efficient pathway to energy localization in biological molecules as well as discrete systems, in general [34,35]. It results from the interplay between nonlinearity and dispersion. Indeed, nonlinear waves and solitons initiated from MI have been showed to be suitable in describing nerve pulse in the neuronal networks with real applications in one and two dimensional couplings [36–38]. Although many research works many been carried out on various neuronal networks, the condition under which modulated impulse wave emerge and propagate in an improved IF neural networks exposed to high–low electromagnetic radiation have not yet been reported. This constitute the main motivation of our findings. In what follows, we shall develop an improved IF neuronal using the additional magnetic flux variable to describe the time varying electromagnetic field, and its feedback on the membrane potential realized using the memristor. We further apply the multiple scale expansion method to solve our resulting highly nonlinear IF model. Using parameters from our analytical predictions, numerical simulations will be performed.

2. Model equations and asymptotic expansion

The Integrate and Fire (IF) neuronal model combines biological rationality and computational efficiency [23,24]. It mimics the electrical activities of cortical neurons. According to Faraday's law of electromagnetic induction, an induced current is set up due to membrane potential fluctuation [29,39,40]. In order to include the effect of the induced current created, the magnetic flux variable and memristor are used. The improved IF neuronal model driven by a simulation current I is given by

$$\begin{aligned} \frac{dx}{dt} &= a - bx - k_1(\alpha + 3\beta\phi^2)x + I, \\ \frac{d\phi}{dt} &= kx - k_2\phi, \end{aligned} \tag{1}$$

where x and ϕ describe the membrane potential and magnetic flux variable, respectively. The term $k_1(\alpha + 3\beta\phi^2)x$ represents the induced current set up across the membrane of neuron due to membrane potential fluctuation. k_1 is the memristor coupling that bridges the membrane potential and the magnetic flux and hence the effect of electromagnetic induction is realized. $\alpha + 3\beta\phi^2$ represents memory conductance of flux-controlled memristor, in which, α represents constant conductance, β indicates the feedback rate of magnetic flux, and both depend on the memristor. k_2, and k are induction coefficients dependent on the media.

When synaptic connections are considered, neuronal network are designed, suitable for investigating the collective behaviors of neurons via pattern formation and synchronization. Based on the new IF model with electromagnetic induction, synaptic gap junction coupling with nearest neighbors interaction is proposed to enhance information exchange in the network. The dynamical equations for chain diffusive neuronal network under high–low frequency electromagnetic radiation ϕ_{ext} is given by

$$\begin{aligned} \frac{dx_n}{dt} &= a - bx_n - k_1(\alpha + 3\beta\phi_n^2)x_n + I + D(x_{n+1} - 2x_n + x_{n-1}), \\ \frac{d\phi_n}{dt} &= kx_n - k_2\phi_n + \phi_{ext}, \end{aligned} \tag{2}$$

where $\phi_{ext} = A\cos(2\pi ft)+B\cos(2\pi Nft)$. f and Nf are the frequencies of the magnetic radiation, with respective amplitudes A and B. N is a frequency factor describing the disparity in the two frequencies. The term $D(x_{n+1} - 2x_n + x_{n-1})$ represents the synaptic gap junction coupling term in the chain neural network with nearest neighbors interaction. The subscript n represents the node position in the network, $n = 1, \ldots, J$. J and D represents the number of neurons and strength of the gap junction, respectively. The parameters are selected as $a = 1.05, b = 1.80, I = 1.04, k = 0.9, \alpha = 0.40, \beta = 0.02, k_2 = 1.50, D = 0.50$ and $J = 500$. We use the above system of equations above to determine the conditions under which modulated plane wave solutions in the array becomes unstable, resulting in the formation of localized wave patterns with solitonic traits. The effect of electromagnetic induction via the memristor coupling are investigated under magnetic radiation.

The system of coupled nonlinear discrete differential equations represented by Eq. (2) is very difficult to be resolved analytically. In this light we proceeded by applying the powerful multiple scale expansion method [41,42] so as to derive a more suitable amplitude equation on which linear stability and instability have been successfully applied. In the process, the first lattice site in the network annotated $n = 1$ is stimulated at the original frequency Ω. It is with this natural frequency the system evolves in the absence of nonlinear effect. However, nonlinear effects are inherent in most biological systems including biological neural networks due to the nonlinear transmission of ions. Consequently, the natural frequency of our network deviates such that we can express the actual frequency and wave number as $\omega = \Omega + \epsilon\nu$ and $q_0 = q + \epsilon\frac{\nu}{u_g} + \epsilon^2 c_g \nu^2 + \cdots$, such that the group velocity and group velocity dispersion are expressed respectively as $\frac{1}{u_g} = (\frac{\partial q}{\partial \omega})_\Omega$, and $2c_g = (\frac{\partial^2 q}{\partial^2 \omega})_\Omega$. ω and q are the actual frequency and wave number, respectively. Indeed, ν is simply a small deviation from Ω. It is worth noting that at actual frequency simplifies to the natural frequency in case $\epsilon = 0$. We designed a state vector solution for Eq. (2) as $P_n(t) = \{x_n(t), \phi_n(t)\}$ having the generalized unperturbed forms given by

$$\begin{aligned} x_n(t) &= \int d\omega \hat{\chi}(\omega) e^{i(\omega t + q_0 n)}, \\ \phi_n(t) &= \int d\omega \hat{\phi}(\omega) e^{i(\omega t + q_0 n)}. \end{aligned} \tag{3}$$

where $\hat{P}(\omega) = \{\hat{\chi}(\omega), \hat{\phi}(\omega)\}$. We use the change of variables $\tau_n = \epsilon(t + n/u_g)$ and $\zeta_n = \epsilon^2 n$, with $c_g = 1$. The trial generalized solutions are then represented in the form

$$\begin{aligned} x_n(t) &= A(n,t)\chi(\zeta_n, \tau_n), \\ \phi_n(t) &= A(n,t)\phi(\zeta_n, \tau_n). \end{aligned} \tag{4}$$

with $A(n,t) = e^{i(qn+\Omega t)}$. This approach introduces a new network number m which supports a large grid. For a given n, the available the set of network points that can be considered are $\ldots, n-N, n, n+N, \ldots$, written as a function of the slow variable m as $\{\ldots, (n-N) \to (m-1), n \to m, (n+N) \to (m+1)\ldots,\}$. We set $\epsilon^2 = 1/N$ due to the pronounced discreteness effects.

By making use of the Fourier series in power of the parameter ϵ

$$\begin{aligned} x_n(t) &= \sum_{p=1}^{\infty} \epsilon^p \sum_{l=-p}^{p} \chi_p^l(\chi_n, \tau_n) A^l(n,t), \\ \phi_n(t) &= \sum_{p=1}^{\infty} \epsilon^p \sum_{l=-p}^{p} \phi_p^l(\zeta_n, \tau_n) A^l(n,t) \end{aligned} \tag{5}$$

With $\chi_p^{-l}(m,\tau) = (\chi_p^l(m,\tau))^*$ and $\phi_p^{-l}(m,\tau) = (\phi_p^l(m,\tau))^*$. We further proceed by substituting Eq. (5) in Eq.(2);

$$\begin{aligned} &\sum_{p=1}^{\infty} \epsilon^p \sum_{l=-p}^{p} \Big[\epsilon \frac{\partial}{\partial \tau} \chi_p^l(m,\tau) + i\omega l \chi_p^l(m,\tau)\Big] A^l(n,t) = a - b\Big(\sum_{p=1}^{\infty} \epsilon^p \sum_{l=-p}^{p} \chi_p^l(m,\tau) A^l(n,t)\Big) + I - k_1 \Big[\alpha + \\ &3\beta\Big(\sum_{p=1}^{\infty} \epsilon^p \sum_{l=-p}^{p} \phi_p^l(m,\tau) A^l(n,t)\Big)^2\Big] + D\Big[\sum_{p=1}^{\infty} \epsilon^p \sum_{l=-p}^{p} 2(\cos(ql)-1)\chi_p^l(m,\tau) + \epsilon(\frac{2i}{V_g})\sin(ql)\frac{\partial}{\partial \tau}\chi_p^l(m,\tau) \\ &\qquad + \epsilon^2(\frac{1}{V_g})^2 \cos(ql)\frac{\partial^2}{\partial \tau^2}\chi_p^l(m,\tau) + \epsilon^2 \times i\sin(ql)(\chi_p^l(m+1,\tau) - \chi_p^l(m-1,\tau))\Big] A^l(n,t), \end{aligned} \tag{6a}$$

$$\sum_{p=1}^{\infty} \epsilon^p \sum_{l=-p}^{p} \Big[\epsilon \frac{\partial}{\partial \tau} \phi_p^l(m,\tau) + i\omega l \phi_p^l(m,\tau)\Big] A^l(n,t) = k\Big(\sum_{p=1}^{\infty} \epsilon^p \sum_{l=-p}^{p} \phi_p^l(m,\tau) A^l(n,t)\Big) - k_2\Big(\sum_{p=1}^{\infty} \epsilon^p \sum_{l=-p}^{p} \phi_p^l(m,\tau) A^l(n,t)\Big). \tag{6b}$$

We solve the above coupled system Eq. (6a)–(6b) at different orders of ϵ, with the corresponding harmonics l. At the order $(1, l)$, with $l = 0$, we obtain

$$\chi_1^0(m,\tau) = \phi_1^0(m,\tau) = 0. \tag{7}$$

For $l = 1$, we obtain the dispersion relation

$$\Big[i\Omega - 2D(\cos(q) - 1) - b - \alpha k_1\Big]\Big[i\Omega + k_2\Big] = 0, \tag{8}$$

for which our system admits non-trivial solutions;

$$\begin{aligned} \chi_1^1(m,\tau) &= \chi(m,\tau), \\ \phi_1^1(m,\tau) &= \frac{k}{k_2 + i\Omega} \times \chi(m,\tau). \end{aligned} \tag{9}$$

At the order $(2, l)$, for $l = 0$, we obtain the solution

$$\chi_2^0(m,\tau) = \phi_2^0(m,\tau) = 0. \tag{10}$$

At $l = 1$, a system of equations with a zero determinant is obtained, satisfying the Fredholm condition given by

$$V_g = 2iDsin(q). \tag{11}$$

We search for the solution in the form

$$\begin{aligned} \psi_2^1(m,\tau) &= \pi(m,\tau), \\ \phi_2^1(m,\tau) &= \frac{k_1}{k_2 + i\Omega} \times \pi(m,\tau) - \frac{k_1}{(k_2 + i\Omega)^2}\frac{\partial \pi(m,\tau)}{\partial \tau} \end{aligned} \tag{12}$$

with $\chi(m,\tau)$ is being arbitrary function. At the order, for $l = 2$, we obtain solutions in the form

$$\chi_2^2(m,\tau) = \phi_2^2(m,\tau) = 0. \tag{13}$$

Finally, by resolving the system for $\chi_3^1(m,\tau)$ and $\phi_3^1(m,\tau)$, at $p = 3$ and $l = 1$, it yields the nonlinear amplitude equation;

$$-i\gamma(\chi_{m+1} - \chi_{m-1}) + \alpha_2\frac{\partial^2 \chi_m}{\partial \tau^2} + \beta_2|\chi_m|^2\chi_m = 0 \tag{14}$$

where

$$\begin{aligned} \gamma &= D\sin(q), \\ \beta_2 &= \frac{cos(q)}{4Dsin^2(q)}, \\ \alpha_2 &= 3\beta k_1 k^2\Big[\frac{1}{(k_2 + i\Omega)^2} + \frac{2}{(k_2)^2 - (i\Omega)^2}\Big] \end{aligned} \tag{15}$$

Eq. (14) is a nonlinear amplitude differential equation with coefficients γ, β_2 and α_2 dependent on the electromagnetic induction feedbacks and synaptic coupling strength between neurons. This spatiotemporal confirms information processing in the brain is not localized in a given neuron but it is done collectively within networks in both space and time. The global forms of Eq. (14) are well documented equations, already obtained in other domains of nonlinear physics including charge transport in DNA [43] and myocardial action potential propagation [44]. Eq. (14) will be used in the next section only for the linear stability analysis, while the direct numerical experiments will be performed on original model equation Eq. (2).

3. Linear stability analysis and modulated wave patterns

We consider the plane wave $\chi_m(\tau) = Ae^{i(\nu m - \Delta\tau)}$ as the solution for the amplitude Eq. (14). The complex amplitude and frequency are related to the perturbation wave number ν via the nonlinear dispersion relation

$$\Delta^2 = \frac{-\beta_2}{\alpha_2} \times \Big[|A|^2 + \frac{2D\sin(q)}{\beta_2}\sin(\nu)\Big]. \tag{16}$$

The wave solution above will be unstable for $\Delta^2 < 0$. This condition depends simultaneously on the signs of the terms $\frac{-\beta_2}{\alpha_2}$ and $|A|^2 + \frac{2D\sin(q)}{\beta_2}\sin(\nu)$. By fixing $\sin(\nu) = 1$, unstable wave will be generated for

$$|A|^2 > \frac{2D\sin(q)}{\beta_2} = A_{cr}^2, with \frac{-\beta_2}{\alpha_2} < 0. \tag{17}$$

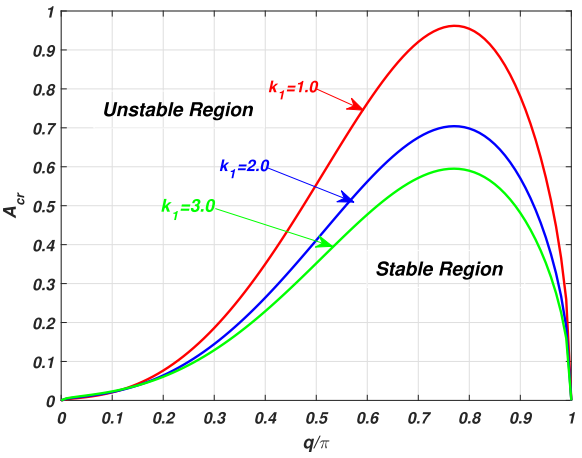

Fig. 1. Critical amplitude vs. wave number with $D = 0.50$, $k = 0.9, \alpha = 0.40, \beta = 0.02$ and $k_2 = 1.50$. The stable and unstable regions of modulational instability are presented. The growth rate of instability decreases with increases in the memristor coupling.

It is understood from the instability condition given by Eq. (14) that when the parameters fall inside the unstable zone, unstable wave pattern emerges in the network following the mechanism of modulational instability (MI). We plot the growth rate of instability versus the wave number q and present the results in Fig. 1. More so, the stable and unstable regions are clearly displayed. It is found that smaller values of the wave number falls in the unstable region and hence favors the formation of localized wave patterns. When performing our numerical simulations, we select $q = 0.1\pi$. Furthermore, by varying the values of the memristor coupling, it is observed that the growth rate of instability decreases. That is higher electromagnetic induction feedback reduces the critical amplitude. In order to validate this analytical prediction, we integrate numerically our generic model.

Indeed, the linear stability analysis cannot give impulse information about the long-time evolution of the modulated waves evolving in the network because it is based on the linearization around an unperturbed plane wave. In order to verify our analytical predictions, Eq. (2) is integrated numerically using the fourth-order Runge–Kutta computational scheme, with step size $h = 0.001$. The transient period for calculation is set at 10 000 time units. Initial conditions are chosen in accordance to the plane wave solution of Eq. (14). Indeed, initial conditions are perturbed plane waves having amplitude $A = 0.20$, wave number $q = 0.1\pi$ and modulation wave number $\nu = 0.5\pi$ picked from the unstable regions of the modulational instability as indicated on Fig. 1. To discern the effect of electromagnetic induction through the memristor coupling, on the bearing of localized structures by our discrete system, we set $k_1 = 1.20$, where the network is exposed to a high–low frequency electromagnetic radiation $\phi_{ext} = 25\cos(2\pi ft) + 25\cos(2\pi Nft)$, with $f = 0.04$ and $N = 10$. We note the intrinsic parameter values selected correspond to a point which belongs to the unstable region of the growth rate presented in Fig. 1, which according to the figure obtained, the instability is predicted for plane waves with these wave numbers. The 3D pattern of the emerging pattern of nerve impulse for a network of 500 identical cells is presented in Fig. 2, while the spatiotemporal pattern is presented in Fig. 3 [panel (a)] and the corresponding time series at the node position $n = 100$ [panel b_1], $n = 200$ [panel b_2] and $n = 400$ [panel b_3] are presented in Fig. 3.

It is found that the 3D pattern obtained in Fig. 2 are nonlinear waves with temporal periodic-like structures. Fig. 3 [panel (a)] presents the spatiotemporal pattern of the membrane potential of 500 neurons in the network, where Time runs from top to bottom and Lattice site from left to right. It consist of alternate band of bright and dark regions. In the bright regions, the neurons fires while in the dark regions, the neurons are at quiescent state. In this bright regions, different firing patterns are expected. The spatiotemporal patterns clearly portrait bright bands with different intensities brightness, suggesting mixed or irregular firing patterns. The time series presented in Fig. 3 presents mixed/irregular firing patterns of the network. These irregular firing patterns could be clearly due to the exposure of the network to electromagnetic radiation. This confirms the work reported in Ref. [45,46]. Furthermore, the time series taken at different lattice site and presented in Fig. 3 [panel $(b_1) - (b_3)$] show nonlinear waves pattern with similar dynamics, suggesting synchronization. This could be very powerful from biophysical perspective where intermittent neural synchronization is reported to be associated with Parkinson's disease [47]. The improved IF model exposed to high–low frequency electromagnetic radiation could thus be a vital prototype relevant for understanding the potential mechanism of intermittent synchrony in Parkinson disease. It is well known that depending on the value of the memristor coupling k_1 selected, one should expect different behaviors of the system. By increasing the strength of k_1, its effect on pattern formation are presented Fig. 4.

It is found in Fig. 4 that the spatiotemporal patterns are greatly modified as the value k_1 are changed. This confirms are analytical prediction, presented in Fig. 1. Indeed, higher electromagnetic induction feedback gain suppresses excitability ($k_1 = 2.90$ in Fig. 5(b) and $k_1 = 3.10$ in Fig. 5(c)), by reducing the spatiotemporal pattern to a homogeneous and quiescent

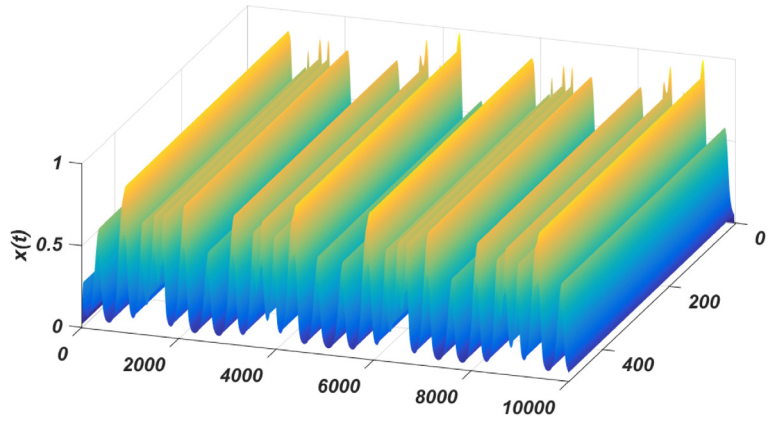

Fig. 2. 3D feature of the nerve pulse in a lattice with 50 cells and recorded over a period of t=10000, where k_1=1.20, D=0.50, A=25.0, B=25.0, f=0.04, N=10.

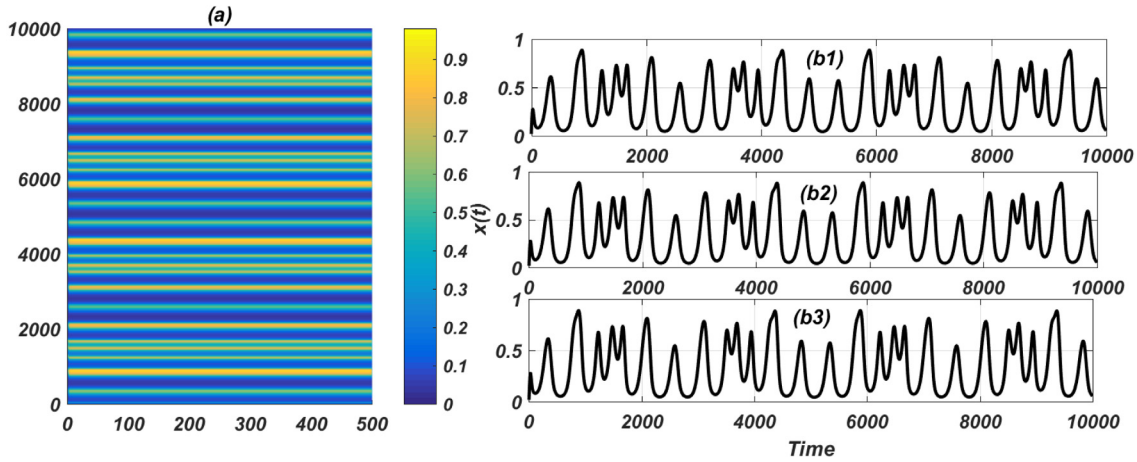

Fig. 3. Spatiotemporal (a) and temporal features (b) of the nerve impulse presented in Fig. 2.

state. Furthermore, we examine the effect of high–low frequency electromagnetic radiation on our network dynamics. Since we are using a superposition of two fields, we concentrate on the effect of disparity in frequency (N) of the two fields. The results are presented in Figs. 5 and 6.

It is observed that Fig. 5, as the value of N are increased, the localized patterns are modified. At a small value of N ($N = 1$ in Fig. 5(a)), the system presents regular spatiotemporal pattern, whereby the bright bands correspond to the regions where the neurons are firing. Indeed, the thin structures found in Fig. 5(a) correspond to individual spikes inside a burst. This is confirmed by the corresponding time series presented Fig. 6(a), where spikes are observed. It is found that as N increases as in Figs. 5(b) and 5(c), mode transition in firing state occurs(Figs. 6(b) and 6(c)). This factor (N) thus proofs efficient in ensuring rich dynamic states in the network. As future work, it could be interesting to investigate synchronization in memristive neurons with no synapse coupling [48].

4. Concluding remarks

Based on the law of electromagnetic induction, the Integrate and Fire neuronal model is improved to include the effects of electromagnetic induction and radiation using the magnetic flux variable. The memristor is used to bridge the magnetic flux and membrane potential. High–low frequency electromagnetic radiation is imposed on the magnetic flux variable as external stimuli. A network of the proposed model, created using synaptic connection with nearest neighbor interaction is used to study both analytically and numerically the emergence and propagation of localized wave patterns via the theory of modulational instability. It is found that the collective behaviors of neurons as well as the electrical activities are dependent on the distribution of magnetic flux. It reveals that electromagnetic induction can modulate the formation of wave patterns and mode in electrical activities. Under high–low frequency electromagnetic radiation,

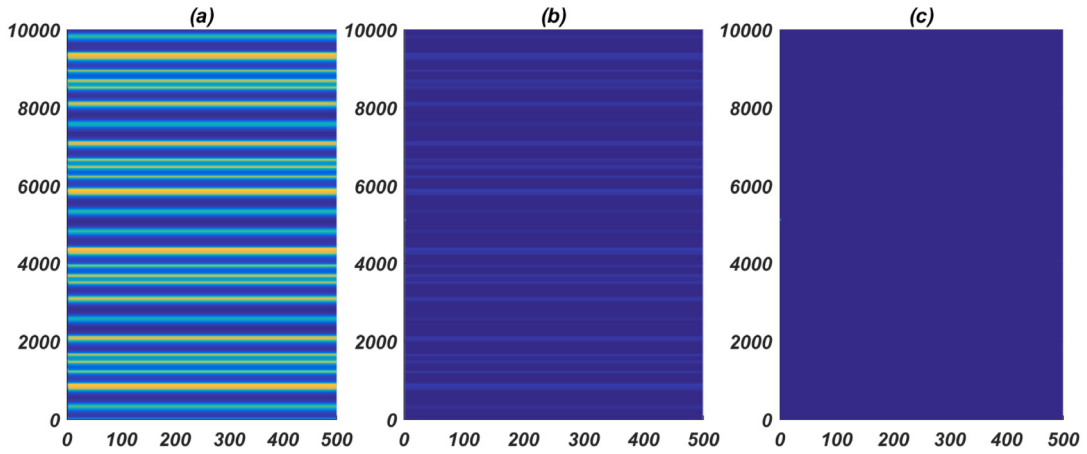

Fig. 4. Spatiotemporal patterns (a) k_1=2.50 (b) k_1=2.90 (c) k_1=3.10.

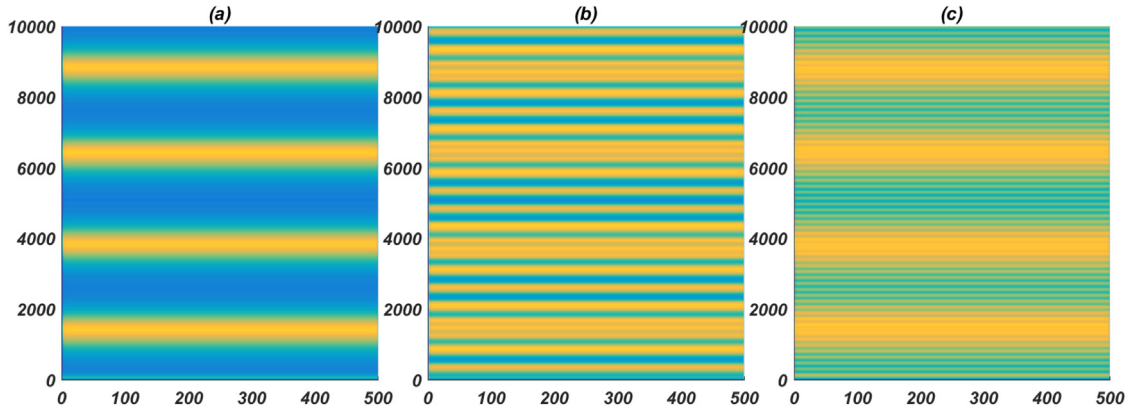

Fig. 5. Spatiotemporal patterns for n=200 (a) N=1 (b) N=10 (c) N=25.

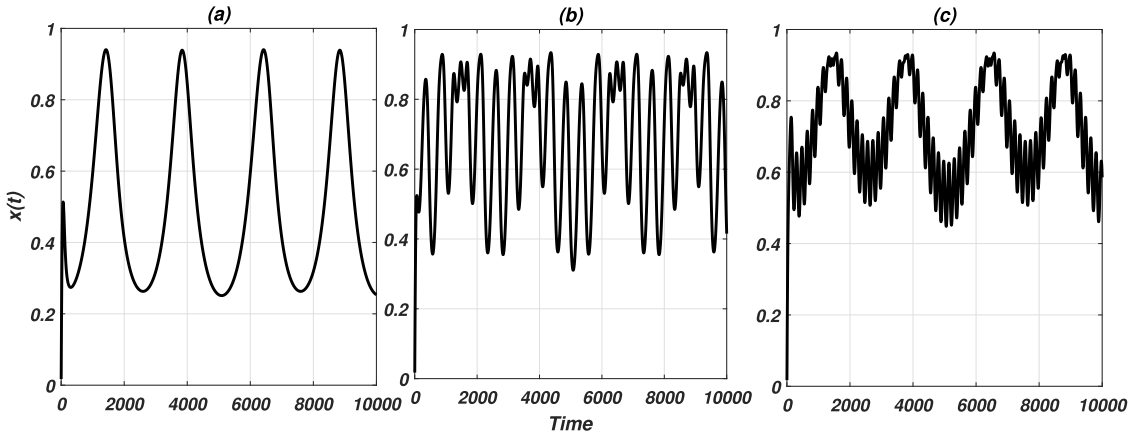

Fig. 6. Membrane potential time series patterns for n=200, I=1.04 (a) N=1 (b) N=10 (c) N=25.

the electromagnetic induction feedback gain via the memristor could effectively suppress excitability to a homogeneous spatiotemporal pattern, with quiescent state. Indeed, neuronal network can be deformed and wave propagation destroyed when exposed to continuous diverse electromagnetic radiations.

CRediT authorship contribution statement

C. Ntahkie Takembo: Conceptualization, Methodology, Software. **P. Nyifeh:** Data curation, Writing – original draft, Visualization, Investigation. **H.P. Ekobena Fouda:** Supervision. **T.C. Kofane:** Writing – review & editing.

Declaration of competing interest

The authors declare that they have no known competing financial interests or personal relationships that could have appeared to influence the work reported in this paper.

Data availability statement

The data sets generated during and/or analyzed during the current study are available from the corresponding author on reasonable request.

References

[1] C. Wang, J. Ma, Internat. J. Modern Phys. B 6 (2018) 32.
[2] S. Majhi, B.K. Bera, D. Ghosh, M. Perc, Phys. Life Rev. 28 (2019) 100–121.
[3] S. Majhi, D. Ghosh, Chaos 28 (2018) 083113.
[4] S. Doubla Isaac, Z. Tabekoueng Njitacke, J. Kengne, Int. J. Bifurcation Chaos 11 (2020) 30.
[5] I. Maina, C.B. Tabi, H.P. Ekobena, A. Mohamadou, T.C. Kofane, Chaos 25 (2015) 043118.
[6] C.N. Takembo, M. Ekonde Sone, Heliyon 7 (1) (2021) e06132.
[7] C.B. Tabi, A.S. Eteme, A. Mohamadou, T.C. Kofane, Chaos Solitons Fractals 123 (2019) 116.
[8] X.J. Sun, M. Perc, Q.S. Lu, J. Kurths, Chaos 20 (2018) 033116.
[9] A.S. Eteme, C.B. Tabi, A. Mohamadou, Commun. Nonlinear Sci. Numer. Simul. 43 (2017) 211.
[10] G. Zhang, C. Wang, F. Alzahrani, F. Wu, X. An, Chaos Solitons Fractals 108 (2018) 15–24.
[11] C.S. Herrmann, A. Klaus, Int. J. Bifurcation Chaos 14 (2) (2004) 623–633.
[12] E. Yilmaz, V. Baysal, M. Ozer, M. Perc, Physica A 444 (2016) 538–546.
[13] A. Mvogo, C.N. Takembo, H.P. Ekobena, T.C. Kofane, Phys. Lett. A 381 (2017) 2264–2271.
[14] H.T. Wang, Y. Chen, Nonlinear Dynam. 85 (2016) 881–891.
[15] Q.Y. Wang, M. Perc, Z. Quan, G. Chen, Nonlinear Dynam. 80 (2009) 026206.
[16] J. Ma, F.Q. Wu, C.N. Wang, Internat. J. Modern Phys. B 31 (2017) 1650251.
[17] A.L. Hodgkin, A.F. Huxley, J. Physiol. 117 (1952) 500–544.
[18] R. FitzHugh, Biophys. J. 1 (6) (1961) 445–466.
[19] J. Nagumo, S. Arimoto, S. Yoshizawa, Proc. IRE 50 (1962) 2061–2070.
[20] J.L. Hindmarsh, R.M. Rose, Nature 296 (1982) 162–164.
[21] C. Morris, H. Lecar, Biophys. J. 35 (1981) 193–213.
[22] M.S. Kafraj, F. Parastesh, S. Jafari, Chaos Solitons Fractals 137 (2020) 109782.
[23] A.N. Burkitt, Biol. Cybern. 95 (2006) 1–19.
[24] W. Teka, T.M. Marinov, F. Santamaria, PLoS Comput. Biol. 10 (2014) e1003526.
[25] E.M. Izhikevich, IEEE Trans. Neural Netw. 14 (2003) 1569–1572.
[26] M. Lv, C. Wang, R. Guodong, J. Ma, X. Song, Nonlinear Dynam. 85 (2016) 1479–1490.
[27] G. Wang, Y. Xu, M. Ge, L. Lu, Y. Jia, Int. J. Electron. Commun.(AEU) 120 (2020) 153209.
[28] M. Lv, J. Ma, Y.G. Yao, F. Alzahrani, Sci. China Tech. Sci. 62 (2019) 448–457.
[29] C.N. Takembo, A. Mvogo, H.P. Ekobena, T.C. Kofane, Nonlinear Dynam. 95 (2) (2019) 1067–1078.
[30] Y. Xu, Y. Jia, J.B. Kirunda, J. Shen, M. Ge, L. Lu, Q. Pei, Complexity 2 (2018) 1–13.
[31] M. Ge, Y. Jia, Y. Xu, L. Lu, H. Wang, Y. Zhao, Appl. Math. Comput. 352 (2019) 136–145.
[32] Y. Liu, J. Ma, Y. Xu, Y. Jia, Int. J. Bifurcation Chaos 29 (2019) 1950156.
[33] Z. Hou, J. Ma, X. Zhan L. Yang, Y. Jia, Chaos Solitons Fractals 142 (2021) 110522.
[34] T. Dauxois, M. Peyrard, Physics of Solitons, Cambridge University Press, Cambridge, 2006.
[35] A.S. Tankou, C.N. Takembo, G.H. Ben-Bolie, P. Owona Ateba, PLoS ONE 14 (6) (2019) e0214989.
[36] C.N. Takembo, A. Mvogo, H.P. Ekobena, T.C. Kofane, Nonlinear Dyn. 381 95 (2) (2019) 1079–1098.
[37] C.N. Takembo, A. Mvogo, H.P. Ekobena, T.C. Kofane, Nonlinear Dynam. 96 (2019) 1083–1093.
[38] C.N. Takembo, A. Mvogo, H.P. Ekobena, T.C. Kofane, Internat. J. Modern Phys. B 32 (2018) 1850165.
[39] M. Lv, J. Ma, Neurocomputing 205 (2016) 375–381.
[40] J. Ma, F. Wu, T. Hayat, P. Zhou, J. Tang, Physica A 486 (2017) 508–516.
[41] J. Leon, M. Manna, Phys. Rev. Lett. 83 (1999) 2324.
[42] C.B. Tabi, I. Maïna, A. Mohamadou, H.P.F. Ekobena, T.C. Kofané, Physica A 435 (2015) 1–14.
[43] C.B. Tabi, A. Mohamadou, T.C. Kofane, Chaos 19 (2009) 043101.
[44] C.N. Takembo, H.P. Ekobena, Sci. Rep. 10 (1) (2020) 15087.
[45] Y. Zhang, F. Wu, C. Wang, J. Ma, Physica A 521 (2019) 519–530.
[46] M. Ge, Y. Yia, Y. Xu, L. Yang, Nonlinear Dynam. (2018) 515–523.
[47] L.L. Rubchinsky, C. Park, R.M. Worth, Nonlinear Dynam. 68 (2012) 329–346.
[48] Q. Zhou, D.Q. Wei, Nonlinear Dynam. 105 (2021) 753–765.

International Journal of Modern Physics B
(2024) 2450200 (12 pages)

DOI: 10.1142/S021797922450200X

World Scientific
www.worldscientific.com

Unstable wave patterns of information in neural network under light illumination and magnetic field

P. Nyifeh*, Z. T. Njitacke†,‡, C. N. Takembo*,†,§, A. Mvogo*,
H. P. Ekobena Fouda* and J. Awrejcewicz†

*Laboratory of Biophysics, Department of Physics,
Faculty of Science, University of Yaounde I, P.O. Box 812,
Yaounde, Cameroon

†Department of Electrical and Electronic Engineering,
College of Technology, University of Buea, P.O. Box 63, Buea, Cameroon

‡Department of Automation, Biomechanics and Mechatronics,
Faculty of Mechanical Engineering, Lodz University of Technology,
Lodz, Poland
§takembo.ntahkie@ubuea.cm

Received 19 January 2023
Revised 10 March 2023
Accepted 12 March 2023
Published 26 May 2023

Functional neurons built from neural circuits are capable of perceiving and processing external signals such as light illumination and magnetic radiation, by converting the physical signals into modulated bioelectric signals called action potential with diverse forms and shapes. Through modulational instability (MI), modulated wave formation and pattern transition are studied in a chain memristive network of 100 photosensitive neurons. Memristors and photocells are incorporated in a simple FitzHugh–Nagumo neuron to detect and process the external magnetic flux and light illumination. To determine regions of modulated wave formation, linear stability analysis is performed on a nonlinear envelope equation which resulted from the asymptotic expansion of the generic dynamical equations. The growth rate of MI is plotted and the distinct zones of stable/unstable MI are presented. We confirm the analytical result through numerical simulations whereby the initial plane wave solutions lead to the emergence of localized structures with traits of spiking, bursting and chaotic states. High-frequency photocurrent changes orderly localized patterns to chaotic-like patterns while high-frequency magnetic flux promotes pattern transition from bursting to 2-period spiking state and a 4-period spiking state. This could provide an adequate way to influence the behaviors of artificial neurons as well as potential mechanism of information coding in the nervous system.

Keywords: Neural network; photocell; memristor; asymptotic expansion; solitons; bifurcation.

PACS numbers: 87.19.La; 05.45.–a; 02.60.Cb; 05.45.Tp; 05.45.Xt; 05.45.Yv.

§Corresponding author.

1. Introduction

Advances in artificial intelligence and brain science have drew much attention recently as they have largely contributed new knowledge on the potential mechanism of information processing in the nervous system related to learning, memory, choosing and cognition.[1–3] Also, proper understanding of the intelligent brain-like algorithm could be helpful in inventing and improving deep learning calculation and theory,[4–6] which are very useful tools in designing intelligent controllers and equipments.[7,8] To estimate various neural activities within the brain and its environ, many biophysical laws governing the underlined neural activities have been derived based on various neural models and maps. Various characteristic states such as quiescent, bursting, spiking and chaotic have been accurately mimicked as observed from biological experiments. Recent characteristic state called chimera state[9,10] has equally been detected in neuronal systems. These states are very essential in monitoring the normal electrical activities of the nervous system. They are equally vital elements in predicting abnormal behaviors especially when the nervous system is either attacked or injured thereby preventing collapse and death in extreme cases.

Hodgkin and Huxley[11] developed the first neuronal model, describing neuronal potential in quantitative terms using the dynamics of ion current via gated channels in a squid axon. Afterwards, many other simplified and computationally efficient models were derived to reproduce the essentials of neuronal electrical activity. These include FitzHugh–Nagumo model,[12,13] Morris Lecar,[14] Integrate and Fire model,[15] Izhikevich model[16] and many others.[17,18] The criterion for choosing a particular neural model is principally based on its ability to mimic the natural expressions of neurons and neural networks as well as the computational efficiency.

In neurodynamics and computational neuroscience, many neural models have been built from diverse neural circuits to replicate the processes of neural signals.[19,20] Reliable nonlinear circuits can be designed and tamed to reproduce consistently the various characteristics states of neurons as obtained from real biological experiments. In light of this, simple and coupled neural circuits could be used to realize complex dynamical and collective-cooperative processes related to wave propagation, pattern formation and synchronization.[21,22] From the knowledge of synaptic plasticity, various memristive and hybrid synapses derived respectively, from memristor and a combination of capacitors, inductor, resistor have been used to achieve field coupling between circuits. Josephson junction[24,25] has equally been employed in coupling two circuits as well as to discern the effect of magnetic flux. In order to encode optical signal, phototube is incorporated in oscillating circuit. For example, Liu *et al.*[26] used photocell to activate a simple FitzHugh–Nagumo neuron and an external optical signal is imposed to excite the photocell in order to generate a time-varying current source. The main characteristics of biological neurons such as quiescent, spiking, bursting, and even chaotic behaviors were observed by activating the phototube. Zhang *et al.*[27] used magnetic flux-controlled memristor and an ideal Josephson junction to build a simple neural circuit and estimate the effect of the magnetic field

on neural activities. It's very relevant to build a reliable FitzHugh–Nagumo (FHN) neural network by incorporating memristors and photocells in the simple FHN network so as to replicate the processes of neural signals as obtained in biological experiments.

The excitability properties of neurons and neuronal networks related to learning, information coding, memory and disease state are greatly affected by filtered signals. Yu *et al.*[28] studied the filtering characteristic of Hodgkin–Huxley neuron and observed that the filtering capability of the neuron is modulated by the excitation level received from the filtered signal, and is stronger around the excitation threshold. Noise and many other external signals could enhance the ability of neuron to detect weak signals. Wang *et al.*[29] investigated chaotic resonance in a neuron subjected to electromagnetic induction and found that there exists an optimal chaotic current intensity that ensures the excellent detection of weak signal in an isolated Izhikevich neuron. Furthermore Hou *et al.* [30] studied the firing response of a Hindmarsh–Rose neuron exposed to a depolarization field and then external current forcing. It was found that the firing pattern is transformed from single busting to intermittent multimodel busting as the frequency and amplitude of electric field were increased. Furthermore, a reliable neural network would permit the adequate evaluation of the sufficient conditions under which modulated impulse signals emerge and propagate in the nervous systems. The mathematical basis for the formation of modulated signals in nonlinear lattices is modulational instability (MI).[31–34]

MI is one of the direct and efficient techniques to detect wave pattern structures related to information coding in neuronal networks under the permanent competition between nonlinear and dispersive effects.[35] MI became so useful after having observed that solitons and nonlinear waves were appropriate to describe nerve impulses. MI has been widely applied in discussing modulated information transport along nonlinear electrical transmission lines.[36,37] Within the neural network and cardiac tissue, MI has been widely used in discussing interneural communication and information processing related to various physiological and pathological phenomena.[38,39] In Refs. 38 and 39 the conditions under which slightly perturbed plane wave impulse solutions become unstable in cardiac tissue were discussed in one dimension and two dimensions. Under suitable balance between nonlinear and dispersive effects, plane impulse waves break into trains of soliton-like structures whose behaviors are very sensitive to parameter variations. Despite several investigations reported on pattern formations in coupled neural circuits and networks, no contribution has so far been dedicated towards modulated wave stability formations in photosensitive neural networks exposed to external magnetic field.

In this paper, we apply the powerful discrete asymptotic expansion method to solve the generic system of equations derived from memristive network of photosensitive neurons. This results in an envelope equation on which linear stability analysis is performed. Using data from the analytical results, numerical experiments are carried out and the presence of modulated signals sensitive to light illumination and magnetic radiation are confirmed.

2. Model, Scheme and Discussion

Phototube and memristor incorporated into the branches of a nonlinear circuit could yield an output voltage controlled by light illumination and electromagnetic induction, respectively. In this way, the biological neuron is thought of as an intelligent and smart processor such that functional nonlinear circuit could be built to perform similar functions. The memristive neuron has been presented in Refs. 15 and 16 while the photosensitive neuron has been presented in Ref. 22. The memristive photosensitive neuron was presented by Njitacke *et al.* in 2023.[23] Dimensionless equations of the memristive photosensitive neuron are given by

$$\begin{cases} \dot{x} = (1-\varepsilon)x - \dfrac{1}{3}x^3 - y + a_1\sin(\omega_1 t + l_a) - k_0(-\alpha - 3\beta\varphi^2)(x - e_f), \\ \dot{y} = c(x + a - by), \\ \dot{\varphi} = k_1 x - k_2\varphi + a_2\sin(\omega_2 t). \end{cases} \tag{1}$$

The term $a_1\sin(\omega_1 t + l_a)$ is a time varying external forcing that maps the periodic photocurrent from the phototube due to light illumination. Indeed, a periodic photocurrent is used as it is controlled by external illumination. The term $-k_0(-\alpha - 3\beta\varphi^2)(x - e_f)$ is the negative feedback memristive current originating from electromagnetic induction due to the internal effect of bioelectricity from ions exchange across the cell membrane as well as exposure to external magnetic flux. k_0 is the memristive coupling strength that couples the membrane potential (x) and the magnetic flux variable (φ).[40,41] Also, e_f denotes a reversal potential in the memristive channel. The term $a_2\sin(\omega_2 t)$ is a periodic stimulus that maps external magnetic flux forcing controlled by electromagnetic radiation exposure.[42] The variable y is the slow current or recovery variable meanwhile $-k_2\varphi$ measures the magnetic flux leakage.

The photosensitive memristive neurons are considered to be coupled locally in a chain with nearest neighbor interaction. The network can be written as follows:

$$\begin{cases} \dot{x}_i = (1-\varepsilon)x_i - \dfrac{1}{3}x_i^3 - y_i + a_1\sin(\omega_1 t + l_a) - k_0(-\alpha - 3\beta\varphi_i^2)(x_i - e_f) \\ \qquad + D(x_{i+1} - 2x_i + x_{i-1}), \\ \dot{y}_i = c(x_i + a - by_i), \\ \dot{\varphi}_i = k_1 x_i - k_2\varphi_i + a_2\sin(\omega_2 t), \end{cases} \tag{2}$$

with $i = 1, 2, \ldots, N$. N is the scale of the network while D is the strength of the synaptic coupling, and i is the location of the node. The rest of the model parameters are set at $\epsilon = 0.25, D = 0.05, a = 0.7, b = 8.0, a_1 = 0.6, a_2 = 0.6, \alpha = 0.01, \beta = 0.3, k_0 = 5.7, k_1 = 0.01, k_2 = 1.8, \omega_1 = 0.5, \omega_2 = 10, l_a = 0.1$ and $e_f = 0.99$. In what follows, we apply the discrete asymptotic expansion method to solve the above generic system of equations.

3. Discrete Asymptotic Expansion Method

Based on the discrete asymptotic expansion method, the solutions to the system of equations given by Eq. (2) are considered as wave packets, whereby the amplitudes and carrier waves are kept discrete.[31] This approach permits us to obtain a more manipulable equation from Eq. (2) for which linear stability analysis will be discussed.

In the process, the stimulation of the first neuron in the chain network initiates an action potential (wave packet) having oscillation angular frequency ω and wave number k. Due to nonlinear effects within the network, ω and k deviate by ϑ from the natural frequency ω' and k'. This is summarized by the relation: $\omega = \omega' + \epsilon\vartheta$ and $k = k' + \epsilon\frac{\vartheta}{u_g} + \epsilon^2 c_g \vartheta^2 + \ldots$, with $u_g = \frac{\partial\omega}{\partial k}$, and $\frac{1}{2c_g} = \frac{\partial^2\omega}{\partial^2 k}$. Furthermore, by introducing a new network number m that supports a large grid in such a way that for any i, possible sets of network points $\ldots, i-N, i, i+N, \ldots$, are taken as a function of the slow variable m as $\{\ldots,(i-N)\to(m-1),\ i\to m,\ (i+N)\to(m+1)\ldots,\}$. Consequently, the solutions of Eq. (2) can be expressed as Fourier expansions, whose components are calculated in a Taylor series in powers of ϵ given as follows:

$$U_i(t) = \sum_{p=1}^{\infty} \epsilon^p \sum_{s=-p}^{s=p} \hat{U}_p^{\,s}(\zeta_i, \tau_i) e^{j(ki+\omega t)}, \tag{3}$$

with $U_i(t) = \{x_i(t), y_i(t), \varphi_i(t)\}$ and $\hat{U_p^s}(\zeta_i,\tau_i) = \{\hat{x_p^s}(\zeta_i,\tau_i), \hat{y_p^s}(\zeta_i,\tau_i)), \hat{\varphi_p^s}(\zeta_i,\tau_i)\}$ being the slowly modulated amplitude of the plane wave $e^{j(ki+\omega t)}$, where $j^2 = -1$, $\tau_i = \epsilon(t + i/u_g)$ and $\zeta_i = \epsilon^2 i$. The slowly modulated amplitude $\hat{U}_p^{(l)}$ respects the reality condition $\hat{U}_p^{(-l)} = (\hat{U}_p^{\,l})^*$. By substituting Eq. (3) in Eq. (2), we obtain the system of equations:

$$\begin{aligned}
&\sum_{p=1}^{\infty} \epsilon^p \sum_{s=-p}^{p} \left[\epsilon \frac{\partial}{\partial\tau} x_p^s(m,\tau) + j\omega s x_p^s(m,\tau)\right] A^s(i,t) \\
&\quad = (1-\varepsilon)\sum_{p=1}^{\infty}\epsilon^p\sum_{s=-p}^{p} x_p^s(m,\tau)A^s(i,t) - \frac{1}{3}\left(\sum_{p=1}^{\infty}\epsilon^p\sum_{s=-p}^{p} x_p^s(m,\tau)A^s(i,t)\right)^3 \\
&\qquad - \sum_{p=1}^{\infty}\epsilon^p\sum_{s=-p}^{p} y_p^s(m,\tau)A^s(i,t) - k_0\left[-\alpha - 3\beta\left(\sum_{p=1}^{\infty}\epsilon^p\sum_{s=-p}^{p}\varphi_p^s(m,\tau)A^s(i,t)\right)^2\right] \\
&\qquad \times \left[\sum_{p=1}^{\infty}\epsilon^p\sum_{s=-p}^{p} x_p^s(m,\tau)A^s(i,t) - e_f\right] + D\left[\sum_{p=1}^{\infty}\epsilon^p\sum_{s=-p}^{p}\big(2(\cos(ks)-1)x_p^s(m,\tau)\right. \\
&\qquad + \epsilon\left(\frac{2j}{u_g}\right)\sin(ks)\frac{\partial}{\partial\tau}x_p^s(m,\tau) + \epsilon^2\left(\frac{1}{u_g}\right)^2\cos(ks)\frac{\partial^2}{\partial\tau^2}x_p^s(m,\tau) + \epsilon^2(j\sin(ks)) \\
&\qquad \left.\times\ (x_p^s(m+1,\tau) - x_p^s(m-1,\tau))\right] A^s(i,t) + a_1\sin(\omega_1 t + l_a),
\end{aligned} \tag{4a}$$

$$\sum_{p=1}^{\infty}\epsilon^p\sum_{s=-p}^{p}\left[\epsilon\frac{\partial}{\partial\tau}y_p^s(m,\tau)+j\omega s y_p^s(m,\tau)\right]A^s(i,t)$$
$$=c\left[\sum_{p=1}^{\infty}\epsilon^p\sum_{s=-p}^{p}x_p^s(m,\tau)A^s(i,t)+a-b\left(\sum_{p=1}^{\infty}\epsilon^p\sum_{s=-p}^{p}y_p^s(m,\tau)A^s(i,t)\right)\right], \quad (4b)$$

$$\sum_{p=1}^{\infty}\epsilon^p\sum_{s=-p}^{p}\left[\epsilon\frac{\partial}{\partial\tau}\varphi_p^s(m,\tau)+j\omega s\varphi_p^s(m,\tau)\right]A^s(i,t)$$
$$=k_1\left(\sum_{p=1}^{\infty}\epsilon^p\sum_{s=-p}^{p}x_p^s(m,\tau)A^s(n,t)\right)+k_2\left(\sum_{p=1}^{\infty}\epsilon^p\sum_{s=-p}^{p}\varphi_p^s(m,\tau)A^s(i,t)\right)$$
$$+\ a_2\sin(\omega_2 t). \quad (4c)$$

For different values of p, Eqs. (4a)–(4c) are solved at different orders of ϵ. At the first order $p=1$, the order ϵ^1, gives the system

$$\sum_{s=-1}^{s=1}[(js\omega-1+\varepsilon+\alpha k_0-2D(\cos ks-1))x_1^s+y_1^s]A^s(i,t)=0,$$
$$\sum_{s=-1}^{s=1}[-cx_1^s+(js\omega+bc)y_1^s]A^s(i,t)=0, \quad (5)$$
$$\sum_{s=-1}^{s=1}[-k_1x_1^s+(js\omega+k_2)\varphi_1^s]A^s(i,t)=0.$$

Solving Eq. (5) for $s=0$ yields $U_1^0(m,\tau)=0$ $(x_1^0(m,\tau)=y_1^0(m,\tau)=\varphi_1^0(m,\tau)=0)$. At $s=1$, we obtain a linear system of equations in terms of x_1^1, y_1^1 and φ_1^1 summarized by

$$AU_1^1(m,\tau)=0, \quad (6)$$

with,

$$A=\begin{pmatrix}j\omega-1+\varepsilon-\alpha k_0-2D(\cos(k)-1) & 1 & 0\\ -c & j\omega+bc & 0\\ -k_1 & 0 & j\omega+k_2\end{pmatrix} \text{ and } U_1^1=\begin{pmatrix}x_1^1\\ y_1^1\\ \varphi_1^1\end{pmatrix}.$$

Since $U_1^1(m,\tau)\neq 0$, it implies the determinant of A is null, giving the relation

$$[j\omega-1+\varepsilon-\alpha k_0-2D(\cos(k)-1)]\times(j\omega+bc)+c=0. \quad (7)$$

The dispersion relation given by Eq. (7) above is dependent on the memristive coupling k_0. The corresponding group velocity is obtained as

$$u_g=\frac{2jD\sin(k)(j\omega+bc)}{2j\omega+bc-1+\varepsilon+\alpha k_0-2D(\cos(k)-1)}. \quad (8)$$

If we let $x_1^1(m,\tau) = x_m$ then we can solve for $y_1^1(m,\tau)$ and $\varphi_1^1(m,\tau)$ in Eq. (6) such that

$$\begin{aligned} y_1^1(m,\tau) &= \left(\frac{c}{j\omega + bc}\right) x_m, \\ y_1^1(m,\tau) &= \left(\frac{k_1}{j\omega + k_2}\right) x_m. \end{aligned} \tag{9}$$

In the same manner, for $p = 1, 2$, the order ϵ^2,$s = 0$ gives a system of equations in terms of x_2^0, y_2^0 and φ_2^0;

$$\begin{aligned} x_2^0(m,\tau) &= \frac{6\beta k_0 e_f k_1^2}{(\varepsilon - 1 - \alpha k_0 + 1/b)((j\omega)^2 - k_2^2)} |x_m|^2, \\ y_2^0(m,\tau) &= \frac{6\beta k_0 e_f k_1^2}{b(\varepsilon - 1 - \alpha k_0 + 1/b)((j\omega)^2 - k_2^2)} |x_m|^2, \\ \varphi_2^0(m,\tau) &= \frac{6\beta k_0 e_f k_1^3}{k_2(\varepsilon - 1 - \alpha k_0 + 1/b)((j\omega)^2 - k_2^2)} |x_m|^2 \end{aligned} \tag{10}$$

and for $s = 1$ we obtain a system of equations in terms of x_2^1, y_2^1 and φ_2^1 such that with $x_2^1 = \delta(m,\tau)$, we obtain:

$$\begin{aligned} y_2^1(m,\tau) &= \frac{c}{(j\omega + bc)} \delta(m,\tau) - \frac{c}{(j\omega + bc)^2} \frac{\partial x_m}{\partial \tau}, \\ \varphi_2^1(m,\tau) &= \frac{k_1}{(j\omega + k_2)} \delta(m,\tau) - \frac{ck_1}{(j\omega + bc)^2} \frac{\partial x_m}{\partial \tau} \end{aligned} \tag{11}$$

and for $s = 2$ we obtain a system of equations in terms of x_2^2, y_2^2 and φ_2^2:

$$\begin{aligned} x_2^2(m,\tau) = \Lambda x_m^2 &= \frac{-3\beta k_0 e_f k_1^2 (2j\omega + bc)}{[(2j\omega + bc)(2j\omega + \lambda) + c](j\omega + k_2)^2} x_m^2, \\ x_2^2(m,\tau) &= \frac{-3c\beta k_0 e_f k_1^2}{[(2j\omega + bc)(2j\omega + \lambda) + c](j\omega + k_2)^2} x_m^2, \\ \varphi_2^2(m,\tau) &= \frac{-3\beta k_0 e_f k_1^3 (2j\omega + bc)}{[(2j\omega + bc)(2j\omega + \lambda) + c](j\omega + k_2)^2 (2j\omega + k_2)} x_m^2, \end{aligned} \tag{12}$$

with $\lambda = -1 + \varepsilon - \alpha k_0 - 2D(\cos(2k) - 1)$. Finally, when $p = 1, 2, 3$, the order ϵ^3 gives a system of equations in x_3^s, y_3^s and φ_3^s. For $s = 1$ we obtain a system of equations in terms of x_3^1, y_3^1 and φ_3^1 such that by making use of previous relations, where $x(m,\tau) = x_m(\tau)$, we obtain

$$jP(x_{m+1} - x_{m-1}) + Q\frac{\partial^2 x_m}{\partial \tau^2} + R|x_m|^2 x_m = 0, \tag{13}$$

where

$$P = D\sin(k),$$
$$Q = \frac{-D\cos(k)}{(ju_g)^2} - \frac{c}{(j\omega + bc)^3}, \tag{14}$$
$$R = 3\beta k_0 k_1^2\left(\frac{1}{(k_2 + j\omega)^2} + \frac{2}{(k_2)^2 - (j\omega)^2}\right) - 1 - \frac{6\beta k_0 e_f k_1^2 \Lambda}{(k_2 - j\omega)(k_2 + 2j\omega)}.$$

Equation (13) obtained above is a nonlinear differential difference equation having features of Cubic Nonlinear Schrödinger Equation (CNSE). In the next section, we will perform linear stability analysis.

4. Stability Analysis and Modulated Wave Patterns

Due to MI in nonlinear and dispersive media, a plane impulse wave could become unstable under modulation. By injecting a perturbation $x_m(\tau) = x_0 e^{j(\mu m - \pi\tau)}$ into Eq. (13), the nonlinear relation obtained is given by

$$\pi^2 = \frac{1}{Q'} \times \left(\frac{-2D\sin(k)\sin(\mu)}{R} + |x_0|^2\right), \tag{15}$$

with $Q' = \frac{Q}{R}$. Modulated wave emerges when $\pi^2 < 0$. By taking into consideration discreteness effect, $\sin(\mu)$ is bounded and thus we set $\mu = \frac{\pi}{2}$. If $Q' < 0$ then unstable wave is possible when

$$|x_0|^2 > \frac{2D\sin(k)}{R} = x_{\text{cr}}^2. \tag{16}$$

The graph of growth rate related to the critical amplitude $x_{\text{cr}} = x_{\text{cr}}(k)$ is plotted for synaptic coupling strength $D = 0.04$ and presented in Fig. 1.

The critical amplitude-wave number parameter space in Fig. 1 is divided into two distinct regions, namely the Stable Region (SR) and Unstable Region (UR). It is expected from numerical findings that when parameters are picked from UR, modulated wave will emerge from the network lattice. In numerical simulation, we used fourth-order Runge–Kutta computational scheme, with step time $h = 0.01$ and periodic boundary conditions. The initial conditions are selected to correspond to slightly modulated plane waves, having corresponding normal and perturbed wave numbers set at $k = 0.1\pi$ and $\mu = 0.5\pi$. Numerical simulation permits the study of the long-time evolution of the modulated waves evolving in the network under memristive, photosensitive parameter. This evolution in patterns is related to the hidden structure of information coding in the network.[35]

First, we examine the effect of light illumination on the spatiotemporal patterns of membrane potential. We fix the amplitude at $a_1 = 0.4$ and we evaluate the possible dependence on information coding on the frequency ω_1. The results are presented in Figs. 2(a)–2(c). In Fig. 2(a), $\omega_1 = 0.10$, in Fig. 2(b), $\omega_1 = 0.18$ and in Fig. 2(c), $\omega_1 = 0.20$.

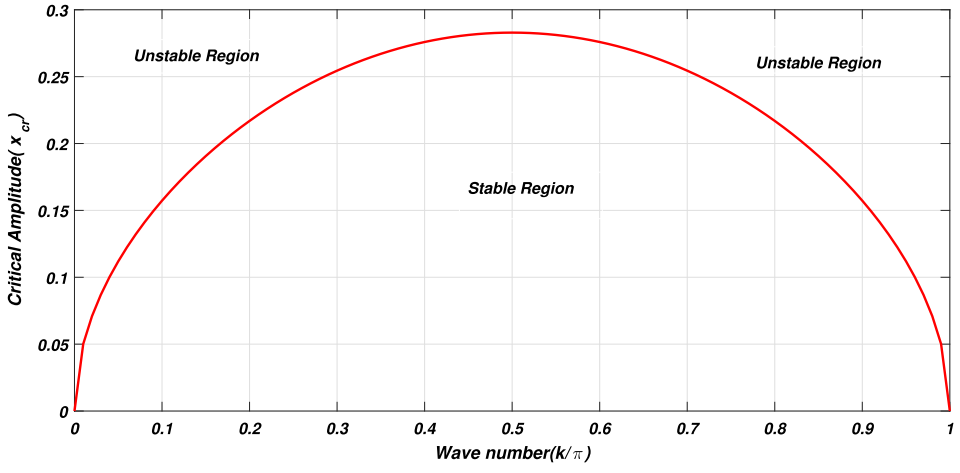

Fig. 1. (Color online) Critical amplitude versus wave number for $D = 0.04$, $k_0 = 5.7$ and $b = 0.8$. The Stable Region (SR) and Unstable Region (UR) of modulational instability (MI) are presented.

The results in Fig. 2 confirm that evolution of collective dynamical behaviors via pattern formation in the network depends on the external stimuli from light illumination on each node. At low frequency exposure in Fig. 2(a), the network presents a state characterized by alternate quiescent and firing patterns. This structure corresponds to the spiking state of the network. As the frequency of light exposure is increased to greater value in Fig. 2(c), there is destruction of the initially coherent pattern into a partially disordered state which could be linked to chaotic state. These results prove that a variety of different collective electrical activities could be induced under different frequency of light illumination. Photosensitive neurons can thus capture and convert external optical signals thereby realizing the encoding of the signal. Remarkably, the obtained patterns in Fig. 2(c) might also be a route to chimera states which has been widely discussed recently in neuronal system.[43,44]

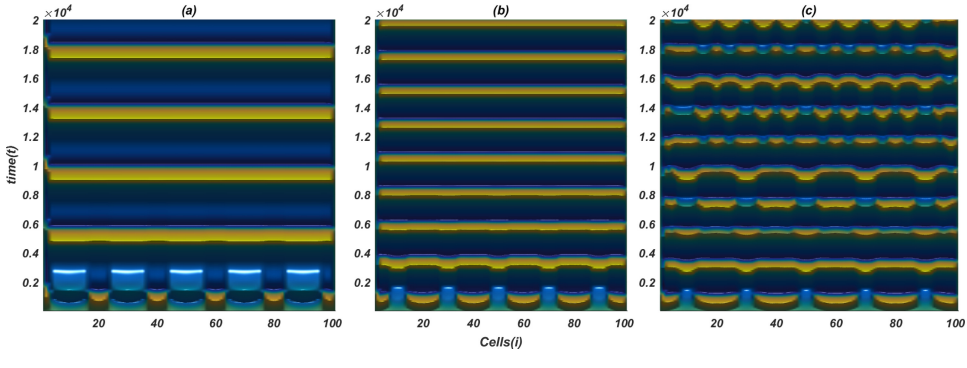

Fig. 2. (Color online) Spatiotemporal patterns of membrane potential calculated for each frequency of photocurrent from light illumination; (a) $\omega_1 = 0.10$, (b) $\omega_1 = 0.18$, (c) $\omega_1 = 0.20$, with $a_1 = 0.4$.

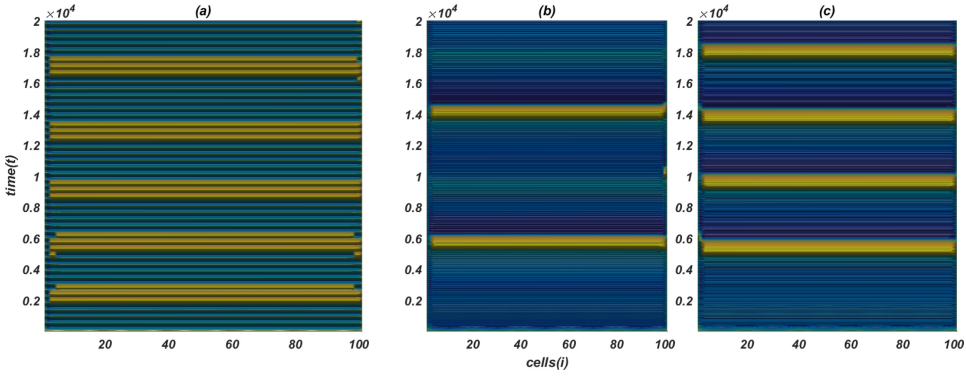

Fig. 3. (Color online) Spatiotemporal patterns of membrane potential calculated for each frequency of external magnetic flux; (a) $\omega_2 = 0.5$, (b) $\omega_2 = 8$, (c) $\omega_2 = 10$, with $a_2 = 4.0$.

Furthermore, we evaluate the dependence of patterns on the frequency of external magnetic flux related to the electromagnetic radiation. We fix the amplitude at $a_2 = 4.0$ and we vary the angular frequency ω_2. The results are presented in Figs. 3(a)–3(c), where $\omega_2 = 0.50$ in Fig. 3(a), $\omega_2 = 8.0$ in Fig. 3(b) and $\omega_2 = 10$ in Fig. 3(c).

The results in Fig. 3 confirm varieties of firing patterns such as bursting state as well as 2-period and 4-period spiking states can be induced in the network under electromagnetic radiation exposure. At low frequency external magnetic flux in Fig. 3(a), the spatiotemporal pattern presents localized patterns corresponding to bursting state. In Fig. 3(b), the 2-period spiking state is observed and at a higher frequency in Fig. 3(c), we observe a 4-period spiking state. From the numerical results, we observed that the double periodic stimuli respectively for periodic photocurrent controlled by external illumination and periodic magnetic flux controlled by external magnetic field applied on the simple neuron each promote mode transition. However, the periodic photocurrent is more sensitive to mode transition than the periodic magnetic flux.

Apart from light illumination and magnetic field, thermal fluctuation can significantly modulate excitability of neurons by influencing gated channel conductance. It is expected that in future project, a thermistor can be incorporated into a functional circuit to detect temperature fluctuation.[45,46] In that way, the effect of thermal fluctuation on the potential mechanism of information coding in brain micro-circuits could be uncovered.

5. Conclusion

Modulated impulse formation and pattern transition in a chain network of memristive photosensitive neurons have been discussed through MI. By applying the discrete asymptotic expansion method, the dynamical equations are solved to obtain an envelope equation suitable for linear stability analysis. Linear stability analysis is

performed such that the conditions and regions under which modulated signals emerge in the network are determined. These analytical predictions are confirmed through numerical experiments. Using parameters taken from the unstable zone, the longtime evolution of initial plane wave solutions confirm the presence of localized modulated impulses with features of spiking and bursting states as obtained in real biological experiments. Respective frequencies of photocurrent from light illumination and external magnetic flux are shown to significantly modify the obtained localized structures via pattern transition. This could be very useful in constructing intelligent and useful sensory networks.

References

1. J. Stajic, *Science* **356**, 497 (2017).
2. D. Hassabis *et al.*, *Neuron* **95**, 245 (2017).
3. M. Musib *et al.*, *Science* **357**, 28 (2017).
4. S. Hegelich, *Cogn. Syst. Res.* **45**, 59 (2017).
5. D. Shen, G. Wu and H. I. Suk, *Ann. Rev. Biomed. Eng.* **19**, 221 (2017).
6. O. Inam *et al.*, *Appl. Magn. Reson.* **48**, 1055 (2017).
7. M. Kalla, B. Singh and S. S. Murthy, *IEEE Trans. Ind. Electron.* **64**, 264 (2017).
8. P. Ioannou and K. Tsakalis, *IEEE Trans. Automat. Control* **31**, 1033 (1986).
9. N. Kushwaha *et al.*, *Front. Phys.* **9**, 513969 (2021).
10. S. Majhi *et al.*, *Phys. Life Rev.* **28**, 100 (2019).
11. A. L. Hodgkin and A. F. Huxley, *J. Phys.* **117**, 500 (1952).
12. R. FitzHugh, *Biophys. J.* **1**, 445 (1961).
13. J. Nagumo *et al.*, *Proc. IRE* **50**, 2061 (1962).
14. C. Morris and H. Lecar, *Biophys. J.* **35**, 193 (1981).
15. C. N. Takembo *et al.*, *Physica A* **593**, 126891 (2022).
16. Y. Yang *et al.*, *Cognitive Neurodyn.* **15**, 265 (2021).
17. J. L. Hindmarsh and R. M. Rose, *Nature* **296**, 162 (1982).
18. N. F. Rulkov, *Phys. Rev. Lett.* **86**, 183 (2001).
19. M. Chen *et al.*, *AEU Int. J. Electron. Commun.* **110**, 152840 (2019).
20. J. H. Zhang and X. F. Liao, *AEU Int. J. Electron. Commun.* **75**, 82 (2017).
21. C. Wang *et al.*, *Mod. Phys. Lett. B* **34**, 2050323 (2020).
22. Y. Liu, Y. Xu and J. Ma, *Commun. Nonlinear Sci. Numer. Simul.* **89**, 105297 (2020).
23. Z. T. Njitacke *et al.*, *Chaos Solitons Fractals* **167**, 113014 (2023).
24. Y. Zhang *et al.*, *Chin. J. Phys.* **71**, 72 (2020).
25. A. Mishra *et al.*, *Chaos* **31**, 052101 (2021).
26. Y. Liu *et al.*, *Front. Inf. Technol. Electron. Eng.* **21**, 1387 (2021).
27. Y. Zhang *et al.*, *Nonlinear Dyn.* **102**, 1848 (2020).
28. D. Yu *et al.*, *Commun. Nonlinear Sci. Numer. Simul.* **117**, 106894 (2023).
29. G. Wang *et al.*, *Nonlinear Dyn.* **107**, 3945 (2022).
30. Z. Hou *et al.*, *Chaos Solitons Fractals* **142**, 110522 (2022).
31. C. N. Takembo *et al.*, *Indian J. Phys.* **167** (2022), doi: 10.1007/s12648-022-02368-2.
32. C. B. Tabi, S. Veni and T. C. Kofane, *Phys. Rev. A* **104**, 033325 (2021).
33. Y. S. Kivshar and M. Peyrard, *Phys. Rev. A* **46**, 3198 (1992).
34. E. Kengne and A. Lakhssassi, *Chaos, Solitons Fractals* **160**, 112240 (2022).
35. C. N. Takembo, *Mod. Phys. Lett. B* **36**, 2250021 (2022).
36. E. Kengne *et al.*, *Nonlinear Dyn.* **104**, 1 (2021).
37. E. Tala-Tebue *et al.*, *Eur. Phys. J. Plus* **132**, 272 (2017).

38. C. N. Takembo *et al.*, *Int. J. Mod. Phys. B* **32**, 1850165 (2018).
39. C. B. Tabi, A. S. Eteme and T. C. Kofane, *Nonlinear Dyn.* **100**, 3799 (2020).
40. J. Ma *et al.*, *Physica A* **486**, 508 (2017).
41. A. Mvogo *et al.*, *Phys. Lett. A* **381**, 2264 (2017).
42. J. Ma *et al.*, *Chaos, Solitons Fractals* **89**, 219 (2017).
43. S. S. Muni *et al.*, *Chaos Theory Appl.* **4**(3), 119 (2022), doi: 10.51537/chaos.1144123.
44. M. Mehrabbeik *et al.*, *Math. Biosci. Eng.* **18**, 9394 (2021).
45. Y. Xu and J. Ma, *Commun. Nonlinear Sci. Numer. Simul.* **111**, 106426 (2022).
46. Y. Xu *et al.*, *Appl. Math. Comput.* **385**, 106426 (2020).